AD-A063 733 ARMY ENGINEER WATERWAYS EXPERIMENT STATION VICKSBURG MISS F/G 13/10
STUDY AND PARAMETRIC ANALYSIS OF TRAFFICABILITY, RUNNING GEAR, --ETC(U)
DEC 78 G W TURNAGE, W C SEABERGH

UNCLASSIFIED WES-TR-M-78-3 NL

1 OF 2
AD
A063733

LEVEL II

TECHNICAL REPORT M-78-3

STUDY AND PARAMETRIC ANALYSIS OF TRAFFICABILITY, RUNNING GEAR, AND STABILITY CONSIDERATIONS FOR NEARSHORE BOTTOM-CRAWLING VEHICLES

by

Gerald W. Turnage, William C. Seabergh

Geotechnical Laboratory
U. S. Army Engineer Waterways Experiment Station
P. O. Box 631, Vicksburg, Miss. 39180

December 1978

Final Report

Unclassified

SECURITY CLASSIFICATION OF THIS PAGE (When Data Entered)

REPORT DOCUMENTATION PAGE

READ INSTRUCTIONS BEFORE COMPLETING FORM

1. REPORT NUMBER (14) WES-TR-Technical Report M-78-3	2. GOVT ACCESSION NO.
3. RECIPIENT'S CATALOG NUMBER	
4. TITLE (and Subtitle) (6) STUDY AND PARAMETRIC ANALYSIS OF TRAFFICABILITY, RUNNING GEAR, AND STABILITY CONSIDERATIONS FOR NEARSHORE, BOTTOM-CRAWLING VEHICLES.	5. TYPE OF REPORT & PERIOD COVERED (9) Final report. Feb 77–Feb 78
	6. PERFORMING ORG. REPORT NUMBER
7. AUTHOR(s) (10) Gerald W. Turnage, William C. Seabergh	8. CONTRACT OR GRANT NUMBER(s)
9. PERFORMING ORGANIZATION NAME AND ADDRESS U. S. Army Engineer Waterways Experiment Station, Geotechnical Laboratory, P. O. Box 631, Vicksburg, Miss. 39180	10. PROGRAM ELEMENT, PROJECT, TASK AREA & WORK UNIT NUMBERS
11. CONTROLLING OFFICE NAME AND ADDRESS (11) Civil Engineering Laboratory, Naval Construction Battalion Center, Port Hueneme, Calif. 93041	12. REPORT DATE December 1978
	13. NUMBER OF PAGES 180
14. MONITORING AGENCY NAME & ADDRESS (if different from Controlling Office) (12) 188 p.	15. SECURITY CLASS. (of this report) Unclassified
	15a. DECLASSIFICATION/DOWNGRADING SCHEDULE

16. DISTRIBUTION STATEMENT (of this Report)

Approved for public release; distribution unlimited.

17. DISTRIBUTION STATEMENT (of the abstract entered in Block 20, if different from Report)

18. SUPPLEMENTARY NOTES

19. KEY WORDS (Continue on reverse side if necessary and identify by block number)

Coastal zone
Mathematical models
Mobility
Ocean bottom vehicles
Surfzone Transition Analytical Methodology (STAM)
Trafficability
Vehicle performance

20. ABSTRACT (Continue on reverse side if necessary and identify by block number)

The Surfzone Transition Analytical Methodology (STAM) is a computerized mathematical model that was developed to predict the trafficability and stability performance of bottom-crawling vehicles operating in the nearshore region (from shoreline to 150-ft water depth). STAM input requires detailed mathematical descriptions of (a) the vehicle's design characteristics, (b) its performance requirements, and (c) the specific nearshore environment. From these descriptions, STAM predicts (a) vehicle trafficability performance in terms of vehicle/obstacle interference and vehicle ability to negotiate soft soil,

DD FORM 1 JAN 73 1473 EDITION OF 1 NOV 65 IS OBSOLETE

Unclassified

SECURITY CLASSIFICATION OF THIS PAGE (When Data Entered)

20. ABSTRACT (Continued)

develop drawbar pull, and maintain tractive force while operating on either a fine-grained or a coarse-grained ocean bottom, and (b) vehicle stability performance in terms of vehicle resistance to lateral and to longitudinal overturn, plus vehicle ability to maintain forward motion and to resist side sliding. STAM predicts the performance of only two-track, single-chassis bottom-crawling vehicles because this well-developed chassis/running gear combination was judged most suitable for near-future nearshore operations. Detailed guidelines are presented to assist the user of STAM in (a) evaluating the potential of a particular vehicle design to satisfy stated performance requirements in a specified nearshore environment, and (b) making tradeoffs in the selection of vehicle design parameter values to define the optimum design that most closely satisfies the vehicle's performance requirements within a specified nearshore environment.

THE CONTENTS OF THIS REPORT ARE NOT TO BE USED FOR ADVERTISING, PUBLICATION, OR PROMOTIONAL PURPOSES. CITATION OF TRADE NAMES DOES NOT CONSTITUTE AN OFFICIAL ENDORSEMENT OR APPROVAL OF THE USE OF SUCH COMMERCIAL PRODUCTS.

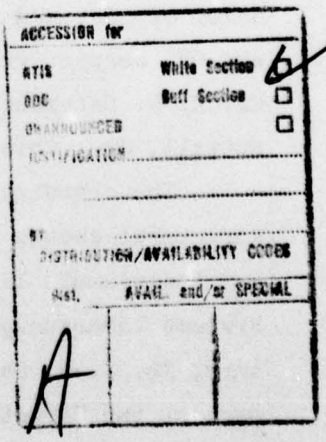

PREFACE

The study reported herein was conducted from February 1977 to February 1978 by personnel of three organizational units of the U. S. Army Engineer Waterways Experiment Station (WES)--the Mobility Research and Methodology Branch (MRMB), Mobility Systems Division (MSD), Mobility and Environmental Systems Laboratory (MESL); the Coastal Branch (CB), Wave Dynamics Division (WDD), Hydraulics Laboratory (HL); and the Operations Branch (OB), Soil Dynamics Division (SDD), Soils and Pavements Laboratory (SPL). The work was requested and sponsored by the Civil Engineering Laboratory (CEL), U. S. Naval Construction Battalion Center, Port Hueneme, California.

Mr. W. C. Seabergh (CB) developed a mathematical description of the major water forces that act on nearshore bottom-crawling vehicles and prepared the section of the report that deals with that subject. Mr. D. E. Barnes (OB) computer-coded the overall model that describes nearshore vehicle performance and exercised this model in the several applications described in the report. Mr. G. W. Turnage (MRMB) was the principal investigator, directed the analysis included in the report, and along with Mr. Seabergh prepared the report.

The study was performed under the general supervision of Messrs. W. G. Shockley, H. B. Simmons, and J. P. Sale, Chiefs of the MESL, HL, and SPL, respectively; Messrs. A. A. Rula and E. S. Rush, former and present chief, respectively, of MSD, and Dr. J. G. Jackson, Chief of SDD; and Dr. C. L. Vincent and Mr. R. C. Sloan, Chiefs of CB and OB, respectively. The study was under the direct supervision of Mr. H. G. Herrmann, III, Ocean Engineering Department, CEL; Mr. C. J. Nuttall, Jr., Chief of MRMB; and Dr. R. W. Whalin, Chief of WDD.

The organization of laboratories at the WES has undergone a structural change since this study was conducted. The organizations and individuals listed above as part of the Mobility and Environmental Systems Laboratory (MESL) are now included in the Geotechnical Laboratory, Mr. J. P. Sale, Chief. Also, the Soil Dynamics Division is now part of the Structures Laboratory, Mr. Bryant Mather, Acting Chief.

COL J. L. Cannon, CE, was Director of the WES during this study, and Mr. F. R. Brown was Technical Director.

CONTENTS

CONVERSION FACTORS, U. S. CUSTOMARY TO METRIC (SI)
UNITS OF MEASUREMENT

U. S. customary units of measurement used in this report can be converted to metric (SI) units as follows:

Multiply	By	To Obtain
cubic feet	0.02831685	cubic metres
degrees (angular)	0.01745329	radians
feet	0.3048	metres
feet per second	0.3048	metres per second
feet per second squared	0.3048	metres per second squared
horsepower (550 ft-lbf/sec)	745.6999	watts
horsepower (550 ft-lbf/sec) per ton	83.82	watts per kilonewton
inches	2.54	centimetres
inches per minute	2.54	centimetres per minute
kips (force)	4448.222	newtons
knots (international)	0.5144444	metres per second
miles (U. S. statute) per hour	1.609344	kilometres per hour
pounds (force)	4.448222	newtons
pounds (force) per second	4.448222	newtons per second
pounds (force) per square inch	6.894757	kilopascals
pounds (force) per square inch per inch	0.27145	megapascals per metre
pounds (force)-seconds squared-inches	0.1129848	newtons-seconds squared-metres
pounds (mass)	0.4535924	kilograms
pounds (mass) per cubic foot	16.01846	kilograms per cubic metre
square feet	0.09290304	square metres
square inches	6.4516	square centimetres
tons (2000 lb, mass)	907.1847	kilograms

STUDY AND PARAMETRIC ANALYSIS OF TRAFFICABILITY, RUNNING GEAR, AND STABILITY CONSIDERATIONS FOR NEARSHORE, BOTTOM-CRAWLING VEHICLES

PART I: INTRODUCTION

Background

1. The survey, construction, and maintenance of nearshore underwater facilities are important tasks of the U. S. Navy. To do this work efficiently requires the use of bottom-crawling vehicles designed to operate in specified environmental conditions at stated performance levels. Unfortunately, a methodology for such vehicle design has been largely lacking.

2. An earlier study,[1] conducted by the U. S. Army Engineer Waterways Experiment Station (WES) for the U. S. Naval Civil Engineering Laboratory (so-named at that time), provided preliminary information regarding seafloor characteristics on a worldwide basis and existing seafloor-crawling vehicles. The state of the art of land trafficability and mobility research was described, and some observations were made concerning the merits and limitations of various seafloor vehicle running gears and the measurement and interpretation of seafloor soil strength properties. This earlier study was quite comprehensive, but generally qualitative in nature and attempted neither to quantify any aspect of seafloor trafficability nor to predict the performance characteristics of specific seafloor-crawling vehicles.

3. The present study is less comprehensive than the earlier one in that it deals only with seafloor vehicles operating nearshore (from shoreline to 150-ft* water depth). This study should be a useful extension of the earlier one, however, because it stresses development

---

* A table of factors for converting U. S. customary units of measurements to metric (SI) units is presented on page 6.

of a quantitative methodology for designing seafloor-crawling vehicles to satisfy stated performance requirements in specified seafloor environments.

Purpose

4. The purposes of the study reported herein were to:

   a. Summarize existing information in the fields of vehicle trafficability, running gear/chassis configuration, and stability as they affect the performance of seafloor-translating vehicles operating primarily in the nearshore region.

   b. Develop a methodology for the selection and preliminary design of a vehicle's running gear and chassis configuration, given a vehicle mission with specified nearshore environmental conditions and required operational performance characteristics.

Scope

5. The present study can be considered an extension of the one described in Reference 1 and thus deals primarily with information that has become available since publication of the earlier study. Purpose a above was satisfied by analyzing results from a detailed search of the literature. The methodology to satisfy purpose b was developed by (a) incorporating into a single mathematical model those relations needed to describe water forces acting on a seafloor-crawling vehicle, vehicle/seafloor interactions that are essentially the same as would be obtained in a terrestrial environment, and vehicle/seafloor/water force interactions that are peculiar to vehicle operation on the seafloor, and (b) providing guidance relative to the use of this model in nearshore vehicle design analyses.

PART II: REVIEW OF PERTINENT SEAFLOOR TRAFFICABILITY INFORMATION

6. Before the rational design or selection of any ground-crawling vehicle for trafficability purposes can begin, it is necessary to understand the environment in which the vehicle will operate. Further, it is necessary to determine what practical vehicle hardware concepts are available and what guidance real-world experience provides toward choosing the most appropriate concept. A review of the above types of information is particularly important when the environment of concern is as foreign (by present-day standards) to ground-crawling vehicle traffic as is the nearshore environment.

Environmental Conditions

7. For the purpose of this study, the nearshore is defined as that region of the seafloor from the shoreline to the 150-ft water depth. The environmental conditions to be considered are those that can be expected to have most influence on nearshore vehicle trafficability, namely, (a) water forces acting on a vehicle, (b) seafloor soil strength, (c) seafloor surface microrelief (local slope* and obstacles), and (d) turbidity. A description of these environmental conditions must take into account that (a) the parameters selected will be used in the methodology developed later in this report for predicting nearshore vehicle performance quantitatively--thus these parameters must be quantifiable; and (b) essentially no nearshore areas have been described before in terms specifically designed to promote the prediction of nearshore vehicle trafficability. It is thus beneficial to set forth at least general guidelines for measuring the values of the appropriate nearshore parameters.

Water forces

8. Water forces per se adversely affect the performance of bottom-crawling vehicles in that they promote vehicle sliding and/or overturning

---

* Local slope is seafloor slope within one vehicle length of the front and rear ends of a given vehicle.

and may resist vehicle movement in the direction desired. A subsequent section of this report develops a detailed mathematical description of the several types of forces that water exerts on a bottom-crawling vehicle operating nearshore (paragraphs 70-96). For the present, it is sufficient to mention that (a) there are four major types of water forces involved--buoyant, lift, drag, and inertial; (b) these forces sometimes momentarily take very large values--up to several times the gross vehicle weight for drag force, for example; and (c) predictions of water force values can be made only if values are specified for a number of vehicle design, vehicle operational, and sea-related parameters such as vehicle length, width, height, and geometry; vehicle speed and heading angle;* and water depth, general slope,** wave height, wave period, and current velocity.

9. Values of pertinent vehicle design parameters needed as input information for the prediction of water forces can easily be measured for existing vehicles or specified for design vehicles. Vehicle operational parameters are also relatively easy to deal with since vehicle speed on the seafloor ordinarily is very low and heading angles can be specified in terms of reasonable limits.

10. Unfortunately, accurate values of the required sea-related parameters are usually more difficult to determine, primarily because of two problems. First, the very presence of a layer of opaque seawater makes the seafloor remote. Thus, except for combinations of relatively small nearshore area and shallow water depth, measurements of seafloor macrorelief (water depth and general slope) must be made by remote instead of direct (rod- and level-type) means. For use in predicting water forces acting on seafloor-crawling vehicles, remote sensing (by sonic, seismic, or electromagnetic means) can produce sufficiently

---

* Vehicle heading angle is measured from a straight reference line drawn perpendicular to the shoreline, which is also taken herein to be a straight line. Incoming and backwash water forces are considered to act parallel to the reference line.

** General slope is the average seafloor slope over at least 50 ft of horizontal distance.

precise measurements of seafloor macrorelief--water depths to the nearest foot and general seafloor slope to the nearest percent. Satisfactory description of macrorelief for a given nearshore area usually depends on the availability and scale of existent seafloor topographic maps or on the funds available to develop new maps, whether by direct or remote means.

11. The second problem arises from the transitory nature of sea action, which causes values of the sea-state parameters (wave height, wave period, and current velocity) to vary both on an areal basis and on a time basis (minute-to-minute, hour-to-hour, etc.). The most practical way to deal with this situation is to estimate the values of these parameters.

12. To decide whether to operate a given seafloor-crawling vehicle within a given nearshore area on a short-term basis (day-by-day), it probably is sufficient to make first-cut estimates of the sea state from related weather predictions and to then refine these estimates by on-site measurements. To <u>design</u> a vehicle to operate in a particular nearshore area, however, requires that values of the sea-state parameters be estimated on a more long-term basis.

13. The techniques of extremal statistics can be used to estimate the largest value of a given sea-state parameter to be expected within time periods ranging up to many years. For example, Figure 1[2] shows the probability of exceeding a given wave height (y-scale), both on the usual nondimensional probability basis (lower x-scale) and in terms of one occurrence per unit of time (upper x-scale). Relations like those in Figure 1 depend on the long-term distributions of both wave height and wave period; these can be determined only by modeling the behavior patterns of these two parameters statistically as they are observed (and recorded) to occur for a reasonably long period of time (e.g., several months). For instance, from a relation like that in Figure 1, the wave height that might be used in designing a nearshore, bottom-crawling vehicle would be the once-a-week value.

14. A second approach to establishing such a design value is to observe the proposed vehicle operation site over a time period of at

least several days during which the sea-state at times is approximately as severe as would be considered acceptable for subsequent vehicle operation. A sufficient number of measurements of each sea-state parameter should be taken to allow the parameter's sampling distribution* to be closely approximated by a standard mathematical representation. The design value of the particular sea-state parameter (say, current velocity) could then be taken as, say, the 75th percentile or, more restrictively, the 90th.[3]

15. In summary, paragraph 8 described in general terms those vehicle design, vehicle operational, and sea-related parameters needed for input to a mathematical model of water forces acting on bottom-crawling vehicles operating nearshore. Paragraphs 9-14 described in more detail applicable approaches for measuring the values of the three types of parameters, particularly the sea-related ones.

Seafloor soil strength

16. In nearshore applications, even more so than in terrestrial ones, prediction of ground-crawling vehicle trafficability depends on being able to accurately measure or predict soil strength in the contact region. This situation arises because, on average, seafloor soils are weaker. (Here, only seafloor soils are considered, as opposed to rock, sandstone, coral, etc., which are considered impediments to trafficability, primarily as obstacles to be overridden.) From Reference 1, seafloor "...clay deposits can be assumed to be primarily normally consolidated. This, in combination with the presence of water, results in 100 percent saturated clay deposits of lower density and strength than found in terrestrial deposits. Also, sensitivity is higher. For sands, density--and hence the angle of internal friction and shear strength--is, in general, less for marine deposits than for terrestrial deposits. Shear strength of marine sand deposits is further reduced since only the submerged weight of the material can be considered..."

---

* The abscissa of a sampling distribution represents the value of the parameter measured; the ordinate denotes the proportion of the total number of measurements that produced the value.

17. Three methods of measuring nearshore soil strength can be considered:

a. Remote sensing. This most desirable approach cannot be used at present since the state of the art does not allow sufficient precision in estimating seafloor soil strength.

b. Laboratory testing of seafloor soil samples. This approach has the advantage of permitting determination of a number of basic soil properties (internal friction, cohesion, density, particle-size distribution, etc.) and indicators of soil strength (vane shear, cone index, etc.). However, obtaining seafloor soil samples is usually an expensive, cumbersome undertaking, and until a few years ago provided "little chance of obtaining really undisturbed samples. Even with good samples, the possible variations of soil properties due to changes in the ambient pressure conditions and to storage could not be accounted for."[1] Slightly later, however, good success was reported in correlating vane shear and cone index data of seafloor soil measured in situ with that measured in laboratory core samples.[4] Still, further work is needed to develop sampling and laboratory testing techniques that assure that laboratory-measured seafloor soil properties accurately depict the properties of the seafloor soil in place.

c. In situ soil strength measurements. For the immediate future, this least glamorous of the three approaches appears to be the most useful. Because of the remoteness of the seafloor, the strength-measuring apparatus used should be simple to operate and lend itself to either direct or remote control. Two such apparatus--the cone penetrometer and the vane shear device--satisfy these requirements and have been used widely in evaluating seafloor soil strength.[1,4,5]

18. For use in a system to predict nearshore, bottom-crawling vehicle trafficability, the cone penetrometer is of particular interest. Average cone index, CI* (an indicator of soil strength obtained with the WES standard cone penetrometer),[6] is the soil strength term used in a methodology that has been successfully used for a number of years to predict vehicle terrestrial trafficability. Subsequent analysis herein shows that appropriate parts of that methodology can also be used in describing vehicle nearshore trafficability.

---

* For convenience, symbols and unusual abbreviations are listed and defined in the Notation (Appendix D).

19. Cone index is defined as the average force required to penetrate a soil vertically within a prescribed soil depth at 72 in./min with a right circular steel cone of 30-deg-apex angle, divided by the cone's base area, 0.5 sq in. The soil depth over which values of CI should be averaged depends on the soil strength profile and on the weight and type of vehicle whose performance is to be predicted. For one-pass vehicle performance, this is usually the 0- to 6-in. layer; for 50-pass performance, the 6- to 12-in. layer. CI provides an index of soil strength and does not purport to represent a specific soil property; hence CI's implied units of pound per square inch ordinarily are dropped, and values of CI are presented as undimensioned indices.

20. For ordinary circumstances, it is recommended that the standard WES 0.5-sq-in.-base-area cone be used in seafloor soil strength evaluations. Where increased sensitivity in the measurement of soil penetration resistance is needed for instance, in describing the strength of extremely low-strength fine-grained soils (oozes) that are found over parts of the seafloor,* larger sizes of cones can be used. Easily applied relations are available for converting values of cone index obtained with nonstandard size cones to those of the 0.5-sq-in cone (if cone shape and material are held constant).[6]

21. For a range of fine-grained soils, linear relations exist between measurements of cone index and vane shear.[4,7] Vane shear (an indicator of a soil's shear strength obtained with an apparatus that includes four rectangular vanes, or blades, at the end of a small-diameter shaft) is measured by (a) forcing the vanes vertically into the soil until the midheight of the vanes is at the depth where the measurement is to be made, (b) rotating the vane horizontally through 90 deg, and (c) dividing the torque required for vane rotation by the product, surface area of the displaced soil cylinder times the appropriate torque arm. Because vane shear values may later be shown to provide information that complements cone index values, it is recommended that measurements of both cone index and vane shear be taken routinely in seafloor site

---

* Soil this weak would probably support only vehicles of extremely low-ground contact pressure, e.g., 2 psi and less.

evaluations. Further, it is recommended that a sample of seafloor soil be taken near the location of each cone index-vane shear pair of measurements, for two reasons: (a) so that the slope of the linear relation between these two terms can, over a period of time, be correlated with soil type, and (b) more importantly for the immediate future, so that the value of average cone index can be interpreted properly.*

Seafloor microrelief

22. Seafloor microrelief (local slope and obstacles) may adversely affect vehicle trafficability primarily in three ways: (a) by increasing the tractive force required by the vehicle to overcome grade resistance, (b) by creating possible geometric interference between the vehicle and the seafloor, and (c) by placing the vehicle in a more precarious attitude for resisting overturn by water forces. Local slope is defined in the footnote on page 9. Obstacles are considered as any rise or depression in the seafloor of at least 3-in. height (or depth) at an angle of at least 5 deg; both measurements are relative to the adjacent local seafloor slope.

23. As with all other pertinent features of the seafloor environment, the more precise the description obtained for seafloor microrelief, the better the chance of accurately predicting its influence on vehicle trafficability. A reasonable balance must be struck, however, between the time and cost required to develop a description of microrelief for a possibly quite large seafloor area and the precision with which tractive force, geometric interference, and vehicle overturn can be modeled. The stylized description of microrelief illustrated in Figure 2 is considered to reflect such a balance. Values taken for the heights, lengths, widths, angles, and spacings of the stylized obstacles should be selected to describe a microrelief as severe as its actual counterpart. Such values might be taken as 75- or 90-percentile values based on standard mathematical representations of measurements taken at the vehicle operational site.

---

* The methodology subsequently developed for predicting nearshore vehicle trafficability separates soils into two classes, (a) coarse-grained soils, and (b) fine-grained soils and sands with fines.

Turbidity

24. Turbidity, which is the disturbance of sediment causing a darkening or obscuring in water of what was or should be clear, degrades seafloor trafficability by reducing or eliminating the ability of the vehicle driver to determine by visual means where he should direct his vehicle. Of the four most important environmental conditions relative to seafloor trafficability (see paragraph 7), turbidity is presently the least quantifiable or predictable.

25. Essentially no formal testing, model or full-scale, has been done to evaluate the amounts of turbidity produced by the various types of running gears; consequently, only qualitative estimates of seafloor turbidity can be made. These estimates may or may not agree, depending on the viewpoint. For instance, better manueverability by wheels than tracks within a restricted area argues for less turbidity by wheels in some situations; possibly smaller values of slip by tracks than by wheels for the same vehicle load and soil strength suggests less turbidity by tracks for other cases. Turbidity is not treated in the methodology developed herein for predicting seafloor trafficability. It is recommended that systematic studies be undertaken to quantify turbidity and to develop a means for predicting the value of this variable as a function of pertinent seafloor, sea-state, vehicle, and vehicle operational parameters.

Existing Hardware Concepts

26. In this report, "hardware" is defined as the running gear and chassis of a given ground-crawling vehicle. From Reference 1, running gear is defined as "the vehicle component that remains in constant physical contact with the ground during vehicle motion, regardless of whether or not it provides propulsion force (i.e., active or passive running gears)." Chassis is defined as the frame upon which the body of the vehicle is mounted. For this study, "existing hardware concepts" are known running gear/chassis configurations that have the possibility of successfully trafficking the seafloor.

27. Evaluation of the relative merits of various hardware concepts requires that consideration be given to (a) the missions that the parent vehicles must perform and (b) the environment in which these missions will take place. In a subsequent part of this report, five types of bottom-crawling vehicles representative of the Navy's anticipated mission requirements in the nearshore region are considered--underwater bulldozer, plus survey, transport, work platform, and trencher vehicles. To accomplish its missions in the complex nearshore environment, each of these types of vehicles must be (1) self-propelled (powered from an on-board source or through an umbilical); (2) steerable; and according to current thinking, (3) mobile to and from a work site. Further, the most demanding features of nearshore environment relative to vehicle trafficability are that (1) water forces of sometimes extremely large values are encountered; (2) soft soil and obstacle negotiation problems are at least as great as onshore; and (3) operation and recovery of a given ground-crawling vehicle are much more difficult and hazardous than onshore.

28. These common features among nearshore vehicle mission requirements and environmental conditions allow preliminary establishment of desirable hardware criteria in qualitative terms. The ideal nearshore, bottom-crawling vehicle should:

a. Be powered and steerable (to satisfy typical mission requirements).

b. Be streamlined (to miminize water forces felt by the vehicle).

c. Be rugged (to withstand water forces).

d. Be low and wide, with a low center of gravity (to resist overturning).

e. Have low ground contact pressure (to promote soft-soil negotiation).

f. Have running gear outer faces configured to gain maximum available tractive force (to climb slopes, override obstacles, and resist slipping).

g. Have chassis and running gear configured to provide maximum obstacle override capability.

29. In choosing the one or more hardware concepts that most nearly satisfy the above criteria, it is necessary also to take into account such practical considerations as the state of development, proven successful use, and maintenance requirements of a given hardware concept. In making this choice, it is useful to consider the vehicle running gear and chassis first separately and then together.

Vehicle running gear

30. In Reference 1, Wiendieck summarized the seafloor performance characteristics to be expected of the eight types of basic vehicle running gear (Figure 3)--the sled, roller, unpowered wheel, hanging chain, powered wheel, track, screw, and mechanical leg, mentioned roughly in order of their historical development. Findings in the following new summary agree largely with those of Wiendieck, but are tempered by the preliminary considerations of paragraphs 26-29.

a. The sled. A modern version of this oldest of the basic running gear, towed by a surface ship, has been used successfully to lay and bury communications cables over hundreds of miles of the seafloor.[8] Reliance on a surface vessel for developing tractive and control forces, however, is impractical for the typical device nearshore travel route. A recent conceptual study suggests that better cable-laying performance would result by using a vehicle supported on skids and self-powered by thrusters.[9] Very low maneuverability and obstacle-climbing capability appear to negate this variant of the sled as the prime mover for the type vehicles of interest herein (see paragraph 27).

b. The roller. A modern variation of this primitive type of running gear is the "rolligon" vehicle. It features liquid- or gas-filled flexible rubber bags fitted outside a large frame on each side of the vehicle and driven by powered rollers in contact with the bags along their peripheries (away from the ground contact area). Power transfer is accomplished solely by friction forces.[10] For near-future applications in the nearshore, this concept is rejected because (1) reduced friction underwater could present major problems of power transfer, and (2) not enough investigation of the "rolligon" concept has been done to rate it as a practical nearshore running gear contender.

c. The unpowered wheel. For nearshore applications, only the powered version of the wheel will be considered.

d. The hanging chain. This unusual device (shown in Figure 4 in a prototype version) has only minimal contact with the seafloor and will function only in water depths at which the main body will float. It has the advantages of very low ground contact pressure and good obstacle traversal performance. Its disadvantages include low stability (i.e., inability to maintain position in any but still-water conditions) and inability to provide a solid base for doing useful work (bulldozing, trenching, etc.). This running gear appears marginally suited only to the survey mission among the five missions referred to in paragraph 27; even there it is rejected for near-future applications because it clearly is unsuited for beach and surfzone operation without use of one of the other running gears in a supplementary role.

e. The powered wheel. It is useful to consider the powered wheel's performance characteristics relative to the criteria (items a-g) in paragraph 28 by contrasting them with those of tracks. In the nearshore, a major strength of the wheel is its excellent maneuverability (item a), which is probably somewhat better than that of a skid-steered track if turbidity caused by sharp turns is considered. Even with low, wide, flexible tires, the maximum amount of tire-ground contact area per unit of vehicle planform area is much less than that attainable with tracks[11] (item e). Wheeled running gears weigh less, making less contribution to a low vehicle center of gravity and resultant vehicle stability (item d), and are less rugged than tracks (item c). The low, wide tires required to promote low ground contact pressure promote about the same degree of vehicle streamlining as tracks (item b). Tires, even with aggressive lugs or chains, develop less tractive force than tracks with aggressive treads (item f). Finally, tires generally are unable to negotiate obstacles as well as tracks (item g). The wheel is mechanically much less complicated than a track, so that maintenance problems for wheels are anticipated to be smaller for underwater applications. The wheel is the most versatile and most investigated of all types of running gear for terrestrial purposes; the track, second-most.

f. Tracks. In effect, the performance characteristics to be expected of tracks in the nearshore environment were reviewed under item e above. Relative to all criteria examined there, the track was better than or nearly equal to the wheel. In particular, the track excels in the most important criteria mentioned in paragraph 28, items c through g. Finally, published reports on the performance

of tracked vehicles in underwater applications indicate that maintenance problems can be held within acceptable limits.[12]

g. The screw. The screw, designed to negotiate very soft, swampy areas and liquid mud, performs very well in these types of terrestrial environments.[13] However, it may churn the soil more than any of the other types of running gear considered here, in which case it would cause greater turbidity problems in the nearshore environment. Its relatively new state of development further argues against the screw for near-future nearshore applications, though this device should receive serious consideration on a long-term basis.

h. The mechanical leg. This most recent type of running gear is complex, unproven, and can be ignored for near-future nearshore applications.

31. In summary, paragraph 30 capsulized the relative performances expected of the basic types of vehicle running gear, primarily in terms of the criteria (see paragraph 28) deemed necessary to satisfy anticipated mission requirements and environmental conditions (see paragraph 27). On this basis, the track is judged to be significantly the best running gear, and considerations hereafter will deal only with tracked running gears.

Chassis

32. The chassis is the frame upon which the body of the vehicle is mounted. Types of vehicle chassis differ primarily in terms of (a) the number of chassis units--one, two, or more; (b) the relative locations of these units when there are more than one--usually in line longitudinally, but sometimes in tricycle or other arrangement; and (c) the way in which these units are connected to one another--more details are given in paragraphs 33-38.

33. First-generation nearshore bottom-crawling vehicles should be built using hardware concepts that are simple and proven. This suggests that any increase in the number of chassis units be made only if that increase provides known, definite advantages in the vehicle's ability to traffic soft soil and override obstacles (item (a) in paragraph 32). If there are more than one chassis unit, the units should be aligned longitudinally since changes in vehicle performance caused by using

other relative unit locations have been evaluated only on a few experimental or special-purpose vehicles (item (b) above). The important concept that needs to be examined relative to the way chassis units are connected is vehicle articulation, or jointing, between units (item (c) above).

34. In Reference 11, C. J. Nuttall, Jr., states: "A vehicle's frame (chassis) may be articulated, or jointed, at one or several places. Each joint may allow relative motion between connected units in the pitch plane, the steering or yaw plane, and/or about a roll axis. The uses and advantages of articulation vary with the particular motions permitted." For a multi-unit tracked vehicle, articulation in the yaw plane to provide steering allows the length-to-width ratio of the overall vehicle to be much larger than for a conventionally skid-steered vehicle (up to 5:1 or more versus about 2:1, respectively),* but at the sacrifice of pivot and very small radius turning capability. The opportunity to increase vehicle length is a real advantage for terrestrial applications, because it allows better longitudinal stability and ride characteristics, particularly for travel at high speeds. For seafloor-crawling applications, these advantages are minimized since seafloor travel need be made only at very low speed. An advantage of articulated steering that is applicable to bottom-crawling operations is that this steering generates less soil disturbance during vehicle turning than does skid steering, leading to reduced turbidity problems (which remain to be quantified). Further, combined yaw and pitch articulation, particularly if the pitch articulation is controllable, holds promise of significantly better obstacle negotiation capability than is possible with rigid frame, skid-

---

* Limits on the vehicle length-to-width ratio for skid-steered tracked vehicles result primarily from limits on the ℓ/t ratio (ℓ = track contact length when the track is on a flat, hard surface; t = distance between center lines of tracks, or track tread). For high-speed, straight-line vehicle stability, ℓ/t should be greater than about 1.2. For steering on a hard surface without excessive power losses, ℓ/t should be less than about 1.8. For slow tracked vehicle operation on soft seafloor soils, these ℓ/t limits can be relaxed somewhat, e.g., $\ell/t < 2$.

steered vehicles (see paragraph 36). Overall, articulated steering has the potential of providing much better bottom-crawling vehicle performance than conventional skid-steering.

35. From Reference 11, "Articulation to provide some significant degree of roll freedom between units helps the vehicle as a whole to maintain its footing (for traction and control) and equalize...track loadings on the ground....Some of the advantage of roll freedom is lost unless the running gear of each unit can conform longitudinally.... Of course, where roll freedom is allowed, each unit individually must have adequate roll stability." For nearshore, bottom-crawling tracked vehicles, lateral rollover is a prime danger due to the sometimes very large values of water forces. Thus, articulation about a roll axis requires careful, detailed evaluation and may not be desirable in some cases.

36. From Reference 11, "Pitch articulation permits longitudinal conformance to the terrain, which is an advantage in weak soils, and more important, greatly improves vertical obstacle crossing ability... A pitch joint may profitably be made lockable under driver control, so that the entire vehicle length can, when needed, be exploited in trench crossing. If further it is selectively powered, so that the ends or the middle of the vehicle may be raised under driver control, obstacle crossing capabilities...can be still further enhanced..." This last advantage has been dramatically demonstrated in two test beds.[14,15]

37. Of the three types of possible chassis articulation control (yaw, roll, or pitch), pitch appears to offer the most promise of improved performance above that of a single-unit tracked vehicle operating nearshore, particularly in terms of obstacle negotiation. At least two points argue against use of pitch articulation in early-stage, bottom-crawling vehicles, however. First, active (lockable) pitch articulation "...is largely experimental and has higher technical risk.... The required control and monitoring systems are more complex and costly."[16] And secondly, no adequate mathematical description of the

obstacle override performance of a pitch-articulated vehicle presently exists for modeling such performance.*

38. In the end, the choice of chassis type for near-future bottom-crawling tracked vehicles is based primarily on considerations of (a) the design characteristics forced on the vehicle by its anticipated environment and (b) the availability and proven performance of chassis types. The sometimes extremely large water forces to be encountered on the seafloor require, foremost, that the bottom-crawler be rugged and be highly resistant to lateral overturn (i.e., be low and wide). The chassis type should be of relatively simple design, be proven by successful field use, and be commercially available (preferably). Multi-unit, active-pitch-articulated chassis hold promise for the future in terms of greatly improved obstacle negotiation and possible slight increases in soft soil negotiation. For the near future, however, rugged single-unit chassis are the chassis of choice--to be mounted on two wide, rugged tracks.**

Offshore Experience

39. Interest in trafficking the seafloor with bottom-crawling vehicles has intensified within the past few years. In part, this has occurred because the earth is becoming ever more crowded and its minerals ever more depleted, leading man to look to the sea as a new frontier for farming and mining. Further, man now recognizes that bottom crawlers have the potential for significantly improving his

---

* Work is being done at the WES to eliminate this deficiency, and it is anticipated that in follow-on work for CEL on nearshore bottom-crawlers, a mathematical model of the obstacle override performance of pitch-articulated, multi-unit tracked vehicles will be available and used.

** Where obstacle override is a problem, the tracked nearshore bottom-crawler in many cases could be assisted in overriding the obstacle by on-board buoyancy tanks and/or an umbilical cable-winch retrieval unit (to be operated from shore or from an attending surface ship).

ability to do many types of important sea-related work--trenching and laying cable in the seafloor; building or placing stable platforms for various support structures (oil rigs, deepwater roadbeds, wharfs, etc.); seafloor dredging; and various other types of civil and military ocean-bottom construction works. The common recognized need is to bring to the job a work vehicle that is as controllable as possible, both in the sense of (a) moving about precisely relative to a seafloor location and (b) when needed, delivering useful force to a desired location. Properly designed bottom-crawling vehicles are the logical choice to satisfy these requirements.

40. Significant efforts have been made worldwide during the past few years to build special bottom-crawling vehicles to do particular seafloor jobs (References 17-21). Owing to the very large expenses involved, most of these vehicles have been built largely from terrestrial vehicle parts and tested or operated on the seafloor on a sporadic basis. All of the vehicle designs have taken seafloor trafficability requirements into account to one degree or another. However, the literature describing seafloor tests or operations with existent bottom-crawlers has several points in common: it usually describes the vehicle in detail (in terms of its weight, dimensions, power supply, control systems, etc.); seldom describes the operational environment in detail (beyond geographical location and broad estimates of soil type and strength, water depth and current); and almost never describes seafloor trafficability performance in detailed, quantitative terms (ability to traffick a stated seafloor soil strength, to develop a stated amount of drawbar pull, to climb a stated slope, etc.). In fact, "Data on seafloor trafficability and vehicle performance is extremely limited and of little value in assessing the state-of-the-art."[22]

41. The reason for this paucity of seafloor environmental and trafficability data is clear--such data are difficult and expensive to obtain. Still, some lessons can be learned from the offshore experience of bottom-crawling vehicles to date. Probably the best sources are the Japanese, largely because they consider development of the capability to perform "...seabed civil and construction works in the deep sea..." to

be a "...national project." Accordingly, "...equipment makers in various fields in Japan started in 1971 development of a series of entirely new seabed engineering works systems (SEW) necessary for seabed construction works under the subsidy of the Japan Society for the Promotion of Machinery Industry..."[23]

42. It is not surprising, then, that the Japanese appear to have done the most work of any nation in recent years to design, build, test, and use bottom-crawling vehicles to do a variety of civil construction jobs--underwater trenching, dredging, surveying, bulldozing, excavating, etc.[5,23,24,25] And, according to the literature, these vehicles do their jobs well.

43. Two common features are found in the literature on details of the Japanese underwater tractor designs and their operational characteristics:

a. Essentially all of the vehicles have tracked running gears (several with track shoes that are triangular in cross section, and that are "...considered suitable for travelling on the seabed surfaces"[5])

b. Particularly for deep-sea operations, but also in many nearshore applications, many of the vehicles work with a surface ship that supplies power and remote control to the bottom-crawler through umbilical lines (Figures 5 and 6, for example). This control usually includes shipboard selection of both (a) direction of vehicle movement on the seafloor (in conjunction often with elaborate electrical, sonar, and sometimes television surveillance equipment monitored on ship), and (b) vehicle effective weight and vertical location of the vehicle (by means of air ballast tanks controlled on ship and a lift cable/winch system capable of bringing the bottom crawler to the sea surface).

44. Reference 25 is representative of Japanese thinking about the common features mentioned above. The author states that for an underwater tractor (bulldozer, back hoe, dredger, etc.) "... large mechanical thrust and high mobility are two basic requirements to be met and, in this regard, the endless track type of running gear now prevalent among land tractors is likely to come into vogue for underwater vehicles." Surface control is usually preferred to man-in-the-sea or submerged control because "...the floor of the sea...is usually dark with turbid

water." Further, to "...work the tractor at the seafloor safely and effectively (requires) continuous surveillance over the constantly changing conditions surrounding the tractor at work." Variable buoyancy of the bottom-crawler is desirable to allow the vehicle to (a) extricate itself from sinking into a soft seafloor, (b) override obstacles not otherwise negotiable; and (c) quickly surface "...toward the service ship and remain awash to be towed..." homeward or to the next work site.

45. In Reference 5, the authors describe a Survey and Inspection Robot (SIR) System aimed at "...surveying undulations on the sea bottom and testing soil in advance of underwater construction works, as well as watching other underwater machinery, and inspecting the result of construction works." This system rides on a tracked running gear that includes triangular-shaped shoes like those mentioned in paragraph 43 (Figure 7); can be lifted to the sea surface by a "...cable-rope winch unit..." if it "...cannot advance any more due to a precipice, rocks, and extremely soft sediment..."; and features for its in situ soil testing devices "...a cone penetrometer, a vane shear tester, and a soil sampler to examine the nature of the upper layer soil on the sea bottom..." (Figure 8).*

46. Essentially all aspects of the Japanese approach to designing seafloor work vehicles outlined in paragraphs 43-45 are considered to be reasonable. Most of these designs feature simple, rugged, two-track hardware, the same type hardware recommended in this report for near-shore, bottom-crawling vehicles on the basis of evaluating the running gear criteria in paragraphs 28 and 29 and the chassis considerations in paragraphs 35-38. Probably the most important design feature suggested by Japanese experience for nearshore, bottom-crawling vehicles that has not been mentioned heretofore, but which should be carefully evaluated in relation to weight, space, cost, and utility in critical subzones of

---

* The same three types of in situ devices were recommended for this purpose in paragraph 21.

the nearshore environment, is that such vehicles should have buoyancy tanks mounted on them and also preferably be attached to an umbilical cable/winch retrieval system operated either from a surface ship or from shore.

PART III: DEVELOPMENT OF THE SURFZONE TRANSITION ANALYTICAL METHODOLOGY (STAM)

47. Since the nearshore environment is still essentially virgin territory for trafficking by bottom-crawling vehicles, the best first step in designing vehicles to operate there is to develop a realistic mathematical model that describes the essential elements of (a) the vehicle involved, (b) the nearshore environment, and (c) the performance to be expected of the vehicle in that environment. It is in the nearshore region that the surfzone, or breaking wave zone, occurs. As will be seen, this zone is probably the most demanding one in the nearshore region as far as bottom-crawling vehicle trafficability and stability are concerned. Because of this and the fact that "surfzone" is a much better known word than "nearshore" to the general readership, the name chosen for the mathematical model is "Surfzone Transition Analytical Methodology," or STAM. A description of the development of STAM follows.

Purpose and General Approach

Purpose

48. The basic purpose of STAM is to provide a rational, realistic scheme whereby a bottom-crawling vehicle can be designed to satisfy stated performance requirements in a specified nearshore environment. The following types of information must be supplied:

a. Vehicle characteristics:

- Chassis dimensions
- Dimensions of loaded cargo volume
- Payload weight and center of gravity
- Loaded chassis dry and submerged weights and center of gravity
- Limits on available horsepower and torque
- General description of vehicle shape

b. Performance requirements:

- Maximum drawbar pull
- Maximum heading angle
- Maximum vehicle operational speed
- Whether or not vehicle must resist large dynamic loads and/or have its running gear serve as a rigid base

c. Nearshore environment information:

- Type of seafloor material (sand, mud, rock, etc.)
- Strength of seafloor material (in terms of cone index)
- Seafloor slope (local and general)
- Obstacle geometry, size, and spacing
- Sea current velocity
- Deepwater wave height
- Deepwater wave period
- Maximum water depth for vehicle operation

General approach

49. The overall structure of STAM is illustrated in Figure 9. Stripped to its essentials, STAM's approach is to:

a. Make a preliminary design of the vehicle based on the vehicle, performance, and environment information supplied (upper part of block 1 in Figure 9).

b. Calculate the values of important water forces that the vehicle will encounter (block 2).

c. Evaluate the ability of the vehicle to traffick the seafloor while doing its job (block 3).

d. Check to see whether the vehicle design provides adequate stability against vehicle overturn and against denial of desired vehicle movement or position (block 4).

e. Based on iteration adjustments to the preliminary vehicle design and perhaps to criteria for acceptable performance (blocks 3, 4, and lower part of block 1), develop a final vehicle design.

50. The remainder of Part III of this report provides detailed descriptions of the methodologies developed to accomplish each of steps

a-d above.* These methodologies feature quantitative determinations that, in effect, "flesh out" the largely qualitative insights that were gained from the analyses in Part II. Further, the computer programs, or subroutines, developed for blocks 2, 3, and 4 are exercised in "example selection problems" supplied by the sponsor to demonstrate STAM's practical application.

Vehicle Design Considerations

General considerations

51. To satisfy the range of performance/environment requirements typical of a nearshore, bottom-crawling work vehicle, the vehicle must be able to:

a. Operate sometimes on soil of very low strength.

b. Override obstacles, develop drawbar pull, and climb slopes, all at low vehicle translational velocity.

c. Be steerable.

d. Maintain its stability against overturn when acted on by the combined effects of obstacles, seafloor slope, and water forces (each of which may take very large values).

e. Withstand severe operational conditions dependably.

52. Thus, the typical bottom-crawling vehicle should:

a. Have low ground contact pressure.

b. Have usable tractive force sufficient for low-speed operation in sometimes very difficult conditions.

c. Have values of track length, width, and spacing that are reasonable when considered in combination.

d. Be short and wide, with a low center of gravity.

e. Be ruggedly constructed using state-of-the-art design.

53. Based on the above considerations (and on the analyses of vehicle running gears and vehicle chassis in paragraphs 30-31 and 32-38, respectively), all types of bottom-crawling vehicles considered by this study should have two-track running gears with the single vehicle chassis located between the tracks.

---

* The methodology to accomplish step e is described in detail in Part IV of this report.

Design guidelines

54. To develop design guidelines for bottom-crawling vehicles, it is necessary to answer three types of questions. First, what vehicle/performance/environment information must be supplied? This question was treated in paragraph 48. Secondly, what characteristics should be designed into the vehicle to maximize the vehicle's chances of doing its job well? General guidance to this question was supplied in paragraphs 52 and 53. And thirdly, what is the full range of vehicle design parameters whose values must be known (i.e., computed from the supplied information) if STAM is to be exercised? This question is answered by listing all parameters subsequently called for by blocks 2, 3, and 4 in Figure 9. To expand on the brief, general answers to the three questions just raised and to illustrate the development of reasonable preliminary design guidelines for several bottom-crawling vehicles, it is convenient to analyze the design phase of the five example selection problems to which STAM will be subsequently applied.

55. Vehicle/performance/environment information. Appendix A illustrates for five types of bottom-crawling vehicles the basic vehicle/performance/environment information that must be supplied in order to exercise STAM. The five vehicles in Appendix A are:

Vehicle No.	Vehicle Descriptive Name
1	Seafloor Survey Vehicle
2	Seafloor Transport Vehicle
3	Seafloor Work Platform Vehicle
4	Seafloor Trencher Vehicle
5	Underwater Bulldozer

These vehicles are useful to consider since the types of jobs they are intended to perform are representative of the broad range of types of work anticipated for nearshore bottom-crawlers. Further, the example problems are useful in that the range of environmental conditions considered approximates those anticipated for real-world situations. In summarized form, values of the supplied vehicle and performance parameters for the five example vehicles are listed in Table 1, and the environmental parameters in Table A1.

56. Vehicle design characteristics. All of the general guidelines in paragraphs 52 and 53 apply in designing each example vehicle to do its job well (i.e., accomplish its mission). Additionally, because of the nature of their missions and performance requirements, together with their specified chassis weights, it is clear that vehicles 4 and 5 must have the most rugged running gears among the five vehicles, followed by vehicles 2 and 3. Vehicle 1 need have the least (though still rugged). For each of vehicles 2-5, the specified large chassis/payload weights require that maximum ground contact area per unit of vehicle platform area be provided in order to promote soft soil negotiation. This requirement is best satisfied by nonramped tracks (i.e., tracks that are semicircular at each end). Further, each of vehicles 2-5 has associated with it either large dynamic loads or the requirement to remain nearly stationary during a work cycle. Thus, the track suspension of vehicles 2-5 should be rigid (girderized). The loaded chassis weight of vehicle 1 is small enough to permit sufficiently low ground contact pressure with a ramped track. Ramping vehicle 1's track at each end also enhances the vehicle's obstacle override ability, making vehicle 1 more competitive in this area of performance with larger vehicles 2-5, each mounted on nonramped tracks. The suspension of vehicle 1 should be fairly flexible, leading to better vehicle speed and (again) obstacle override performance, both of which are important for a survey vehicle. Finally, since vehicle 5 will have a blade in front, some of its preliminary design characteristics obviously will be computed somewhat differently from those of vehicles 1-4.

57. Range of vehicle design parameter values. The first column of Table 2 lists all of the vehicle design parameters required by the STAM water force calculations and stability submodels, and all the vehicle design parameters except for a few dummy ones required by the STAM trafficability submodel.* Figure 10 graphically illustrates those

* Detailed information relative to the dummy vehicle design parameters of the STAM trafficability submodel is provided subsequently in paragraph 62.

parameters in Table 2 that describe the geometry of a tracked vehicle. Of those remaining parameters in Table 2, most relate to a given vehicle's weight, its moment of inertia, and to those mechanical or other characteristics of the vehicle that strongly influence its trafficability performance.

58. Several parameters in Table 2 had values assigned to them to notify the trafficability submodel of some particular vehicle characteristic (e.g., vehicle type VT: 0 for tracked and 1 for wheeled). Several other parameters had values assigned to them (e.g., vehicle approach angle VAA). However, the majority of the vehicle design parameters in Table 2 took values that were computed from the preliminary design guidelines shown in Table 3. Paragraphs 59-61 and 65-69 discuss briefly the development of these guidelines. As design iterations progress and more detailed engineering information is developed about component weights and performance factors, these preliminary estimates should, of course, be replaced by actual values for final design decisions and evaluations.

59. In Table 2, note that the STAM trafficability submodel requires considerably more vehicle design parameters for its implementation than do the water force calculations and the stability submodels. Further, the values of most of the vehicle design parameters in the latter two submodels are defined once values of the trafficability submodel vehicle design parameters are known. The starting point, then, as far as designing a vehicle for STAM applications is concerned, is the STAM trafficability submodel. Consequently, it is important to consider two aspects of this submodel. First, the STAM trafficability submodel was developed by (a) extracting applicable parts from the U. S. Army Mobility Model (AMM),[26,27] an existent, comprehensive, field-proven mathematical model for predicting vehicle trafficability in the terrestrial environment, and then (b) modifying these parts to fit the nearshore environment.* Secondly, AMM has been used in the past exclusively to predict

---

* The relations used by STAM in its water force calculations, trafficability, and stability submodels to predict the performance of nearshore, bottom-crawling vehicles are described in detail in subsequent parts of this report.

the performance either of existing vehicles or of drawing-board vehicles generally similar to existing ones. Thus, this study provided the first opportunity for developing guidelines to define vehicle design parameter values for vehicles designed from scratch, i.e., the five example vehicles of Appendix A. These guidelines are presented in Table 3.

60. The approach taken in developing the Table 3 guidelines was to (a) start with the vehicle characteristics provided (those listed in paragraph 48 and supplied in Appendix A for the five example vehicles), then (b) examine the interrelations among the vehicle design parameters listed in Table 2 to determine how each of these parameters could be defined from the vehicle characteristics provided, and finally (c) assure that the vehicle design guidelines developed were rational and provided the example vehicles with the attributes mentioned in paragraph 52. The result of step (b) above was to develop preliminary design guidelines equations in Table 3 in "building block" fashion--i.e., the order of the equations listed in Table 3 is such that the vehicle design parameter of interest is defined in terms of parameters whose values were supplied and/or parameters whose values were determined in an earlier equation in the table. To accomplish step (c) above, an extensive amount of published vehicle design data was studied for existing tracked vehicles that were designed specifically to operate in low-strength, sometimes flooded soil conditions. (Data in References 13 and 28 were particularly useful in this regard.) These design data described vehicles with the desired attributes listed in paragraph 52, and the guideline equations in Table 3 were developed to show close agreement with these data.

61. Exposition of the rationale behind each guideline equation in Table 3 would require more space than need be allotted in this report. Perusal of these equations will reveal, however, that they are rational, suitably interconnected, and self-contained (once general data descriptive of the vehicle characteristics in paragraph 48 are supplied), and that they do define tracked vehicles with the attributes of paragraph 52. It is important to note that these guideline equations were developed to define hypothetical vehicles, such as the five example vehicles, and that

a design analysis of an actual vehicle must be based on carefully measured parameters descriptive of that vehicle.

62. In addition to the vehicle design parameters listed in Table 2, the present form of the STAM trafficability submodel also requires that values be specified for several dummy parameters not listed in this table. This requirement arises because of the particular form of that part of AMM that was used as the foundation of the STAM trafficability submodel. Most of these dummy parameters have essentially no effect on vehicle trafficability in the nearshore region, but values must be supplied for them in order to render the trafficability submodel operational. The dummy parameters and their values are listed below:

Trafficability Submodel Dummy Parameter	Assigned Value
Number of gears	2
All gear ratios	1,2
Number of pairs of points in the obstacle magnitude-vehicle speed curve	2
Coordinates of obstacle magnitude (in.) versus vehicle speed (mph)	0, 100; 100, 0
Number of pairs of points in the surface roughness-speed curve (cross-country)	2
Coordinates of surface roughness (rms) versus vehicle speed (mph)--cross-country	0, 100; 100, 0
Number of pairs of points in the surface roughness-speed curve (roads and trails)	2
Coordinates of surface roughness (rms), vehicle speed (mph)--roads and trails	0, 100; 100,0
Insert 1 if VCI_1 is to be computed by submodel, 2 if value of VCI_1 is to be input	1
Fine-grained VCI_1	1

63. Special notice also needs to be taken of the last type of data listed under "Trafficability Submodel" in Table 2, i.e., the coordinates of the track speed at the drive sprocket (DSS) versus tractive force (TF) curve, because of (a) the way in which vehicle horsepower hp was defined for each of the five example vehicles, and (b) the particular format required of the DSS, TF coordinates in order that the trafficability submodel could be implemented on the computer. Relative to (a), vehicle hp was computed for the five example vehicles as

$$hp = \frac{TF_{max} \times V_{max}}{375}$$

, with TF_{max} being equal to computed in-air gross

vehicle weight (Table 3) and V_{max} equal to maximum vehicle operational velocity (Appendix A and Table 1). Defining vehicle hp at the drive sprocket this way is conservative since such horsepower ordinarily allows full development of available tractive force from the interaction of the soil and the vehicle running gear, even for relatively high soil strength (high values of cone index).* The DSS, TF coordinates describe vehicle performance at the drive sprocket and thus do not reflect inefficiencies in the vehicle drive train.

64. Relative to (b) above, for all except the first and last pairs of DSS, TF coordinates in Table 3, $TF = \frac{375\ hp}{DSS}$, where hp was defined in paragraph 63 and DSS takes values up to V_{max}. The computational procedure in the trafficability submodel is arranged so that the first set of DSS, TF coordinates is 0, TF_1 (with TF_1 equal to the TF of the first DSS value after DSS = 0); the first nonzero DSS value is equal to a value of 0.1-0.2 V_{max}; and the last set of DSS, TF coordinates is V_{max}, 0.

65. In addition to bestowing on the five example vehicles the attributes mentioned in paragraphs 52, 53, and 56, the design equations in Table 3 also provide some flexibility in the vehicle design by defining reasonable ranges within which a number of equation coefficient values can be selected. It is emphasized, however, that the equations and ranges of values for equation coefficients in Table 3 are provided only for general guidance. The final design of a particular bottom-crawler to do a particular job in a particular nearshore environment must consider the values of appropriate vehicle design parameters available to the vehicle designer from actual hardware.

66. In effect, the preliminary vehicle design equations of Table 3 describe tracked vehicles with the largest tracked running gears of

---

* This method of defining hp did prove to be reasonable. For the full range of scenario conditions (A through H), the largest values of available tractive force/vehicle effective weight ranged from 0.66 to 0.81 for the five example vehicles. Thus, at maximum vehicle velocity V_{max}, tractive force that could be developed at the vehicle's drive sprockets was always at least 23-52 percent larger than tractive force available from the soil/vehicle interaction, so that in no case was an example vehicle underpowered.

conventional geometry that are compatible with values of chassis, payload, and weight parameters provided (Table 1). Using the values of the computed vehicle parameters for the five example vehicles in Table 3, preliminary checks can be made relative to the steerability and ground pressure of a vehicle.

67. For reasonably easy skid steering, the ratio TL/(VW - TW) of a given nearshore, tracked bottom-crawler should take a value less than 2 (see footnote for paragraph 34). For the five example vehicles, values of TL/(VW - TW) are, in order, 1.17, 1.18, 1.32, 1.33, and 1.14. For nearshore bottom crawlers, values of vehicle nominal unit ground pressure--defined as GVW/2(TL)(TW)--should be as small as reasonable design allows, down to the value that corresponds to VCI_1 = the smallest cone index for the vehicle's scenarios. VCI_1 is one-pass vehicle cone index, defined as the smallest value of cone index that will support the vehicle during one vehicle pass on level soil, with the vehicle doing no external work.* Mathematically, VCI_1 is defined as a function of mobility index MI, which is in turn a dimensionless function of pertinent vehicle characteristics. Table 4 presents the equation for MI for self-propelled tracked vehicles, and the equations for determining VCI_1 and VCI_{50} (50-pass VCI) as functions of MI . Figure 11 illustrates graphically the relations of VCI_1 and VCI_{50} to MI . For the five example vehicles, values of GVW/2(TL)(TW) are, in order, 2.1, 2.8, 2.8, 4.1, and 4.2 psi; corresponding values of VCI_1 are 4, 4, 4, 6, and 7;** and the smallest scenario cone index (C_s) values for the vehicles (Table A1) are, in order, 2, 4, 2, 2, and 4.

---

* In nearly all applications of STAM described in the text of this report, vehicle trafficability performance is considered on the basis of one vehicle pass. For some actual nearshore situations, performance may be more appropriately considered on a multipass basis. Accordingly, trafficability prediction relations are included in STAM for both one-pass and multipass performance, and a few of these relations are highlighted in the text.

** The GVW/2(TL)(TW) and VCI_1 values in paragraph 67 are based on values of in-air gross vehicle weight. For vehicles 1-5 completely submerged, values of GVW/2(TL)(TW) are, in order, 1.3, 2.0, 2.0, 2.9, and 3.6 psi; and values of VCI_1, again in order, are 3, 3, 3, 4, and 5.

68. Note that if VCI_1 is much less than the smallest cone index of the vehicle's scenarios, then the preliminary vehicle design dimensions can be reduced. From paragraph 67, this was not the case for any of the five design vehicles. If VCI_1 is greater than the cone index of a given scenario, then either (a) that scenario must be altered or omitted or (b) the vehicle design must be altered. Relative to option (b), the design guideline in Table 3 that has most direct influence on the value of GVW (and subsequently VCI_1) is $W_t = k(TW)(TL)$. GVW = dry $W_{LC} + W_t$, and W_{LC} is specified for a given vehicle. In W_t, k is the weight-estimating constant that has been assigned to reflect the ruggedness and load-carrying capabilities required of the track system for the example vehicles. Based on the values of k suggested in Table 3 (Sheet 2 of 5), fairly major latitude is available in the choice of k before a decision on the ruggedness required of the tracked running gear is made. After this decision is made, however, the range of appropriate k values is fairly small.

69. For the five design vehicles, it was felt that the degree of running gear ruggedness initially selected (see paragraph 56) should be maintained. A given vehicle design could be "fine-tuned" by using the smallest value of k listed in Table 3 for a given degree of ruggedness instead of the suggested, more central value of k shown in each W_t equation. This adjustment was judged not necessary for the example vehicles since in no case would it cause the vehicle's VCI_1 value to be lowered enough to cause the vehicle to be able to operate in a scenario denied it by its first-cut VCI_1 value.

Water Forces Acting on a Nearshore, Bottom-Crawling Vehicle

Introduction

70. This section of the report discusses the calculation of dynamic water forces on a bottom-crawling vehicle, given the environmental parameters of deepwater wave height, wave period, water depth, the general seafloor slope, and a constant current applied broadside to the vehicle. A computer program was developed to compute the forces on

vehicles for a two-dimensional bathymetry (depth and distance from shore) with a monochromatic wave field. Thus the model employed is simplistic with regard to a more complex three-dimensional coastal and offshore environment and a more complex wave field composed of a spectrum of wave heights, periods, and directions. This simplified approach is best taken in this study since no particular three-dimensional bathymetry is specified, and the difficulties in determining forces for even a simplified condition precludes the use of a more complex environment or wave field. The important vehicle parameters involved in the force calculations are the dry and submerged weights; dimensions of height, width, and length; and the shape.

Forces due to water action

71. Three basic types of hydraulic forces can be generated in the seafloor environment of a vehicle moving along the ocean bottom:

a. Wave forces.

b. Current forces.

c. Hydrostatic forces.

72. Wave forces. Forces due to the action of short period (3-20 sec), wind-generated water waves can be partitioned into three zones: the offshore zone, the breaking wave zone, and the broken wave zone. In the offshore zone the wave form is moving with little mass transport. The water particle motions are almost orbital in nature and ideally the particle returns to its original position after a cycle of motion. The forces on an underwater vehicle caused by this movement are drag forces due to the orbital velocities, inertial forces due to the orbital accelerations, and lift forces resulting from the asymmetrical velocity distribution around the vehicle on the seafloor. Another force, which has been studied for the case of a vertical pile, is a lateral oscillatory force due to eddies shedding alternately on one side of the pile, then the other. This was not considered significant for the more bluff-shaped nonsymmetric vehicles under study.

73. As a wave propagates from deep water to shore, it undergoes transformations due to the influence of the bottom. The most important transformations arise from refraction, shoaling, and breaking. Wave

refraction or the bending of the wave crest toward alignment with the contours was neglected due to the two-dimensional interpretation of the bathymetry. However, for a particular site study it would probably be necessary to investigate refraction due to its effect on wave heights and wave approach. The effects of vehicle orientation as a function of wave approach were studied by rotating the vehicle to different bearings with respect to a wave front approaching parallel to shore. Shoaling, an increase in wave height as it travels shoreward, is caused by wavelength decrease due to a decrease in wave celerity as the wave propagates into shallow water. Since the period remains constant and energy flux is conserved, the wave amplitude increases. Finally, the wave crest cannot sustain any further increase in height and the wave breaks. Various forms of breaking waves can exist and the type is dependent on bottom slope, deepwater wave steepness, and the ratio of deepwater wave height to the deepwater wave length. The depth at which breaking occurs is roughly equal to the wave height that exists upon breaking. The previously discussed orbital motion is changed to a translatory motion, and a large portion of wave energy is expended in this zone.

74. After the wave has broken, there is a further translation of water mass shoreward, usually in the form of a bore, which gradually dissipates as it runs up the beach slope. This region will be identified as the broken wave zone.

75. Current forces. The second type of force is that due to currents and can be developed by a variety of causes. Some currents, such as tidal currents, may be oscillatory in nature, but their rate of change is sufficiently slow so that their application can be considered steady-state in contrast to wind-wave orbital velocities. Tidal currents in the deep ocean and shelf areas are very low speed, usually less than 1 fps. Those near inlets and bay mouths can be much faster, though usually not greater than 6 fps. Wind stress on the water surface can generate currents as well. Wind waves breaking at an angle to shore set in motion currents moving parallel to shore in the surf zone. These currents can sometimes be deflected oceanward where they become identified as rip currents. Currents can develop due to water density

variations, turbidity, and thermohaline circulations. Also, more permanent currents of the deep ocean, such as the Gulf Stream current, can be included in this group. The net result of these steady currents is to produce the velocity-related forces of drag and lift.

76. Hydrostatic forces. The third type of force is hydrostatic force, which is determined by the fluid weight and depth. For this study, the horizontal hydrostatic pressure distributions are neglected since they have a net force of zero on the submerged or partially submerged vehicle. However, the vertical force of buoyancy, which reduces the inwater weight of the vehicle by the weight of the fluid displaced is important to dynamic considerations.

Analysis of forces

77. An examination of the literature concerning wave forces in the underwater environment or nearshore zone reveals that most of the work performed has related to structural members of symmetrical shape, such as cylindrical piles, which extend through the water column, or to shore protection works such as vertical walls. The basic approach to calculating wave forces on underwater vehicles was finally derived from elements of the above types of studies. Calculating forces of the deep water to the point of wave breaking was based on the Morison equation,[29] originally developed for computing forces on piles. Breaking wave force equations were developed from studies of wave breaking forces by Carr.[30] Also, information was derived from studies of wave forces on submerged pipelines,[31-33] on small submerged structures,[34] and from results of wind tunnel tests of land vehicles.[35] Another group of force studies has been made on structures that are large with respect to wavelength, such as underwater storage tanks. However, due to the large structure size, there is an interaction between the structure and the wave field, and special methods can be applied based on potential theory. The underwater vehicles under study are small with respect to wavelengths of interest. There has been little work done on forces on small structures on the seafloor, and no information was found about forces on seafloor vehicles. Therefore, force relations were derived from the previously mentioned sources.

78. Forces in the offshore zone. Wave forces calculated for the offshore zone were based on the Morison equation which has drag and inertial components:

$$F = \frac{1}{2} C_D \rho A V^2 + C_m A \frac{dV}{dt}$$

where

F = force, lb

C_D = drag coefficient

ρ = water density (w/g, water unit weight/acceleration due to gravity), lb-sec^2/ft^4

A = surface area normal to the flow, ft^2

V = velocity in the direction of force, ft/sec

C_m = mass coefficient

$\frac{dV}{dt}$ = acceleration in the direction of force, ft/sec^2

To evaluate the above expression, values for the coefficients must be determined, and the velocity and acceleration terms calculated at the depth at which the vehicle is located.

79. Drag and mass (or inertial) coefficients are ideally evaluated experimentally for specific hydraulic conditions and object shapes and orientations. Most drag coefficient data for objects such as vehicles are determined from wind tunnel tests; however, the flow field for these tests is normally steady, unlike the oscillatory velocity field in the ocean. Almost all drag coefficient determination tests in oscillatory flow have been made for cylindrical piles or suspended spheres. However, if the oscillatory orbit is long, as it is for large waves and long periods, steady-state tests should give a good approximation for drag coefficients in oscillatory flow if the model and prototype Reynolds numbers are similar. The mass coefficient is related to the size, shape, and orientation of a submerged body and represents the additional fluid mass that must be accelerated with the body. This coefficient can be determined analytically for two-dimensional ideal flow by use of the potential flow theory. For three-dimensional shapes there are a limited number of sources. For box-like shapes, the work of Herbich and Shank[34]

provides coefficient information for a limited number of cases. The work of Riabouchinski[36] provides some information on the variation of the mass coefficient with relative dimensions, but only for two-dimensional cases. A large variety of data were synthesized to determine coefficients for the undersea vehicle.

80. To evaluate the Morison equation, values for the velocity and acceleration terms must be estimated. There are several theories available to determine the wave-induced kinematics under idealized waves. The simplest is called the Airy Theory. Investigators[37,38] have shown that the particle velocity near the sea bottom is best predicted by the Airy Theory. The development of this theory can be found in Ippen.[39] More complex theories provide better approximations to the surface shape of the wave or take mass transport into consideration, but these quantities are not of major interest for this study. Also, the difficulty in evaluating the drag and mass coefficients precludes at this time using a more complex theory.

81. Equations for the water particle velocity V and acceleration $\frac{dV}{dt}$ are

$$V = \frac{\pi H}{T} \frac{\cosh 2\pi \frac{(d+z)}{L}}{\sinh 2\pi \frac{d}{L}} \cos \theta$$

$$\frac{dV}{dt} = \frac{2\pi^2 H}{T^2} \frac{\cosh 2\pi \frac{(d+z)}{L}}{\sinh 2\pi \frac{d}{L}} \cos \theta$$

where

H = deepwater wave height, ft

T = wave period, sec

d = water depth, ft

z = depth to location of velocity and acceleration of interest (referenced to water surface, negative downward), ft

L = wavelength at depth d, ft (determined from $L/L_o = \tanh 2\pi d/L$ with $L_o = 5.12T^2$ = deepwater wave period)

θ = phase angle, deg

It is seen that the velocity and acceleration are 90 deg out of phase. Experimental data by Wiegel et al.[40] have shown that in actual wave structure interaction, especially as depths become shallower, the

horizontal inertial force tends to occur nearer the wave crest, where $\theta = 0$ deg, the time of maximum drag force. Therefore, in this study the individual maximums of the drag and inertial forces were summed for the maximum total frontal force on the vehicle. Also, since the force function is sinusoidal, there will be an oscillation in the direction of force application, with one maximum in a shoreward direction and another in the offshore direction during one wave cycle. Therefore, in regard to power requirements, if the vehicle is moving onshore or offshore, movement will be aided half the time and impeded the other half. The average force over a one-half cycle period will be 0.636 times the maximum force.

82. The lift force is defined similarly to the drag force and will be directed upward for a seafloor vehicle. The relation is

$$F_L = \frac{1}{2} C_L \rho A V^2$$

where

C_L = lift coefficient

ρ = water density, lb-sec^2/ft^4

A = frontal area, normal to the velocity, ft^2

V = velocity, as defined previously, ft/sec

Once again, little empirical data are available for defining the lift coefficient of a body in oscillatory flow. Work on pipelines on the seafloor[41] does provide some guidance for choosing coefficients. The lift force depends on the proximity of the object to the seafloor; that is, how "tight" the vehicle is to the bottom and how much flow can occur between the vehicle bottom and the seafloor. The more "leakage" in this region, the smaller the lift force. Vehicle shape is also an important factor. For example, Beckman[31] suggests $C_L = 0.5$ for a circular pipe lying on the bottom, but for a pipe of trapezoidal cross section he suggests $C_L = 0.0$. Wilson and Reed[41] in a discussion of Beckman's work recommend $C_L = 1.0$ for a circular pipe. It appears that for most of the relatively rectangular-shaped vehicles involved in the study, the lift coefficients would be very low, on the order of 0.1 to 0.2.

83. Breaking wave forces. The preceding discussion concentrated on forces in the offshore zone. Once the wave reaches the point of breaking, wave theories do not completely describe the water particle motion because of the extreme turbulence and vorticity. There are, however, empirical approaches in analyzing forces in the breaker zone. Much work has been performed to determine forces on seawalls subjected to breaking waves.[42-45] One drawback, when considering this particular study, is that past studies for the most part determined the maximum dynamic pressure on a solid wall that projects from the bottom through the water surface. This peak pressure is a shock pressure, usually located above the mean water level and developed from the compression of air entrapped by the breaking wave. Normally the area over which this pressure acts is relatively small; the pressure is of very short duration (less than 0.005 sec) and does not always occur for each oncoming wave; and the probability of occurrence is reduced as the water surface becomes rougher. The occurrence of a shock pressure on a vehicle of the type under study would appear remote due to the relatively irregular shape of a vehicle when compared with a flat wall, and the fact that the vehicle may be completely submerged for many of the larger wave conditions. An estimation of breaking wave depth can be made using $D = 1.3H$, with H = breaker height and D = depth at breaking. For an 8-ft breaker height, the depth would be 10.4 ft, a depth greater than most vehicle heights. The 8-ft breaker height relates approximately to a 5- to 6-ft deepwater height. So for the very large wave conditions considered in some scenarios of this study, the vehicles will probably be below the mean water level.

84. Therefore, neglecting short duration shock forces, the problem remains to analyze the effective force of the breaking wave. Due to the lack of analytical theories to describe the internal velocity and acceleration field in the breaking wave, the application of a Morison-type equation was precluded. Further complications are due to the variety of different forms of breaking waves that exist and are dependent on the beach slope and the wave steepness (deepwater wave height divided by deepwater wavelength). Final recourse was made to a study

of "Breaking Wave Forces on Plane Barriers" by John H. Carr, 1954.[30] Force data for vertical walls for various beach slopes and wave conditions had been procured from laboratory studies. The approach of this study was suitable for application to seafloor vehicles because, Carr states:

> Since these short-duration high intensity pressures appear in some respects to be unrealistic as the basis for design, this investigation approached the problem by determining the force-time history during the entire wave cycle to permit the evaluation of other aspects of the force function than the singular one of initial impulse.

85. The approach used was based on a momentum method using the solitary wave theory. Force measurements indicated good agreement with an analytical calculation of the momentum. The expression for the momentum of a breaking solitary wave is

$$U_b = 55.5\ H_b^{5/2}$$

where

U_b = momentum, lb-sec/ft (fresh water)

H_b = breaker height, ft

For seawater,

$$U_b = 56.9\ H_b^{5/2}$$

The test results were presented in a variety of plots for constant beach slope as shown in Figure 12. The ordinate and abscissa of the plots are $FT/2U_b$ and H_o/T^2, respectively, where F = maximum force in lb/sec, T = wave period, U_b = momentum (as defined previously), and H_o = deepwater wave height. An examination of the plots shows the scale of the data points beneath the envelope curves. A trend is seen most readily for the variation of $FT/2U_b$ with beach slope among all the data plots. An expression for this variation was determined to be

$$\frac{FT}{2U_b} = 8.0 - 29.3m$$

where m = beach slope. There is also a trend for reduction of $FT/2U_b$ with increasing H_b/T^2, but this was not quantified due to the data

scatter. Knowing the wave momentum U_b, wave period T, and slope m, the force per foot could be calculated. To compensate for the fact that the vehicle might not extend through the water surface as the wall did for the experimental data, a linear force distribution was assumed with the applied force equal to the total wall force multipled by the ratio of vehicle height to total depth. The force distribution assumed was based on an amalgamation of various observations, some of a contradictory nature. For example, the force distribution prediction on a wall according to Minikin[46] shows exponential decay with depth from the water surface, with the maximum force occurring at the mean water level (not the surface water level). According to Miller et al.,[47] the maximum force can be close to the bottom depending on breaker type. In solitary wave theory, sometimes used to approximate the velocity field of a wave just before breaking, the velocity distribution varies from a maximum at the water surface to a value of about one-third the maximum at the bottom.[48] These three examples illustrate a wide variety of ways in which the force distribution might exist in a breaking wave. The force distribution used in this study varied from 0.5 times the average force at the bottom to 1.5 times the average force at the surface. It should be noted that the surface elevation as the wave breaks is not the depth plus one-half the breaker height but is the depth plus 0.75 times the breaker height because a greater portion of the breaking wave is above the mean level.[49]

86. If the vehicle is submerged in the breaker zone, a lift force is to be expected and the velocity to be applied for the lift equation is calculated from an expression based on the solitary wave theory[48]

$$V = 0.534\ g(d + H)$$

where

g = 32.2 ft/sec^2

d = water depth, ft

H = breaker height, ft

87. Broken wave forces. After the wave has broken, the wave height will attenuate with decreasing depth. Relations from Horikawa and Kuo[50] and from Nakamura[51] have been combined by Silvester[49] to an express attenuated wave height H_b' as

$$H_b' = \frac{H_b\ (0.87)D}{DB} + 0.12$$

where

H_b' = breaker height, ft

D = depth, ft

DB = depth of breaker, ft

The proportion of the attenuated wave height above the mean water level AC is derived from curves by Iwagaki[52]

$$AC = H_b' \left[0.94 - (5.26\ \frac{D}{L_o})\right]$$

where L_o = deepwater wavelength, in feet. The maximum pressure of broken waves against a wall is at the mean water level and is represented by[50]

$$P = \frac{KwC^2}{2g}$$

where

K = experimental constant taken as 2.0 (Hayashi and Hattori[53])

w = unit weight of water, lb/ft^3

C = wave velocity at given depth, ft/sec

g = 32.2 ft/sec^2

Wave velocity in shallow water, according to Iwagaki,[52] is

$$C = C_o \left[0.05 + 2.5\ (\frac{D}{L_o})^{0.525}\right]$$

where

C_o = deepwater wave velocity, ft/sec

d = depth, ft

L_o = deepwater wavelength, ft

Combining the previous two equations produces an expression for the maximum pressure

$$P = \frac{gwT^2}{2\pi^2} \left[0.05 + 2.5(\frac{D}{L_o})^{0.525}\right]^2$$

Iwagaki[52] recommends a triangular pressure distribution, which was used to compute the total force on the vehicle in the broken wave zone. Lift forces were calculated if the vehicle was submerged.

The computer program

88. A computer program was developed to provide the necessary hydraulic force data for use in describing bottom-crawling vehicle performance. The range of interest extended to the 150-ft contour. The three previously discussed zones were determined by the location of the breaker zone for the given deepwater wave height, wave period, and bottom slope. To determine the location of breaking waves, an expression of LeMéhauté and Koh[54] was used to determine the breaker height H_b as

$$H_b = H_o \left[0.76 \left(S \cos \alpha_b\right)^{1/7} \left(\frac{H_o}{L_o}\right)^{-1/4}\right]$$

where

H_o = deepwater wave height, ft

S = general bottom slope, percent

α_b = breaker angle with the shoreline, deg

L_o = deepwater wavelength, ft

In this study only waves with $\alpha_b = 0$ were considered, i.e., the wave crest approached parallel to the shore. With the breaker height H_b known, the water depth d_b at the location of the breaking wave was determined from Collins's[55] equation:

$$d_b = \frac{H_b}{0.072 + 5.6S}$$

with variables as identified previously. A zone in which the breaking wave forces would act was then calculated by Galvin's[56] relationship between breaker height H_b, slope S, and zone width x_p as

$$x_p = (4.0 - 9.25S)H_b$$

The depth at the shoreward end of this zone was then calculated, and the breaking wave forces were evaluated at each end of the zone.

89. Knowing the breaker location and slope, the distance to the 150-ft depth was calculated and divided into 10 increments at which force calculations were performed. Likewise, the width of the broken wave zone was calculated and divided into five increments. Thus, force data were calculated at 17 locations (or stations). A summary of the conditions for which force calculations were made is shown in Table 5.

Discussions of results

90. The first tabulation in Figure 13 shows a representative computer printout for the forces on the seafloor transport vehicle 2, scenario D with the environmental parameters as shown. Stations 1-5 represent locations in the broken wave zone at the depths shown in the second column. The broadside and frontal forces increase with depth as the vehicle becomes submerged. Finally, at station 5, the vehicle becomes submerged and a lift force becomes evident. Stations 6 and 7 are the two locations at which breaker forces are calculated. It is seen that the maximum force for the scenario occurs in this zone. This is usually the case, except for some combinations of low-wave and low-bottom slope conditions where maximum forces occur at station 5 when the vehicle surfaces or nearly so. Once the vehicle is completely submerged the broadside force becomes constant. The maximum lift force occurs in the breaker zone unless the vehicle is not submerged; then the maximum occurs at station 8 in the offshore zone. The offshore zone, stations 8-17, shows decreasing forces as the depth increases. The second tabulation in Figure 13 shows the computed velocities, accelerations, wave heights, and wavelengths as the depth varies in the offshore zone (where the same vehicle and sea-state conditions were used for both tabulations). Table 6 shows the coefficients chosen to determine the forces in this zone.

91. The computer program was run for other scenarios and vehicles in the same manner as discussed above. One other variable included in the force calculations was the vehicle's heading angle. The following headings were used in the detailed force calculations: 0 deg (direction normal to the shoreline), 15 deg from this normal, and 90 deg (or parallel to shore). The 15-deg angle was chosen because this was

believed to be a reasonable allowable variation (±15 deg) in heading the vehicle through the breaker zone in order to minimize the possibility of overturning. The 90-deg heading was selected since the vehicle in this orientation would likely be most susceptible to overturning.

92. For the survey vehicle, the coordinates of points for a series of graphs of frontal, lift, and broadside forces versus variations in the environmental parameters were developed by exercising the water force calculations submodel of STAM over a range of environmental parameter values; the resulting relations are shown in Figure 14. From Figure 14a, the survey vehicle receives the greatest frontal and lift forces for a heading of 55 deg. The force versus deepwater wave height plot in Figure 14b shows an expected result of increasing frontal force with increasing wave height. This increase becomes linear when wave height reaches 2.5 ft, the value of H that corresponds to the vehicle's becoming completely submerged. The lift force also increases with wave height. The steady current (broadside) force remains constant for wave height variation. In Figure 14c, frontal force versus wave period shows a hyperbolic variation (or F is proportional to 1/T) because of the nature of Carr's relationship in the breaker zone. Lift shows an increase with wave period while current force is independent of period. Frontal force and lift are independent of current velocity as shown in Figure 14d. Finally, in Figure 14e the variation of frontal force shows an increase with the general bottom slope.

93. In Table 5, as the environmental conditions in general become more severe the slope used is also more severe, indicating that the worst environmental conditions, scenario H for each vehicle, should produce an upper bound for the forces. At the other end, scenario A, which has a very mild slope, would probably have considerable frictional dissipation due to the large horizontal distances, especially in the shallow water region, so forces there should provide a maximum lower bound since frictional dissipation was not considered.

Accuracy of results

94. The evaluation of the calculated forces in each of the zones is a difficult topic. In the offshore zone, the velocity and

acceleration calculations are sufficiently accurate for good force estimates; however, the evaluation of the force coefficient is subjective for the most part without detailed drawings of each vehicle, and even with that information it would be a difficult task to determine coefficients without actual model testing or prototype measurements. The direct addition of the maximum drag and inertial components of force should produce results on the conservative side for this zone.

95. Forces in the breaker zone are also difficult to evaluate in terms of accuracy without actual testing. An examination of model testing of pipeline on the seabottom by Castiel[33] showed that breaking wave forces on the pipeline were approximately double that measured for a similar size wave and period in a nonbreaking wave test. The water force calculations submodel of STAM produced the same order of force ratio or greater for the example vehicle problems. This reasoning, coupled with taking the frontal surface area of a vehicle as being a vertical solid wall when the vehicle was on level ground, indicated that the STAM-computed results are slightly conservative, especially in light of tests with inclined walls, which showed that for a 30-deg inclination, forces were halved when compared with a vertical wall. Due to the difficulties in analyzing forces in this region more exactly, model testing or field testing would produce more confident results. Also, the following example should give some perception of the nature of large breaking wave forces. Concrete blocks of 100 tons, placed alongside the Humboldt jetties in California, were lost and could not be located due to breaking waves on the order of 40 ft in height. This is comparable to breaking conditions for the trencher in scenario H. Also, model studies indicated that breaker heights as low as 22 ft could dislodge the blocks.*

96. Finally, accuracy of the STAM-predicted water force values depends on the magnitudes of all the force-causing agents discussed

---

* Personal communication with D. D. Davidson, Chief, Wave Research Branch, Wave Dynamics Division, Hydraulics Laboratory, WES.

earlier in this section that were not included in STAM's water force calculations submodel, but which may contribute to the actual forces on a seafloor vehicle, depending on the total three-dimensional environment.

Vehicle Trafficability in the Nearshore Environment

The Army Mobility Model

97. By far the most significant advance that has taken place since publication of Reference 1, as far as making it possible to describe nearshore vehicle trafficability is concerned, has been the development and successful use of the U. S. Army Mobility Model (AMM), (References 26, 27, 57, and 58). Basically, AMM is a computerized, mathematical model designed to predict quantitative vehicle performance either on- or off-road by means of fundamental physical laws and relations peculiar to the terrain-vehicle-driver system. The relations in AMM have been developed and validated by many man-years of research and testing, both in the laboratory and in the field. Designed to predict terrestrial vehicle performance, AMM has subroutines that can be used to describe most important aspects of nearshore vehicle trafficability performance--ability to negotiate soft soil, develop drawbar pull,* climb slopes, and override obstacles.

Vehicle ability to traffick the seafloor

98. The subroutines just mentioned are included in the "soils submodel" of Reference 26. In terrestrial applications of this submodel, interest usually centers on predicting vehicle speed-made-good between two specified geographical locations, and secondarily on obtaining GO or NOGO answers to questions of the type, "Can the M48 tank

---

* For tracked vehicles, drawbar pull is the component, acting through the drawbar pin and parallel to the direction of vehicle travel, of the resultant of all soil forces acting on the vehicle. It is positive when the vehicle can perform useful work (pull a load), negative when external force must be applied to maintain vehicle motion, and zero when tractive force from vehicle/soil interaction is just sufficient to allow the vehicle to move.

(a) traffick clay soil of 40 cone index? (b) climb a slope of 25 percent? (c) develop 10,000 lb of drawbar pull? and (d) override a 3-ft obstacle?" For the bottom-crawling applications of interest herein, the situation is just the opposite. Speeds are so low that speed-made-good determinations are usually of secondary interest; it is often more crucial, however, to be able to predict GO or NOGO for a specified vehicle pull requirement and a particular seafloor condition.

99. Not surprisingly, then, a sizeable number of new computer instructions had to be written to interact with and extract desired information from applicable subroutines of the AMM soils submodel, thus producing a new submodel that makes the type predictions of interest herein. The name of this new submodel is the "tracked vehicle, bottom-crawling trafficability submodel," or more simply, the "trafficability submodel." A detailed listing of computer instructions for the trafficability submodel was included among those of the STAM computer routines mailed to the project sponsor. The major functions of the trafficability submodel are to predict in quantitative terms the ability of a bottom-crawling tracked vehicle to (a) negotiate soft soil, (b) develop drawbar pull, (c) climb a slope, and (d) override an obstacle. It is important to examine in detail the approach that the STAM trafficability submodel uses to predict these four aspects of vehicle trafficability performance.

100. Basis of trafficability submodel predictions. Relative to items (a)-(d) in the preceding paragraph, it is convenient, first, to determine whether vehicle/obstacle geometry interference provides a GO or NOGO situation, and then (provided a GO answer is obtained) to determine whether tractive force available from the vehicle/soil interaction is sufficient to satisfy the tractive force requirements of items (a)-(d).

101. To predict vehicle ability to override an obstacle, the trafficability submodel utilizes subroutine OBSTCL modified from

Reference 26.* This subroutine checks first to determine whether or not vehicle hangup occurs because of the relative geometries of the vehicle and the obstacle. For tracks with semicircular ends encountering an obstacle with a 90-deg approach angle, maximum slope height negotiable is one-half the track height. For all other conditions, prediction of geometric interference is more complex and requires comparing the geometric outlines of the vehicle and the obstacle relative to one another as the vehicle attempts obstacle override. The number of parameters required to describe the geometry outlines of the vehicle and the obstacle (Figures 10 and 2, respectively), together with the number of ways that geometry interference can occur, is so large that geometry interference for each vehicle/obstacle combination ordinarily must be evaluated on an individual basis. The trafficability submodel considers only the situation where both tracks of a vehicle encounter the same obstacle squarely and override it point-for-point in the same way, i.e., only two-dimensional bench-type obstacles of length greater than the vehicle width are considered.**

102. The following relations are used by the trafficability submodel to determine whether tractive force available from vehicle/soil interaction is sufficient to satisfy drawbar pull and tractive force requirements of items (a)-(d) in paragraph 99:

$$\text{Available DBP} = \text{DBP} \cos \theta \tag{1}$$

$$\text{Available TF} = (\text{DBP} + \text{SMR}) \cos \theta \tag{2}$$

$$\text{Required } TF_1 = \text{SMR} + \text{VEW} \sin \theta + \text{Required DBP} \tag{3}$$

$$\text{Required } TF_2 = \text{Required } TF_1 + \text{Required } TF_o \tag{4}$$

---

* A detailed listing of computer instructions for subroutine OBSTCL was included in the listing for the trafficability submodel mailed to the project sponsor.

** The vehicle stability submodel described subsequently herein deals also with discrete (as opposed to bench-type) obstacles, where a given obstacle is narrow enough so that only one of the vehicle's tracks contacts the obstacle during obstacle override.

where

DBP = drawbar pull, lb

θ = seafloor local slope, deg

TF = tractive force, lb

SMR = soil motion resistance, lb

VEW = vehicle effective weight, lb

TF_o = tractive force required for obstacle override, lb

Available drawbar pull DBP is the force that the vehicle can develop parallel to the direction of vehicle travel (relative to both the horizontal and the vertical planes) in excess of that force required for the vehicle to overcome prevailing resistances to motion, i.e., DBP is net TF available to do useful work (pull or push a load, etc). Vehicle effective weight is the actual vehicle weight that prevails at a given level of vehicle submergence and ranges from in-air to submerged gross vehicle weight. VEW sin θ is the component of VEW that acts parallel to a seafloor inclined θ deg to the horizontal.

103. On the basis of the relations in paragraph 102, the least demanding situation in terms of required TF is for a vehicle to operate on a flat seafloor with zero drawbar pull required (i.e., the vehicle must be able to move under its own power but is not required to develop any additional pull). In this case, required TF = required TF_1 = SMR. The most demanding situation is for a vehicle to climb a slope, pull or push a load (develop a required drawbar pull), and override an obstacle, all at the same time. In this case, required TF = required TF_2.

104. In applying Equations 1-4, values of θ and required DBP are usually known for a given vehicle/scenario combination, and the value of VEW can be computed by the water force calculations submodel of STAM for a given vehicle and water depth. With values of θ, required DBP, and VEW known, predictions of available DBP and TF and of required TF_1 and TF_2 are defined by predicted values of DBP, SMR, and TF_o. The STAM trafficability submodel was developed to make these predictions.

105. Relative to predicting DBP and SMR, the trafficability submodel uses one approach for fine-grained soils (clays) and another for coarse-grained soils (sands). For the purposes of this study, weak

cohesive soil (mud) was treated as a very low-strength fine-grained soil; coral, cobbles and boulders, and hard rock were all considered as very high-strength fine-grained soils. Among the scenario ground materials then, loose sand was the only coarse-grained soil.

106. Dealing first with the fine-grained soils, the first decision was to choose which of the several options in the AMM soils submodel should be used in the STAM trafficability submodel. The wet-wet option was selected because it is the most conservative one in AMM that describes the influence of soil surface slipperiness on tracked vehicle performance. That is, the wet-wet option accounts for the fact that available DBP and TF are reduced by soil surface slipperiness.

107. The basic soil/vehicle parameter that the trafficability submodel uses to predict DBP and SMR for fine-grained soils is excess cone index CI_x.* CI_x is defined as scenario cone index CI_s minus VCI_1 (or VCI_{50}, as appropriate). That is, CI_x is the excess cone index above that value required for the vehicle to be barely able to propel itself. With no account taken for the effects of soil surface slipperiness, available DBP_{20}/VEW (i.e., drawbar pull coefficient at 20 percent slip) for one vehicle pass is predicted as a function of CI_x as follows:

$$\frac{DBP_{20}}{VEW} = 0.544 + 0.0463\ CI_x - \sqrt{(0.544 + 0.0463\ CI_x)^2 - 0.0702\ CI_x} \quad \text{for } \frac{VEW}{2 \times TL \times TW} < 4 \text{ psi} \tag{5}$$

and

---

* RCI_x ordinarily is used instead of CI_x in computing available DBP_{20}, where RCI_x = excess rating cone index $\cong$ RCI - VCI_1. RCI is rating cone index, which is the product CI x RI, with RI = remolding index. RI is the ratio of CI measured after remolding a soil sample to CI measured before remolding. Computing RCI for nearshore trafficability purposes requires obtaining a seafloor soil sample and testing it under conditions closely matching those of the soil in place, a process which the present state of the art does not allow for seafloor soils.

$$\frac{DBP_{20}}{VEW} = 0.4554 + 0.0392\ CI_x - \sqrt{(0.4554 + 0.0392\ CI_x)^2 - 0.0526\ CI_x}$$

$$\text{for } \frac{VEW}{2 \times TL \times TW} \geq 4 \text{ psi}^* \qquad (6)$$

The trafficability submodel accounts for soil slipperiness effects on DBP_{20}/VEW available to a tracked vehicle with grousers (i.e., without road pads) by the following scheme:

a. For $CI_x < 20$, Equations 1 and 2 are used.

b. For $20 \leq CI_x \leq 100$, DBP_{20}/VEW is predicted as the average of DBP_{20}/VEW from Equations 1 or 2 and $(DBP_{20}/VEW)_{low}$, computed as

$$\left(\frac{DBP_{20}}{VEW}\right)_{low} = 0.1 \left(\frac{100}{CI_x}\right)^{1.059} \qquad (7)$$

c. For $CI_x > 100$, DBP_{20}/VEW is predicted as the average of DBP_{20}/VEW from Equations 1 or 2 and $(DBP_{20}/VEW)_{low} = 0.1$.

Figure 15 illustrates the relation of predicted DBP_{20}/VEW to CI_x based on the scheme described above.

108. Soil motion resistance coefficient, SMR/VEW, is predicted for one vehicle pass by the trafficability submodel as a function of CI_x as follows:

$$\frac{SMR}{VEW} = 0.045 + \frac{2.3075}{CI_x + 6.5} \text{ **} \qquad (8)$$

---

* For many-pass tracked vehicle performance, the relations corresponding to Equations 5 and 6 are:

$$\frac{DBP_{20}}{VEW} = 0.419 + 0.0146\ CI_x - \sqrt{(0.419 + 0.0146 CI_x)^2 - 0.021\ CI_x}$$

for tracked vehicles with grousers greater than 1-1/2 in.

and $$\frac{DBP_{20}}{VEW} = 0.425 + 0.146\ CI_x - \sqrt{(0.425 + 0.0146\ CI_x)^2 - 0.0198\ CI_x}$$

for tracked vehicles with grousers less than 1-1/2 in.

** For many-pass tracked vehicle performance, the relations that correspond to Equation 8 are:

$$\frac{SMR}{VEW} = 0.6 - 0.00885\ CI + \sqrt{(0.6 - 0.00885\ CI)^2 + 0.001\ CI + 0.027}$$

for tracked vehicles with GVW of 75,000 lb or more

$$\frac{SMR}{VEW} = 0.4167 - 0.01052\ CI + \sqrt{(0.4167 - 0.01052\ CI)^2 + 0.1886}$$

for tracked vehicles with GVW of 10,000 lb or less

Note that in these two equations, cone index CI, not excess cone index CI_x is used.

Equation 8 applies to all tracked vehicles with grousers operating in fine-grained soils. Figure 16 illustrates the relation of predicted SMR/VEW to CI_x described by Equation 8.

109. For tracked vehicles operating in coarse-grained soils, the trafficability submodel predicts DBP_{40}/VEW (drawbar pull coefficient at 40 percent slip) and SMR/VEW as follows:

$$\frac{DBP_{40}}{VEW} = 0.50 \tag{9}$$

$$\frac{SMR}{VEW} = 0.100 \tag{10}$$

Equations 9 and 10 apply for tracked vehicles with flexible suspensions; Equations 11 and 12 apply for tracked vehicles with rigid (girderized) suspensions.

$$\frac{DBP_{40}}{VEW} = 0.56 \tag{11}$$

$$\frac{SMR}{VEW} = 0.074 \tag{12}$$

110. Using predictions of available DBP at 20 percent slip for fine-grained soils and available DBP at 40 percent slip for coarse-grained soils is conservative because available DBP increases slightly in both of these types of soils as tracked vehicle slip increases from about 15 to 100 percent. The relations in paragraphs 107 and 108 for tracked vehicle operation in fine-grained soils are defined in terms of CI_x, a parameter that lends itself to analysis of the effects of soil and vehicle parameters on vehicle performance. The relations in Equations 9-12 for tracked vehicle operation in coarse-grained soils are rather simplistic and are based on evaluated data from a limited amount of full-scale tracked vehicle testing in dry-to-moist sands. For the range of operational conditions of likely interest for nearshore applications, however, Equations 9-12 are adequate, as verified by the following observations.

111. An extensive laboratory investigation of model track performance in dry sand has revealed that DBP_{20}/VEW and SMR/VEW can be predicted

as functions of the dimensionless prediction term $N_s = [G(TW \times TL)^{1.5}/VEW]\left(VEW/VEW_t\right)^{0.5}[d/(TL/2)]^n$ .59 Here, N_s is the sand-track mobility number; G is the gradient, or slope, of a cone index versus penetration depth curve; VEW/VEW_t is assigned a value of 0.4 for tracked vehicles with flexible suspensions, 1.0 for those with rigid (girderized) suspensions; d is the distance from the center of the vehicle rear road wheel to a vertical line through the vehicle's center of gravity (with the vehicle resting on a flat, level, rigid surface); and n = 0.5 for $d < TL/2$, n = 1 for $d = TL/2$, and n = 3/2 for $d > TL/2$.

112. To demonstrate the compatibility of predicted in-sand tracked vehicle performance provided by Equations 9-12 and by the relations in Reference 59, consider, first, that Reference 59 shows that values of DBP/VEW remain nearly constant as track slip increases from 20 to 100 percent for N_s values larger than about 50. Thus, values of DBP_{40}/VEW in Equations 9 and 11 can be taken as comparable to those of DBP_{20}/VEW in Reference 59 if $N_s \geq 50$. Next, in Reference 59, 95 percent confidence limits on the relation of DBP_{20}/VEW to N_s at $N_s = 50$ include values of DBP_{20}/VEW from 0.50 to 0.56 (i.e., these limits include values of DBP/VEW from Equations 9 and 11). Further, there is reasonable agreement between predicted values of SMR/VEW for $N_s \geq 50$ in Reference 59 and values of SMR/VEW of 0.100 and 0.074 in Equations 10 and 12. Finally, from Reference 59, values of DBP_{20}/VEW increase slightly and values of SMR/VEW decrease slightly as N_s increases beyond about 50. Overall, then, there is good agreement between results obtained by (a) the equations used by the present version of the trafficability submodel to predict DBP_{40}/VEW and SMR/VEW for tracked vehicles operating in coarse-grained soils (Equations 9-12), and (b) the relations of DBP_{20}/VEW and SMR/VEW to N_s, if the vehicle/scenario combination of concern is described by $N_s \geq 50$.

113. The one value of G considered in the example selection problems is G = 10 psi/in., which may be considered a lower limit likely to be encountered in actual situations. Combining this value of G with the TW, TL, VEW, and d values that resulted from applying the vehicle design guidelines in Table 3 for the five example vehicles produced

values of N_s from 98 to 204. This indicates that the use of vehicle parameter values defined by Table 3 guidelines in combination with even small values of G ordinarily will produce values of N_s much larger than 50.

114. The first step in predicting tracked vehicle DBP and SMR performance in nearshore regions of coarse-grained soil should be to determine the N_s value defined by the vehicle/scenario condition of concern. Nearly always, $N_s \geq 50$, will be obtained. In this event, it is reasonable to use Equations 9-12 to predict DBP and SMR for tracked vehicles in coarse-grained soils. In the unlikely event that a value of $N_s < 50$ is obtained, the vehicle designer can predict DBP_{20}/VEW and SMR/VEW as functions of N_s from relations in Reference 59.

115. The relations in Equations 9-12 describe DBP and SMR performance to be expected from tracked vehicles operating in dry-to-moist sands, not submerged sands that may present special problems for heavy tracked vehicles. There is mixed evidence from actual experience concerning the effects on tracked vehicle performance caused by submerging a sand. From tests of a 1/6 model tracked vehicle in dry, moist, and submerged sand, Reference 60 showed that submerging the sand caused drawbar pull performance to worsen noticeably. On the other hand, the Soil Mechanics Department, Delft Institute, Holland, has found from field experience that conventional tracked vehicles can successfully traffick freshly deposited (saturated) sandy and sandy silt dredged material of extremely low strength. To the present, enough tracked vehicle tests (model or full-scale) have not been conducted in submerged, loose sand to develop a proven methodology for predicting vehicle performance for this soil condition. For the purposes of this study, it is recommended that predicted values of available DBP and SMR from Equations 9-12 be used, but that they be considered tentative and possibly somewhat optimistic.

116. Paragraphs 106-108 and 109-115 have presented equations and pertinent considerations relative to predicting DBP and SMR for tracked vehicles operating in submerged fine-grained soils and in submerged coarse-grained soils, respectively. From paragraph 104, the one

parameter not considered to this point that must be predicted to allow a full description of available DBP and TF and required TF_1 and TF_2 (in Equations 1-4) is required TF_o, tractive force required for obstacle override. The OBSTCL subroutine of AMM determines whether available tractive force is sufficient for obstacle override by determining the maximum angle that the vehicle can climb VA and comparing this angle with the obstacle approach angle A. If VA $\geq$ A, obstacle override is possible; if VA < A, it is not. As modified for use in the STAM trafficability submodel, subroutine OBSTCL still checks VA against A, and if VA < A, predicts that the vehicle cannot override the obstacle. If VA $\geq$ A, however, modified subroutine OBSTCL iterates to determine the value of TF_o that causes VA = A; i.e., subroutine OBSTCL in the STAM trafficability submodel determines the minimum value of TF_o required for obstacle override.

117. Analytical determination of required TF_o is very complex because for a single vehicle/obstacle/scenario situation, subroutine OBSTCL evaluates the possibility of obstacle override for several vehicle/obstacle orientations by means of a different set of equilibrium equations for each orientation. These sets of equations were not designed to solve for required TF_o, and, in fact, computer iteration is the only practical way to obtain a solution. Thus, each vehicle/obstacle/scenario situation must be evaluated on an individual basis to determine required TF_o. The relation of required TF_o to obstacle height in Figure 17 is representative and was obtained by exercising the OBSTCL subroutine for example vehicle 2 (the seafloor transport vehicle), zero seafloor slope, and a range of obstacle heights for an obstacle with a 105-deg approach angle.

118. Example application. Illustration of how the STAM trafficability submodel can be applied and its performance predictions interpreted is accomplished best by an example application. The computerized trafficability submodel was exercised for all of the example vehicle/scenario combinations (vehicles 1-5, scenarios A-H), so that any one of these combinations could be selected to illustrate the submodel's

application.* Before examining the results of applying STAM's trafficability submodel, however, it is useful to consider the vehicle design and seafloor environment input information required by this submodel.

119. Table 2 and paragraph 62, taken together, list all of the input vehicle design parameters required by the STAM trafficability submodel. Table 7 illustrates for example vehicle 2 the parameters required by this submodel to describe seafloor soil strength and geometry for vehicle 2's scenarios A through H. Eleven columns of information are included in Table 7, described as follows:

(1)	Terrain unit no.:	Enter the scenario letter.
(2)	Terrain unit distance, ft:	Enter a distance equal to at least 10 times the vehicle length
(3)	Surface type:	Enter 1 for fine-grained soil (clay);** enter 2 for coarse-grained soil (sand).
(4)	Surface strength:	Enter the average value of cone index of the seafloor material in the 0-to 6-in. seafloor material depth. For this study, use cone index = 10 S_u for clay (where S_u in Table A1 is shear strength obtained by a vane shear apparatus), and cone index = 3 G for sand (where G in Table A1 is the gradient, or slope, of a cone index versus penetration depth curve).† For coral, cobbles and boulders, and hard rock, enter

---

* For each of three submodels of STAM--the water force calculations, vehicle trafficability, and vehicle stability submodels (Figure 9)--copies were sent to the sponsor of results obtained for all of the example vehicle/scenario conditions.

** Consider coral, cobbles and boulders, and hard rock as fine-grained soils for this study.

† The relations CI = 10 S_u and CI = 3 G are only rough approximations for estimating average cone index values for clay and sand, respectively. Relations are yet to be developed that describe nearshore soil strength in terms that reflect the soils' ability to support vehicle trafficability. Such relations must account for (a) the effect that a layer of water has on soil strength, and (b) the proportion of that soil strength that the soil/vehicle running gear interaction can utilize.

		values of 3000, 4000, and 5000, respectively. (These arbitrarily chosen values of cone index are large enough to cause surface strength not to be a consideration in terms of vehicle trafficability.)
(5)	Slope, percent:	From Table A1, enter the value of local seafloor slope.
(6)	Obstacle approach angle, deg:	Enter 105.* Parameters included in columns 6 through 10 of Table 7 are illustrated in Figure 2. An obstacle angle of 105 deg was considered reasonably severe (i.e., reasonably close to 90 deg) to cause the obstacle override capabilities of the five example vehicles to be sufficiently tested.
(7)	Obstacle vertical magnitude, in.:	Enter the value of "obstacle height" from Table A1.
(8)	Obstacle base width, in.:	Enter a value of 1.5 times the vehicle vertical magnitude. (This guideline was somewhat arbitrary but was intended to produce a WB value (Figure 2) small enough to define a discrete obstacle rather than a transition from a low to a high shelf-type elevation.)
(9)	Obstacle length, ft:	Enter 72. This essentially dummy value was used to define an obstacle much wider than the vehicle (i.e., a bench-type obstacle), the only type obstacle considered by the trafficability submodel.
(10)	Obstacle spacing, ft:	Enter a value slightly larger than the vehicle's length. This guideline causes each obstacle to

* The trafficability submodel of STAM, in conformance with the procedures used in that part of AMM on which this submodel is based, accepts descriptions of obstacle approach angles according to the scheme described in Figure 2. In performing calculations that involve these angles, STAM converts the angle values as appropriate to the calculation at hand. (For example, an angle of 105 deg in some STAM calculations should be treated as (105 - 90) = 15 deg; STAM is programmed to make this conversion automatically.)

		be considered separately as far as the ability of a vehicle to override it is concerned.
(11)	Obstacle spacing type:	Enter 2.

Soil strength and geometry files for the other four example vehicles (1, 3, 4, and 5) were developed using the guidelines described in paragraph 119 and appropriate data from Table A1.

120. With a detailed description of the vehicle/seafloor information required by the STAM trafficability submodel in hand, we examine next an example application of this submodel. The tabulation in Figure 18 for vehicle 2, scenario E is representative of the results obtained in the example applications.

121. Taken together, parameters listed in the first nine lines of the tabulation in Figure 18 (i.e., the header information) identify the vehicle/seafloor condition for which the trafficability submodel was exercised. Values for all but three of these parameters were obtained from Table A1. Values of the remaining parameters are defined as follows:

a. Vehicle submerged weight: See Table 3, "SUBWT" under Water Force Calculations Submodel.

b. Required drawbar pull: See Table 1.

c. Wave period: Two values, 8 and 15 sec, were used for every vehicle/scenario combination.

122. The first three columns of output information from the trafficability submodel further define the vehicle/seafloor condition of concern. In column 1, DL stands for "dry land" and 1, 2, 3, ... are the same station numbers as in the water forces submodel. Accordingly, the first entry under the second column is 0 (for water depth) and, under the third column, is the in-air gross vehicle weight. Succeeding entries under columns 2 and 3 take the same values as in the water force calculations submodel for matching stations (for a given vehicle and scenario). The trafficability submodel is exercised for station DL to whichever first station number causes vehicle effective weight VEW to equal vehicle submerged weight. This is done, because, except for vehicle/obstacle geometrical interference, all types of vehicle

performance predicted by the trafficability submodel change as a function of vehicle weight. Except for using vehicle effective weight VEW (from the water forces submodel), the trafficability submodel describes vehicle trafficability on the seafloor in the same way as it would for trafficability on unsubmerged land.*

123. Entries in columns 4-13 of the tabulation in Figure 18 describe five categories of vehicle performance as predicted by the STAM trafficability submodel:

a. The submodel computes the vehicle's VCI_1 values (column 4) and compares them with the scenario cone index CI_s (listed in the header information). If $VCI_1 > CI_s$, the available soil strength is not sufficient and column 5 lists a "NO" answer; if $VCI_1 \leq CI_s$, column 5 lists a "YES" answer. Note that the value of VCI_1 changes monotonically with vehicle effective weight.

b. The submodel determines whether or not the geometry of the vehicle relative to that of the obstacle will cause a vehicle hangup. If this check indicates no problem, column 6 lists a "GO" answer; if it indicates a hangup, column 6 lists a "NOGO NUMBER" answer, where the number matches the figure number in Reference 57 that illustrates the type of hangup predicted. (For example, Figure 19 illustrates a "type 40" hangup.)

c. The submodel determines the amount of drawbar pull available from the interaction of the seafloor material and the vehicle's running gear and lists this value in column 7.** If available DBP $\geq$ required DBP (from the header information), column 8 lists a "YES" answer; if available DBP < required DBP, column 8 lists a "NO."

d. Column 9 lists the value of required TF_1 computed by Equation 3, and column 11 lists the value of available TF computed by Equation 2 and the appropriate relations from paragraphs 107-109. If available TF $\geq$ required TF_1, column 12 lists a "YES" answer; if available TF < required TF_1, a "NO" answer.

---

* The STAM trafficability submodel accounts for the effects on vehicle performance of only one type of water force, buoyancy (since VEW = in-air vehicle weight minus buoyancy). The STAM stability submodel (discussed subsequently in this report) accounts for the effects on vehicle performance of all four types of water forces--buoyancy, broadside, frontal, and lift forces.

** DBP is sampled at 20 percent track slip for all of the scenario ground materials except loose sand (scenario D); for loose sand, DBP is sampled at 40 percent slip.

e. Column 10 lists the value of required TF_2 computed by Equation 4. If available TF (column 11)^2 $\geq$ required TF_2, column 13 lists a "YES"; if available TF < required TF_2, a "NO."

Stability of the Nearshore Bottom Crawler

124. The STAM stability submodel describes tracked vehicle performance on the nearshore ocean bottom in terms of vehicle ability to (a) resist lateral overturn, (b) resist longitudinal overturn, (c) maintain forward motion, and (d) maintain position on a side slope. A detailed listing of computer instructions for each of these types of performance as described by the STAM stability submodel was included among the STAM computer routines mailed to the project sponsor. Before considering the development and an example application of the four STAM subroutines that describe these types of stability performance, it is important to consider some characteristics that are common to each subroutine.

125. The STAM stability subroutines are realistic in that they account for the cyclic nature of wave action by sampling the magnitude of water forces acting on a seafloor vehicle on a time-dependent basis. These submodels are general in that they describe vehicle behavior for any tracked vehicle/vehicle heading angle/scenario combination. Vehicle heading angle is the angle that the longitudinal axis of the vehicle makes with a straight line drawn perpendicular to the shoreline, where the shoreline is also taken to be a straight line.

126. A large part of the input information required by the STAM stability submodels is a description of water forces acting on the bottom-crawling vehicle, as developed in the water force calculations (WF) submodel. To facilitate the descriptions that follow of the stability subroutines, it is useful to consider some basic features of the WF submodel.

127. For each combination of vehicle, scenario, and vehicle heading angle, the WF submodel computes the values of three types of water forces: frontal force, broadside force, and lift force. Additionally, this submodel subtracts vehicle buoyancy from in-air gross vehicle

weight to obtain vehicle effective weight. These computations are made at each of 17 stations from shoreline outward (first tabulation in Figure 13, for example): 1-5 in the broken wave zone; 6 and 7 in the breaking wave zone; and 8-17 in the offshore zone. As defined in this study, frontal force is that water force acting on the vehicle in a direction perpendicuar to the shoreline. Broadside force acts parallel to the shoreline. As the vehicle heading angle changes, the magnitudes of the frontal and broadside forces change due to changes in vehicle areas projected perpendicular to the directions of the forces. However, the directions of the frontal and broadside forces are considered to remain constant. Thus, for a vehicle heading angle of 90 deg, computed frontal force is actually the force acting on the side of the vehicle and is really a broadside force.

128. In applying the stability subroutines to decide whether a given vehicle can operate under a given scenario, it is useful to consider vehicle performance on a "worst case" basis. That is, for a given combination of vehicle, scenario, and type of stability performance, the appropriate stability submodel is exercised at the one or more combinations of vehicle heading angle, local seafloor slope, station, etc. that are most likely to cause the vehicle not to be able to perform satisfactorily. In each description of a STAM stability subroutine that follows, a description of "worst case" testing is given just after a description of the major computational features of the subroutine.

Vehicle resistance to lateral overturn

129. Development of subroutine. For a tracked vehicle resting on a nearshore local slope of angle θ with one track atop an obstacle of height OH that causes the vehicle to be inclined at angle δ relative to the seafloor and angle α relative to the horizontal, Figure 20 illustrates the major forces acting on the vehicle as it experiences water forces acting during the impact and backwash wave cycles, respectively. In cases A and B of Figure 20, the lower track is assumed to be locked (as by rocks) so that it cannot slide and so that vehicle overturn, if it occurs, is about point O. These conditions are considered most severe relative to possible vehicle lateral overturn.

130. Nearshore water forces act on a bottom-crawling vehicle in a cyclic manner. Each wave period WP is described as occurring over a time WP = IT + BT where IT is impact time, the time during which water forces are incoming toward shore, and BT is backwash time, the time during which water forces are moving away from shore. Impact water force F_i, backwash water force F_b, lift force L, and buoyancy B all are described by the lateral overturn subroutine as changing values according to sine functions. For a given wave, the value of F_i changes during time 0 to IT; F_b changes during time IT to WP; L and B change during both 0 to IT and IT to WP. The maximum values of F_i and of F_b are functions of MFF (maximum frontal force) and MBF (maximum broadside force); the maximum value of L is MLF (maximum lift force), and of B is MB (maximum buoyancy, which equals GVW - VEW, in-air gross vehicle weight minus vehicle effective weight). Values of MFF, MBF, MLF, and MB are all taken directly from the water force calculations submodel.

131. To determine the angle α (in radians) relative to the horizontal that the vehicle assumes as it is rotated by overturn action about point 0 requires, first, the calculation of $\ddot{\alpha} = M_o/J_o$, where $\ddot{\alpha}$ is vehicle angular acceleration about point 0, M_o is overturning moment of the vehicle about point 0, and J_o is polar mass moment of inertia of the vehicle about point 0 (i.e., about an axis that projects into the paper through point 0 in cases A and B of Figure 20). Vehicle overturn motion starts when M_o exceeds zero. During the impact cycle (Figure 20a), M_o is defined as

$$M_o = \left[\left(F_i \cos \alpha \times a\right) + \left(F_i \sin \alpha \times \frac{b}{2}\right)\right] - \left\{(VEW - L - B) \times \left[\left(\frac{b}{2} - j \tan \alpha\right) \cos \alpha\right]\right\} \quad (13)$$

where

$F_i = F \sin \frac{\pi T}{IT}$

α = angle between the bottom of the tracked vehicle and the horizontal when the vehicle is viewed from the end

a = distance from bottom of vehicle to point through which $F_i \cos \alpha$ acts

b = distance between centers of the bottom of the vehicle's tracks*

VEW = vehicle effective weight

$L = MLF \sin \frac{\pi T}{IT}$

$B = MB \sin \frac{\pi T}{IT}$

j = height of the vehicle center of gravity (CG) above the bottom of the vehicle

$F = MFF \sin \phi + MBF \cos \phi$

T = time, 0 to IT for the impact cycle

ϕ = vehicle heading angle, deg

132. During the backwash cycle (Figure 20b), M_o is defined as

$$M_o = -\left[\left(F_b \cos \alpha \times a\right) + \left(F_b \sin \alpha \times \frac{b}{2}\right)\right] - \left\{(VEW - L - B) \times \left[\left(\frac{b}{2} - j \tan \alpha\right) \cos \alpha\right]\right\} \quad (14)$$

where

$F_b = -F \sin \frac{\pi T}{IT}$

$L = MLF \sin \frac{\pi T}{IT}$

$B = MB \sin \frac{\pi T}{BT}$

$F = k_1 (MFF \sin \phi + MBF \cos \phi)$

T = time, IT to WP for the backwash cycle**

k_1 = a constant that reflects the balance in energy dissipated by F_b forces during the backwash cycle relative to that dissipated by F_i forces during the impact cycle.

133. The lateral stability subroutine of STAM determines the value of $\ddot{\alpha} = M_o/J_o$ over a full wave period at successive small increments of

---

* This definition of b assumes that the vehicle center of gravity is located on the lateral geometric center line of the vehicle. If this is not the case, Equation 13 should use c, not b/2, where c is the distance from point 0 to a line drawn through the vehicle CG at angle α (where this line is parallel to the sides of the vehicle).

** Time from IT to WP equals BT. In modeling M_o during backwash time, it was simpler to consider T as occurring from 0 to BT then from IT to WP.

time either from time 0 to IT and then from IT to WP--i.e., considering the impact cycle first--or vice versa, from 0 to BT and then from BT to WPT--considering the backwash cycle first. Next, it performs two numerical integrations to determine angle α, the angle that the bottom of the track makes with the horizontal. Thus, α can be evaluated over either the impact or the backwash cycle first. The initial value of α for the second part of the wave cycle is the value of α determined at the end of the first part of the cycle. Instability relative to lateral overturn is considered to occur when either (a) angle α exceeds 0.4 rad at any time during a wave period, or (b) α fails to return to its initial value at or before the end of a wave period.

134. Of the parameters mentioned in paragraphs 131 and 132, parameters k_1, a, T, and ϕ take assigned values--i.e., these parameters are neither vehicle parameters nor parameters whose values are defined by the water force calculations submodel. In every case, values assigned to these parameters should be realistic or slightly conservative--i.e., the assigned values should lead to values of M_o at least as large as are anticipated in actual situations. The following description of the values assigned to k_1, a, T, and ϕ for subsequent use in evaluating the example vehicles is in order.

135. For $k_1 = 1$ and IT = BT, $F_i = F_b$ and energy dissipation is equally balanced between the impact and backwash cycles. This condition was taken always to be present in deep water (offshore stations 8-17). For $k_1 = 0$, all energy dissipation occurs during the impact cycle. Using k_1 values no larger than 0.2 was judged reasonable for the broken wave and breaking wave zones (stations 1-7) where most energy dissipation occurs during the impact cycle.

136. In subsequent computations based on the lateral overturn subroutine, the value of parameter a was taken equal to 2/3 VH_s (vehicle submerged height) for stations 1-7, and 1/2 VH_s for stations 8-17. These estimated values are considered to be slightly conservative.

137. For stations 1-7, impact time IT was assumed equal to 1 sec (and backwash time as WP minus 1 sec). IT = 1 sec is considered conservative since peak values of F almost always occur during the

impact part of the wave cycle (within stations 1-7), and are sustained for considerably less than 1 sec as a wave passes a nearshore vehicle. Sampling values of F for a somewhat longer time than they actually occur leads to conservative (somewhat overlarge) values of M_o. For stations 8-17, impact time and backwash time were taken as being equal, reflecting the balance that ordinarily occurs in deep water.

138. Vehicle heading angle ϕ was assumed to vary between 0 and 15 deg for bottom-crawling vehicles operating within the broken and breaking wave zones (stations 1-7). Vehicle overturn or swamping within stations 1-7 ordinarily is best avoided by keeping angle ϕ as near to zero as possible. The rationale for using an upper limit of ϕ = 15 deg was that a prudent vehicle operator should be able to keep his vehicle heading within an envelope of ± 15 deg within stations 1-7. Within stations 8-17, angle ϕ was allowed to vary from 0 to 90 deg, the assumption being that because the vehicle is either submerged or nearly so within these stations, the vehicle operator will not be able to align his vehicle relative to incoming waves nearly so well as he could in stations 1-7.

139. Worst case conditions. Relative to vehicle lateral overturn, two worst case conditions, A and B, were considered. Case A is for overturn more likely to occur during the impact cycle (Figure 20a). For case A, the worst situation as far as the vehicle's initial inclination to the horizontal is concerned is for seafloor local slope θ to equal 0 and the seaward side of the vehicle to be atop an obstacle.* The largest impact force nearly always occurs in the breaking wave zone, (stations 6 and 7), so k_1 should be set equal to 0 for stations 1-7 to maximize F_i (see paragraph 135).

140. Case B is for vehicle lateral overturn more likely to occur during backwash (Figure 20b). For case B, the worst situation is for θ

---

* The seafloor is taken to be either flat or to increase in depth from shore outward. The maximum value of local seafloor slope is taken as the scenario value, no matter what the vehicle heading angle. Thus, for a given scenario, local slope can vary from 0 deg to its scenario value.

to equal its scenario value; the landward side of the vehicle to be atop an obstacle; and k_1 to equal 0.2 in stations 1-7.

141. Example application. The lateral overturn subroutine was exercised by "worst case" testing each of the five example vehicles in scenarios A-H (see Table A1). The tabulation in Figure 21 for vehicle 2, scenario E is representative of the results obtained.

142. Values in column 5 of the Figure 21 tabulation demonstrate that the overturn subroutine was exercised at increments of 15 deg for vehicle heading angles from 0 to 90 deg. Two wave periods, 8 and 15 sec, were used for each example vehicle/scenario combination; the tabulation in Figure 21 is for 8 sec (column 6). In column 8, the starting value for angle α is $\theta + \sin^{-1} OH/b$ (Figure 20). The lateral stability subroutine was exercised for the local slope values associated with both cases A and B (zero slope and scenario local slope, respectively). Case A was exercised for vehicle heading angles of 0 and 15 deg, and case B for 0, 15, 30,...90 deg since case A applies to stations 1-7 and case B to stations 8-17. Conclusions are summarized relative to case A in columns 10 and 11 of the tabulation in Figure 21 and relative to case B in columns 13 and 14.

143. In columns 11 and 14, each first-line entry includes the (a) maximum value of angle α (AMAX in radians) obtained during a full wave period and (b) number of the first station at which this maximum value occurred. The second-line entry includes the (a) maximum value of α at the finish of a wave period (AFINISH) and (b) number of the first station where this value occurred. Negative values of AFINISH indicate that angle α returned to its starting value (column 8) before the end of the wave period. Column 10 lists a "YES" answer to "ALL GO" in stations 1-7 if results in column 11 show that AMAX is less than 0.4 rad and AFINISH is smaller than the starting value of A; it lists a "NO" answer otherwise. Under the same guidelines (but using the results shown in column 14), column 13 lists "YES" or "NO" answers for stations 8-17.

Vehicle resistance to
longitudinal overturn

144. Development of subroutine. This subroutine was developed in a manner closely paralleling that of the lateral overturn subroutine. Cases 1 and 2 of Figure 22 show major forces acting during the impact and backwash cycles, respectively, on a tracked vehicle resting on a nearshore local slope of angle θ with the vehicle positioned such that the vertical projection of the vehicle center of gravity aligns with the highest point of a bench-type obstacle.* The vehicle positions shown are the most precarious ones relative to longitudinal overturn for a tracked vehicle overriding a bench-type obstacle of height OH that causes the vehicle to be inclined at angle δ relative to the seafloor and angle β relative to the horizontal.

145. The basic aim of the longitudinal overturn submodel is to predict the angle β that the vehicle assumes as it is acted upon by overturn action about point P (Figure 22). The first step is to compute $\ddot{\beta} = M_p/J_p$, where $\ddot{\beta}$ = vehicle angular acceleration about point P, M_p is overturning moment about point P, and J_p is polar mass moment of inertia of the vehicle about point P (i.e., about an axis that projects into the paper through point P in each case of Figure 22). During the impact cycle (Figure 22a), M_p is defined as

$$M_p = \left[\left(F_i \cos \beta \times a \right) + \left(F_i \sin \beta \times \ell_1 \right) \right] - \left\{ (VEW - L - B) \times \left[\left(\ell_1 - j \tan \beta \right) \cos \beta \right] \right\} \quad (15)$$

where

$F_i = F \sin \frac{\pi T}{IT}$

β = angle between the bottom of the tracked vehicle and the horizontal when the vehicle is viewed from the side

ℓ_1 = distance from point P to a line drawn vertically through the vehicle CG when the vehicle rests on a flat, rigid surface. Distance ℓ_1 is less than or equal to distance ℓ_2, where

* Here, a "bench-type" obstacle is one of such width and constant cross-sectional shape that, as a tracked vehicle overrides it, corresponding points along the bottom of both tracks have equal elevation at any given time.

$\ell_1 + \ell_2$ = contact length of the track on a flat, rigid surface.

$F = MFF \cos \phi + MBF \sin \phi$

a, L, B, j, T, and ϕ are defined in paragarph 131.

146. During the backwash cycle (Figure 22b), M_p is defined as

$$M_p = -\left[\left(F_b \cos \beta \times a\right) + \left(F_b \sin \beta \times \ell_1\right)\right] - \left\{(VEW - L - B) \times \left[\left(\ell_1 - j \tan \beta\right) \cos \beta\right]\right\} \quad (16)$$

where

$F_b = -F \sin \frac{\pi T}{IT}$

$F = k_1 (MFF \cos \phi + MBF \sin \phi)$

L, B, T, and k_1 are defined in paragraph 132.

147. Overall, the definitions of M_p in paragraphs 145 and 146 match those of M_o in paragraphs 131 and 132 except that β is used instead of α; ℓ_1 is used instead of b/2; and the locations of cos ϕ and sin ϕ in the definitions of F_i and F_b for M_p are opposite to those of cos ϕ and sin ϕ in F_i and F_b for M_o. Values of parameters k_1, a, T, and ϕ for the longitudinal overturn subroutine are assigned in the same way as for the lateral overturn subroutine (see paragraphs 134-138).

148. Worst case conditions. Relative to vehicle longitudinal overturn, two worst case conditions, 1 and 2, were considered. Case 1 is for overturn more likely to occur during the impact cycle (Figure 22a). The worst situation is for seafloor local slope to equal 0, the landward end of the vehicle to be at the seafloor, and k_1 to equal 0.

149. Case 2 is for vehicle longitudinal overturn more likely to occur during the backwash cycle (Figure 22b). The worst situation is for θ to equal its scenario value, the seaward end of the vehicle to be at the seafloor, and k_1 to equal 0.2 in stations 1-7. In most respects, cases 1 and 2 for the longitudinal overturn submodel parallel cases A and B, respectively, for the lateral overturn submodel.

150. Example application. The longitudinal overturn subroutine was exercised by "worst case" testing each of the five example vehicles in scenarios A-H (see Table A1). The tabulation in Figure 23 for vehicle 2, scenario E is representative of the results obtained.

151. There is essentially a 1:1 correspondence between the columns in the Figure 23 tabulation for the longitudinal overturn subroutine and the columns of the Figure 21 tabulation for the lateral overturn subroutine. In column 8 of the Figure 23 tabulation, the starting value of β is $\theta + \sin^{-1}\left[OH/(\ell_1 - j \tan \delta)\right]$. "YES" or "NO" answers to the "ALL GO" question in columns 10 and 13 of Figure 23 were determined relative to the β angles on the same basis as these answers were determined for corresponding columns in Figure 21 relative to the α angles (see paragraph 143).

Vehicle ability to maintain forward motion

152. Major features of subroutine. The basic aim of this subroutine was to provide a means for evaluating a vehicle's ability to maintain forward motion--i.e., to make a net gain in distance traveled in the direction desired during a full wave period. Development of this subroutine is somewhat lengthy and cumbersome; therefore, it is presented separately in Appendix B. It is useful to examine here the major features of the developed subroutine.

153. The test for determining whether a bottom-crawling vehicle can maintain forward motion in the nearshore region is based on comparing two quantities, G and T, defined as

$$G = \frac{F}{VEW} \tag{17}$$

and

$$T = \frac{\pi H}{2\lambda} \times \frac{1 - \left[\left(\frac{L + B}{VEW}\right)\left(1 - \lambda\right)^2\right]}{1 - \lambda} \tag{18}$$

where

$H = \mu \cos \theta - \sin \theta$

$\lambda = IT/WP$

μ = coefficient of traction between the vehicle tracks and the seafloor soil

F, L, and B are defined in the same way as for the longitudinal overturn submodel (see paragraphs 145 and 146).

Values of G and T are accumulated over a full wave period at each station (water depth location) of interest. If $G < T$, this indicates that forward motion can be maintained at that station; if $G \geq T$, it cannot.

154. Worst case conditions. Within stations 8-17, the impact and backwash water forces balance one another, thus causing G to equal 0 and making a test for maintenance of forward motion unnecessary. Within stations 1-7, the worst case is for the vehicle moving away from shore, since within these stations impact forces greatly exceed backwash forces. The worst situation is for seafloor local slope = 0 and $k_1 = 0$ (in a manner generally paralleling that of case 1 for the longitudinal overturn subroutine).

155. Example application. The tabulation in Figure 24 for vehicle 2, scenario E is representative of results obtained from "worst case" testing vehicles 1-5 in scenarios A-H relative to vehicle ability to maintain forward motion. Values of G, T, and G/T accumulated over a full wave period at each of stations 1-7 are listed in the Figure 24 tabulation for wave periods of 8 and 15 sec and for vehicle heading angles of 0 and 15 deg (the extreme values considered herein for stations 1-7). For vehicle 2, scenario E (and for all other vehicle/scenario conditions examined), all values of G/T were less than one, indicating that forward motion can be maintained.

Vehicle ability to resist side sliding

156. Major features of subroutine. The purpose of this subroutine was to check whether or not a vehicle will slide sideways due to the effects of seafloor local slope and water forces as the vehicle moves along the nearshore ocean bottom. Development of this subroutine is presented in the latter part of Appendix B. A description of some of the major features of the submodel follows.

157. The test for checking whether or not a bottom-crawling vehicle will slide sideways is based on comparing values of I and U, defined as

$$I = \frac{F}{VEW} \tag{19}$$

and

$$U = \frac{\pi H}{2\lambda} \times \frac{1-\left[\left(\frac{L + B}{VEW}\right)(1 - \lambda)^2\right]}{1 - \lambda} \qquad (20)$$

where H and μ are defined in paragraph 153, and F, L, and B are defined in the same way as for the lateral overturn submodel (see paragraphs 131 and 132).

158. Worst case conditions. Relative to resisting side sliding, two worst case conditions were considered. Case 1 is for vehicle side sliding more likely to occur during the impact part of a wave cycle. This likelihood is greatest for that station at which impact force F is greatest (ordinarily station 6 or 7) and seafloor local slope equals 0 (since the direction of impact force is such that a local slope greater than 0 inhibits, rather than promotes, vehicle side sliding--see Figure B2 in Appendix B, for example). Thus, case 1 applies to stations 1-7, with $k_1 = 0$ (to maximize F and, subsequently, F_i). Values of I and U are accumulated over the impact cycle only. If $I < U$, vehicle side sliding is predicted not to occur; if $I \geq U$, it is predicted to occur.

159. Case 2 is for vehicle side sliding more likely to occur during the backwash cycle. This likelihood is greatest for that station where backwash force F is greatest (ordinarily at station 8) and for seafloor slope equal to its scenario value (since the effects of backwash force and slope are cumulative relative to promoting vehicle side sliding). Thus, case 2 applies to stations 8-17, with $k_1 = 1$. Values of I and U are accumulated over the backwash cycle only. If $I < U$, vehicle side-sliding is predicted not to occur; if $I \geq U$, it is predicted to occur.

160. Example application. The tabulation in Figure 25 for vehicle 2, scenario E is representative of results obtained from "worst case" testing vehicles 1-5 in scenarios A-H relative to vehicle ability to resist side sliding. For case 1, stations 1-7, the values of I, U, and I/U accumulated over an impact cycle are listed for that station where maximum I/U was obtained; for case 2, stations 8-17, corresponding values accumulated over a backwash cycle are listed. Vehicle heading angles considered for case 1 are 0 and 15 deg; for case 2, the angles are 0, 15, 30,...90 deg. Both wave periods (8 and 15 sec) are used. For all conditions in the Figure 25 tabulation, values of I/U are less

than one, so that vehicle side sliding is predicted not to occur. In a subsequent section of this report, a summary of results from applying the side-sliding subroutine to all of the example vehicle/operating condition combinations reveals no values of I/U larger than one. This indicates that vehicle side sliding usually is not a major problem, since some severe vehicle operating conditions are considered in this report.

PART IV: EXAMPLE APPLICATION AND PARAMETRIC ANALYSIS OF STAM

Summary of STAM Application to the Example Vehicle Problems

161. Appendix A contains descriptions of vehicle missions and vehicle design/performance/environment requirements for five types of nearshore, bottom-crawling vehicles. The first two requirements of the example vehicle problems were to (a) design five types of example vehicles within the context of the vehicle design/performance/environment conditions stated in the text of Appendix A and (b) use STAM to predict the performance of the example vehicles for the operating conditions described in Table A1.*

Preliminary design of example vehicles

162. Requirement (a) from paragraph 161, which corresponds to the upper part of the first block of STAM (Figure 9), was satisfied in the "Vehicle Design Considerations" section of this report, paragraphs 51-69. Table 1 lists values of the major design and performance parameters from Appendix A. Table 3 summarizes the preliminary design guidelines used to define vehicle parameter values for the five example vehicles. And Table 2 lists the values of vehicle parameters developed for the five example vehicles primarily on the basis of information in Tables 1 and 3.

Prediction of example vehicle performance

163. Requirement (b) from paragraph 161 was satisfied by exercising the next three blocks of STAM--the water force calculations, vehicle trafficability, and vehicle stability submodels--for the five example vehicles designed in paragraphs 51-69. Two copies of the full set of results obtained for these submodels and vehicles and all scenario

---

* STAM was exercised for the example vehicles operating in all scenario conditions; however, the project sponsor instructed that results in this report include only the operational conditions defined at the bottom of Table A1.

conditions were mailed to the project sponsor. Table 8 summarizes the major results obtained from exercising each of the above-named submodels for the example vehicles and operating conditions of Table A1. These results are analyzed in the following paragraphs.

164. Prediction of water forces. Columns 1-10 of Table 8 summarize maximum values of broadside, frontal, and lift forces obtained for all the example vehicle/operating condition combinations, two wave periods (8 and 15 sec), all 17 stations, and three vehicle heading angles (0, 15, and 90 deg). Values in columns 5, 7, and 9 of Table 8 demonstrate that maximum frontal force took values from 6 to 60 times larger than those of maximum lift force and that maximum lift force took values greater than (usually several times greater than) maximum broadside force.* This dominance of frontal force over the lift and broadside forces resulted, because for the purposes of this report, frontal force is defined as that water force acting on the vehicle in a direction perpendicular to the shoreline, no matter what the vehicle heading angle. Furthermore, maximum frontal force can sometimes take rather overwhelming values. Perusal of the values in columns 3 and 7 of Table 8 reveals, for instance, that the largest values of maximum frontal force for the five example vehicles ranged from 4 to 7 times the corresponding in-air gross vehicle weight, with a peak value of over 770,000 lb for vehicle 5, scenario H. If the scenarios considered in this report are realistic, it is clear that bottom-crawling vehicles must sometimes contend with rather awesome water forces in the nearshore region.

165. Values from the water force calculations submodel are subsequently used by STAM in its stability submodel. There, a given type of vehicle performance is evaluated for a given "worst case" (say, vehicle ability to resist lateral overturn, case A) for either stations 1-7 or 8-17. Interest centers on that one station for which worst

---

* The one exception to this statement is for example vehicle 2, scenario H, where maximum broadside force was slightly larger than maximum lift force, 7556 lb versus 7054 lb.

vehicle performance is predicted, whether or not this station is the one at which maximum frontal force occurs. Nearly always, though, it is frontal force, whether it be at its maximum value or not, that is the dominant water force as far as vehicle stability performance is concerned. Thus, it is useful to examine the relations of frontal force to (a) station number, (b) wave period, and (c) vehicle heading angle, three parameters that have significant influence on frontal force for a given vehicle/scenario combination.

166. Station number. The solid curve in Figure 26 shows the relation of frontal force to station number for the conditions described by the tabulation in Figure 13. This relation is representative in that for all the vehicle/scenario combinations, the largest value of frontal force within stations 1-7 nearly always was obtained at station 6, the next largest at station 7.* Within stations 8-17, maximum frontal force always occurred at station 8 and steadily decreased with increasing station number.

167. Wave period. The dashed curve in Figure 26 was developed for the same scenario conditions as the solid curve, except that the dashed curve is based on a wave period of 15 sec. Compared with the 8-sec wave period (solid curve), the 15-sec wave period (dashed curve) caused frontal force values to be smaller at stations 6-9 and to be larger at all other stations. The pattern of influence of the 8- and 15-sec wave periods on predicted frontal force for all of the other example vehicle/scenario combinations was similar to that just described for Figure 26.

168. Vehicle heading angle. Vehicle heading angle ϕ has significant influence on maximum frontal force (MFF), primarily because MFF varies directly with vehicle surface area projected parallel to the shoreline. Because of this, the degree of influence of ϕ on MFF increases as the difference between vehicle side and end surface areas

---

* In those few cases where maximum frontal force was obtained at station 5, the wave period was always 15 sec and a larger value of maximum frontal force was always obtained at a wave period of 8 sec, all other conditions equal.

increases. To demonstrate this, Figure 27 shows the relation of percent increase in MFF to ϕ for the example vehicle whose side area was largest relative to its end area (the seafloor survey vehicle, upper solid curve); for the one whose end and side areas were most nearly equal (the seafloor transport vehicle, lower solid curve); and for a hypothetical vehicle with equal dimensions for its side and end areas (dashed curve). In Figure 27, percent increase in MFF is defined as (MFF at the heading angle of interest ÷ MFF at heading angle = 0 deg) × 100. Scenario C conditions were used in Figure 27, with wave period held constant at 15 sec.

169. The dashed curve in Figure 27 for the vehicle with equal side and end area dimensions is symmetric with a peak ordinate value of 41.4 percent at an abscissa value of 45 deg. The nearly symmetric transport vehicle has a peak ordinate value of about 45 percent at about ϕ = 46 deg, and the more elongated* survey vehicle has a peak ordinate value of about 71 percent at about ϕ = 55 deg. Overall, the major conclusions to be drawn from Figure 27 are that (a) vehicle heading angle has strong influence on maximum frontal forces MFF; (b) for vehicle heading angles up to 90 deg, the increase in MFF from its value at 0-deg heading angle becomes larger as vehicle elongation increases; and (c) the heading angle at which the peak value of MFF occurs increases as vehicle elongation increases.

170. Prediction of vehicle trafficability performance. Columns 1-4 plus 11-27 in Table 8 summarize "worst case" performance predictions by the STAM trafficability submodel for all of the example vehicle/operating condition combinations. For a given vehicle and scenario, columns 12 and 13 in Table 8 list VCI_1 values for the in-air and submerged conditions, respectively. Column 14 lists a double dash under "NOGO" if scenario cone index from column 11 is larger than the VCI_1 values from both columns 12 and 13 to indicate that a vehicle "GO"

---

* Here, elongated means the vehicle side area is larger than the vehicle end area.

relative to soil strength is predicted. For scenario cone index from column 11 smaller than the VCI_1 value from either columns 12 or 13, column 14 lists the first station at which this condition occurred, i.e., the first station where vehicle "NOGO" relative to soil strength is predicted. Where a station is listed in column 14, it is always DL since VCI_1 is always largest on dry land (i.e., VCI_1 values increase monotonically as VEW increases, and VEW is largest on dry land).

171. Note that values of VCI_1 were not predicted for a tracked vehicle operating in sand (scenario D). WES experience from prototype tracked vehicle testing in the field and from model track testing in the laboratory in a variety of dry-to-moist sands indicates that vehicle immobilization almost never occurs due to the strength of sand per se. Furthermore, the experience of the Soil Mechanics Department, Delft Institute, Holland (see paragraph 115) suggests that conventional tracked vehicles can slowly traffick extremely weak saturated sands.* On the basis of this experience, it was judged reasonable to make a double-dash (GO) entry in column 14 for the D scenario of each vehicle.

172. For a given vehicle and scenario, column 15 in Table 8 lists a "YES" or "NO" answer to the question "Does the trafficability submodel predict geometrical interference (hangup) between vehicle and obstacle?" The trafficability submodel does not check for geometrical interference if a "NOGO" is predicted due to insufficient soil strength for both the in-air and submerged conditions (i.e., if entries in columns 12 and 13 are both larger than the one in column 11). A "NO" answer was placed in column 15 when this happened, however, because it only occurred for scenario A, which has a 0.5-ft obstacle height, the smallest obstacle height considered in the eight scenarios.

---

* Operation of vehicles like example vehicles 3 and 4 (the work platform and trencher), which must deliver repetitive loads to submerged sand while the vehicle remains essentially stationary, may greatly weaken the sand due to load liquefaction. Because of this phenomenon and the general dearth of information on vehicle performance in submerged sands, it is hoped that some insights on liquefaction developed for other engineering applications--say, for dams and foundations as in Reference 61--can be applied to bottom-crawling vehicle operations.

173. Column 16 in Table 8 lists values of required drawbar pull specified for the various vehicle/operating condition combinations; columns 17 and 18 list predicted values of available DBP_{20} for the in-air and submerged conditions. Column 19 lists a double dash if available DBP_{20} is sufficient at all stations (all "GO"), or the first station number where available DBP_{20} is not sufficient (a "NOGO"). If a "NOGO" was predicted relative to soil strength (i.e., if a "DL" entry appears in column 14), then values were not computed for columns 17 and 18 and "DL" was entered in column 19. That is, a "NOGO" due to soil strength also indicates a "NOGO" due to drawbar pull (even for required drawbar pull = 0, since the vehicle cannot develop forward motion).

174. Columns 20-25 in Table 8 list computed values of required TF_1, required TF_2, and available tractive force for the in-air and submerged vehicle conditions. Columns 26 and 27 list double dashes for "GO" and either "NOGO" or "DL" for "NOGO" based primarily on comparing required TF_1 versus available TF and required TF_2 versus available TF for corresponding conditions (in-air or submerged) in columns 20-25. Entries in columns 26 and 27 are also based on interpretation of two types of situations reflected in columns 11-15. First, if a "NOGO" was indicated due to soil strength for either the in-air or the submerged vehicle condition or both (i.e., if VCI_1 in columns 12 or 13 or both was larger than scenario cone index in column 11), then corresponding values of required TF_1, required TF_2, and available TF were not computed in columns 20-25. In this situation "DL" was entered in columns 26 and 27 because "NOGO" due to insufficient soil strength necessarily means that tractive force is not sufficient. Secondly, if a "YES" answer was obtained in column 15, i.e., if vehicle/obstacle interference was indicated, then no computations were made for columns 22 and 23 and a "NOGO" entry was placed in column 27. That is, geometric hangup automatically indicates that available tractive force is insufficient to satisfy required TF_2.

175. Prediction of vehicle stability performance. Columns 1-4 and 28-43 in Table 8 summarize a check of the "worst case" seafloor performance predicted by the STAM stability submodel for all of the example

vehicle/operating condition combinations. Results relative to the lateral overturn subroutine appear in columns 28-33 of Table 8. Columns 28 and 30 describe the conditions under which the values in column 29 were obtained; columns 31 and 33 relate to column 32. Entries under columns 29 and 32 reflect the most unstable conditions relative to lateral overturn obtained for a given combination of example vehicle and operating conditions relative to α_{max} and $\alpha_{start}/\alpha_{finish}$, respectively. Lateral instability is taken to occur if either (a) $\alpha_{max} \geq 0.4$ rad in column 29, or (b) $\alpha_{start}/\alpha_{finish} < 1$ in column 32 (i.e., if the vehicle fails to return to its initial position atop the obstacle at or before the end of a wave period).

176. "Worst case" results for the longitudinal overturn subroutine are summarized in columns 34-39 of Table 8. The same criteria used in columns 29 and 32 to define instability relative to α_{max} and to $\alpha_{start}/\alpha_{finish}$, respectively, are used in columns 35 and 38 relative to β_{max} and to $\beta_{start}/\beta_{finish}$, respectively. Columns 34 and 36 relate to column 35; columns 37 and 39, to column 38.

177. Summaries of "worst case" results for the maintenance of forward motion and the resistance to side-sliding subroutines appear in columns 40-41 and 42-43, respectively. Inability to maintain forward motion during a wave period is indicated by a G/T value ≥ 1 in column 40. Inability to resist side sliding is indicated by an I/U value ≥ 1 in column 43.

Evaluation of Vehicle Design Parameter Influence on Predicted Nearshore Vehicle Performance

Evaluation of example vehicle performance capabilities

178. Summary tally. The third requirement of the example vehicle problems (in addition to the two of paragraph 161) was to evaluate the capabilities of the five example vehicles to satisfy the performance/environment conditions described in Appendix A. To aid in this evaluation, the major performance prediction results summarized in Table 8

were further condensed in the summary tally of Table 9. In order, columns 3-13 in Table 9 correspond to columns 14, 15, 19, 26, 27, 29, 32, 35, 38, 40, and 43 in Table 8. Entries in these first five columns in Table 8 summarize results that were interpreted in paragraphs 170-174 in terms of vehicle GO or NOGO relative to exercise of the STAM trafficability submodel. Entries in the latter six columns in Table 8 do the same for the STAM stability submodel (with GO/NOGO interpretations in paragraphs 175-177). In Table 9, each entry under columns 3-13 indicates either a vehicle "GO" or "NOGO" that corresponds to the Table 8 results just described.

179. Evaluation of summary tally results. The last line in Table 9 contains the sums of NOGO's for each of columns 3-13. The larger the value of a given entry in the last line, the greater the problem to successful vehicle operation caused by the type of performance shown in the column heading for that entry. Sums shown in the last line range from 0 to 19 out of a possible sum of 33. For the example vehicles and the performance/operating conditions considered in Table 9, the last line of the table shows that no problems are indicated for maintaining forward motion or for resisting side sliding (sum of 0 for columns 12 and 13). Vehicle/obstacle geometry interference is a minor problem (sum of 2 for column 4), with NOGO's indicated only for vehicle 1 under scenarios G and H. Vehicle inability to negotiate soft soil (column 3) and to develop required drawbar pull (column 5) are also minor problems (sum of 3 for each) and occur in Table 9 only for scenario A. Insufficient tractive force to climb a slope and to develop required drawbar pull at the same time is somewhat more a problem (sum of 6 in column 6), and to do these two types of work plus override an obstacle is the greatest problem considered (sum of 19 in column 7). Overturn instability is a serious problem in terms of lateral overturn (sums of 14 and 9 in columns 8 and 9) and even slightly more so in terms of

longitudinal overturn (sums of 17 and 12 in columns 10 and 11).*

180. Column 14 in Table 9 contains the sum of NOGO's for entries in all but the last line of the table. The larger the sum of NOGO's in a given line of Table 9, the greater the problem to successful vehicle operation caused by the scenario that appears in column 2 for that line. Eleven GO/NOGO possibilities are considered in each line, and the sum of NOGO's shown in column 14 for the 30 lines in the table range from 0 to 6. Scenarios B and C both produced 0 sums in column 14 in every case where they appear in Table 9. Scenario A produced sums of 4 in each of its three appearances in Table 9, reflecting in each case NOGO entries in columns 3, 5, 6, and 7. These NOGO entries resulted because the scenario A cone index value was 2, which is smaller than the VCI_1 values of the three example vehicles for which scenario A was considered a potential operating condition. Scenario D produced all 0 sums for example vehicles 2-5 but a sum of 2 for vehicle 1. These two NOGO's were obtained in columns 10 and 11, both of which relate to the STAM longitudinal stability subroutine. This indicates that one or more design characteristics of example vehicle 1 providing stability against longitudinal overturn were importantly different from those of vehicles 2-5. From Table 3, it is seen that vehicle 1 was by far the smallest and lightest of the five example vehicles.**

181. Scenarios E, F, G, and H produced sums in column 14 of Table 9 according to the following pattern for the five example vehicles:

---

* Using 0.4 rad as the value at which α_{max} and β_{max} indicate instability to overturn is somewhat arbitrary and certainly conservative. If this limit were increased from 0.4 to 0.6 rad, for instance, the sums in columns 8 and 10 would drop to 9 and 12, respectively, the same sums obtained in columns 9 and 11.

** Vehicle 1 was also the only example vehicle with ramped tracks at each end. This feature of vehicle design has very little effect per se on vehicle longitudinal stability as described in paragraphs 144-151.

Example Vehicle No.	Sum in Column 14 of Table 9 for Scenario			
	E	F	G	H
1	5	5	6	6
2	4	4	-	6
3	-	-	5	-
4	2	2	3	6
5	3	3	5	6

From Table A1, it is seen that soil strength values for scenarios E-H are very large. Values of general and local seafloor slope, obstacle height, current velocity, and wave height are also significantly larger for scenarios E-H than for scenarios A-D, with values of each of these parameters increasing steadily as scenario letters progress from A through H. Increases in obstacle height cause NOGO's due to geometry interference to increase as vehicle size decreases (particularly as running gear size decreases). It is not surprising, then, that vehicle A was the only example vehicle for which NOGO's were obtained in column 4 of Table 9 and that these NOGO's were obtained for the largest obstacle heights (those of scenarios G and H). The fact that sums in the above tabulation are largest for example vehicle 1 (first line of tabulation) is also due largely to vehicle 1 being significantly smaller than the other four example vehicles. Scenario H is the most severe of scenarios A-H; so, it follows that the largest sums should be obtained in the last column of the tabulation.

182. Other than the NOGO's mentioned above for example vehicle 1 and for scenarios G and H in Table 9, the sums in the tabulation of paragraph 181 resulted from NOGO's in columns 6-11 of Table 9. Columns 8-11 in Table 9 relate to the lateral and longitudinal stability subroutine of STAM. Column 6 relates to a check of whether available tractive force TF is sufficient to satisfy three TF requirements--those of soil motion resistance, drawbar pull, and grade resistance (Equation 3, paragraph 102). Column 7 relates to satisfying these same three TF requirements plus that of obstacle override (Equation 4, paragraph 102). The likelihood of NOGO's in columns 8-11 of Table 9 increases as the sea state worsens (i.e., as values of general and local seafloor slope,

current velocity, and wave height take larger values) and as obstacle height increases. NOGO's in column 6 of Table 9 increase as the sea state worsens, and NOGO's in column 7 increase as the sea state worsens and as obstacle height increases.

183. Clearly, the tabulation in paragraph 181, together with the information in Tables 8 and 9, demonstrates that the sea state and obstacle height conditions of scenarios E-H were severe enough to cause significant NOGO problems for the five example vehicles. The tabulation in paragraph 181 shows that ability of the example vehicles to cope with the scenario E-H conditions (i.e., to develop small-valued entries in the tabulation) improves for the five example vehicles in the order 1, 2, 3, 5, and 4.* From Table 3, this is the same order in which gross vehicle weight for the five vehicles increases. Also, if the value of vehicle length for example vehicle 5 (the underwater bulldozer) were taken as vehicle length without blade (240 in. instead of the 336 in. shown in Table 3 for vehicle length including blade), then the order of values of VL × VW for the example vehicles would also be 1, 2, 3, 5, and 4. Thus, vehicle performance as indicated by the tabulation in paragraph 181 appears to improve as vehicle weight increases and as vehicle size increases.

---

* Unfortunately for the analysis in paragraph 183, the operating conditions specified by the project sponsor did not include the vehicle/scenario combinations for which dashed entries appear in the tabulation of paragraph 181. In this tabulation, example vehicle 3 was evaluated only for scenario G. Because vehicles 3 and 5 both obtained sums of 5 for scenario G in the tabulation, no clear-cut choice can be made between the two vehicles on the basis of this tabulation. Perusal of Table 8 values for scenario G, vehicles 3 and 5, shows that the NOGO's of vehicle 3 were less severe than those of vehicle 5 (i.e., the margins by which these vehicles failed to meet GO standards were smaller for vehicle 3). This observation agrees with the order of vehicle numbers listed in paragraph 183. Further, all parts of STAM were exercised for all the vehicle/scenario combinations, and these confirmed that vehicle 3 outperformed vehicle 5 in scenarios E-H.

A more general evaluation

184. Need for and basis of evaluation. The evaluations of the Tables 8 and 9 in paragraphs 178-183 (a) described the patterns by which particular example vehicles 1-5 were predicted by STAM to perform in the particular operating conditions of Table A1 and (b) provided some limited insight into how individual vehicle design parameters influence STAM-predicted vehicle trafficability and stability performance. In making a more general evaluation of the influence of vehicle design parameters on STAM-predicted nearshore vehicle performance, it is important to consider two questions. First, how do the subroutines of the trafficability and stability submodels of STAM describe the influence of major vehicle design parameters on predicted vehicle performance? And secondly, what constitutes an unrealistic grouping of values for vehicle design, vehicle performance, and nearshore environmental parameters for each subroutine? Hereafter, supplying answers to these two questions will be referred to as type "a" and type "b" evaluations, respectively.

185. Using the Table 3 vehicle preliminary design guidelines as a baseline, attention will be directed first to predicted trafficability performance and then to predicted stability performance. Later, trafficability and stability performance will be considered together, first in the context of the vehicle design guidelines of Table 3 and then in the context of vehicle design guidelines in general; both contexts will deal with the types "a" and "b" evaluations described in paragraph 184.

186. STAM trafficability submodel evaluation. Vehicle/obstacle geometry interference will be dealt with first, because unlike the other types of performance considered by the STAM trafficability submodel, the interference subroutine reflects vehicle performance on a geometric and on a lateral stability basis. For input to its interference subroutine, STAM uses (a) mathematical descriptions of the geometric outlines of the vehicle and of the obstacle, and (b) a mathematical description of the location of the vehicle's center of gravity (CG). The subroutine then mathematically passes the vehicle over the obstacle, checking at each

point during obstacle override to see whether (1) vehicle/obstacle geometry interference (overlap) occurs and (2) vehicle overturn occurs during override due to an unacceptable orientation of the vehicle's CG and its geometric outline. The number of possible combinations of vehicle outlines, obstacle outlines, and vehicle center of gravity locations is infinite. This, together with the complexity of STAM's mathematical descriptions of vehicle/geometry interference and the several types of interference that the STAM subroutine considers, causes it to be necessary to treat each vehicle/obstacle combination on an ad hoc basis.

187. Still, it is possible to extract some general guidance relative to vehicle design from the STAM interference subroutine. To minimize the possibility of vehicle/obstacle geometry overlap, the size of the vehicle must be sufficiently large relative to the size of the obstacle and the shape of the vehicle's outline must be such as not to cause vehicle/obstacle geometry overlap at any point during obstacle override. To minimize the possibility of vehicle overturn, the interference subroutine suggests that the vehicle's CG should be as low as practical and centered both laterally and longitudinally within the vehicle's outline.

188. To supplement the above guidance, the following simple, preliminary procedure can be used to check whether or not a given vehicle design avoids unacceptable vehicle/obstacle interference. First, scaled sketches of the outlines of the proposed vehicle and of the worst anticipated obstacle should be drawn and cut out, with the vehicle's CG location identified on the vehicle sketch. Then, the vehicle outline should be passed manually over the obstacle outline to check both for (a) vehicle/obstacle overlap and (b) unacceptable alignment of the vehicle's CG during obstacle/override. A more detailed design of the vehicle should then be done by exercising the STAM interference subroutine iteratively, i.e., by systematically changing the values that describe the vehicle's outline and center of gravity location in successive runs of the interference subroutine until a reasonable vehicle design is obtained.

189. The example vehicle problems provide some insight into reasonable choices of track height and the shape of the lower front and rear sides of the vehicle outline (i.e., ramped versus nonramped tracks) for various types of nearshore tracked vehicles. Vehicle 1 had a 36-in.-high track, ramped ends (45-deg approach and departure angles) and was predicted to be unable to override a 36-in.-high obstacle (scenario G). Vehicles 2-5 had track heights from 45 to 55 in., nonramped ends (90-deg approach and departure angles), and were each predicted to be able to override a 60-in.-high obstacle (scenario H). The fact that nonramped vehicles 2-5 were each predicted to override an obstacle of height greater than their track heights is related to the fact that the example problems considered only one value of obstacle approach angle, 105 deg (Figure 2). For 90-deg approach angle obstacles (i.e., "step" obstacles), the maximum obstacle height negotiable by a nonramped tracked vehicle equals 0.5 track height. For such "step" obstacles, tracked vehicles with ramped ends (approach and departure angles in the order of 45 deg) usually can override obstacles taller than one-half their track heights (on a strictly geometric basis). On the basis of these observations, it appears reasonable to use ramped tracks on a seafloor survey vehicle (example vehicle 1), because such a vehicle must explore new seafloor routes and thus may well encounter near-90-deg obstacles. The types of construction vehicles represented by example vehicles 2-5 ordinarily can follow selected, sometimes improved paths where obstacles have angles greater than 90 deg and/or heights less than one-half the vehicle track height; these types of vehicles should use nonramped tracks.

190. The first generation version of STAM developed in this report considers only conventional single-unit, two-track vehicles. The one major change in vehicle configuration that could dramatically increase tracked vehicle ability to override obstacles is use of active pitch articulation between the two (or more) units of a vehicle. Such a breakthrough is presently hindered by (a) limited field testing of such articulated vehicles, (b) nonavailability of proven articulation hardware, in terms of both the joint itself and driver controls of the

AD-A063 733 ARMY ENGINEER WATERWAYS EXPERIMENT STATION VICKSBURG MISS F/G 13/10
STUDY AND PARAMETRIC ANALYSIS OF TRAFFICABILITY, RUNNING GEAR, --ETC(U)
DEC 78 G W TURNAGE, W C SEABERGH

UNCLASSIFIED WES-TR-M-78-3 NL

2 OF 2
AD
A063733

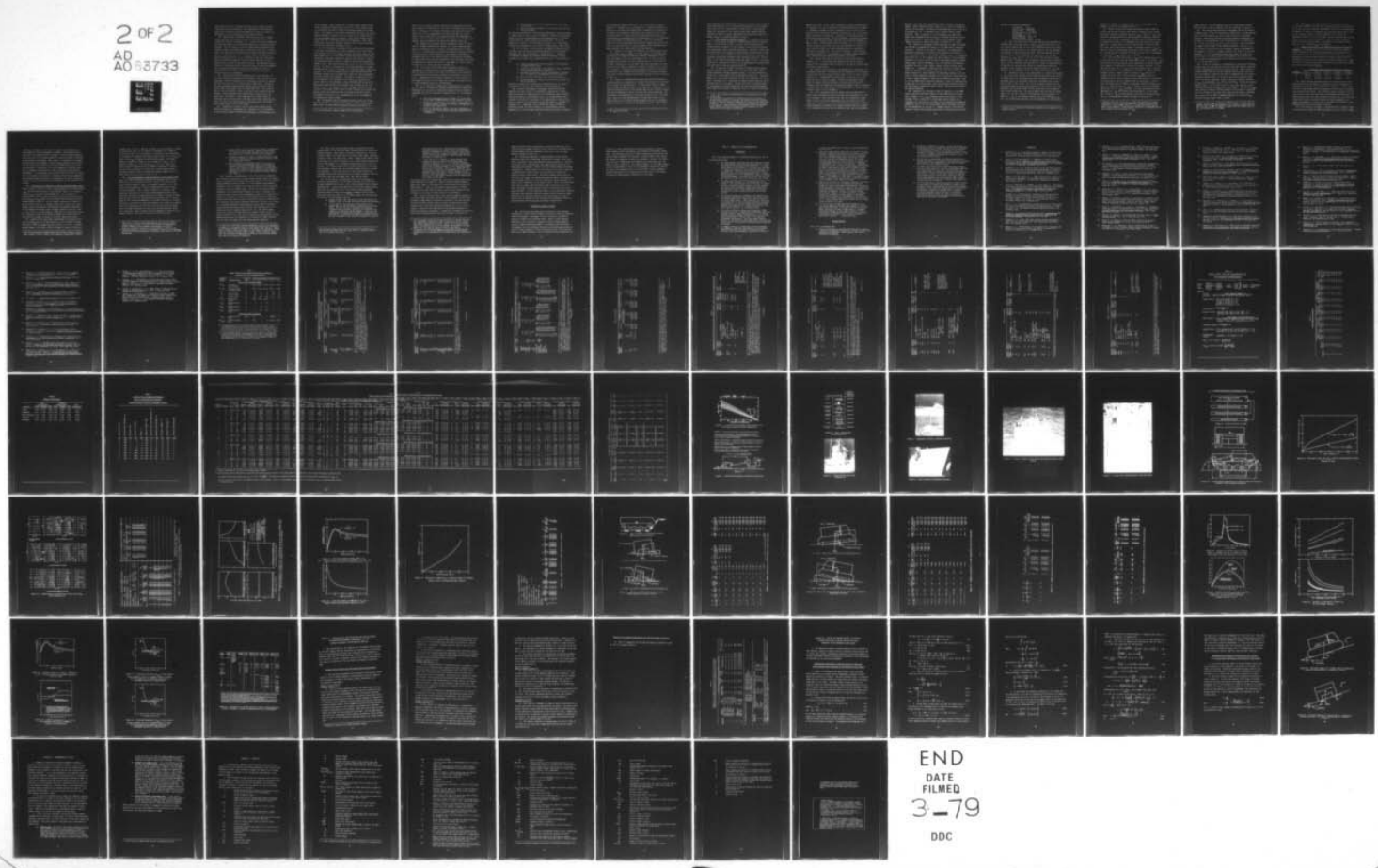

END
DATE
FILMED
3-79
DDC

joint, and (c) lack of a mathematical model that accurately predicts articulated vehicle performance. Work subsequent to that described herein will be done to develop the capability in STAM to describe the performance of active-pitch-articulated tracked vehicles.

191. The analysis in paragraphs 186-190 related only to vehicle/obstacle geometry interference but included both types "a" and "b" evaluations (defined in paragraph 184). Column 15 in Table 8 summarized the predicted results of this type performance for the example vehicle problems. The other parts of vehicle trafficability performance considered in Table 8 are summarized in columns 11-14 and 16-27. Briefly, these other parts deal with three types of vehicle performance--vehicle ability to negotiate soft soil, to develop drawbar pull DBP, and to develop tractive force TF. It is convenient to deal with these three types of performance together, first for vehicle operation in fine-grained soils and then in coarse-grained soils. This approach follows, because for fine-grained soils, these three types of vehicle performance can be predicted as functions of vehicle cone index VCI, while for coarse-grained soils, they are predicted as functions of a quite different vehicle/soil parameter.

192. Dealing first with fine-grained soils, note from Figure 11 that VCI_1 (and VCI_{50}) decreases as MI decreases. Thus, the basic aim in designing a vehicle to negotiate soft, fine-grained soil and to develop DBP and TF in such soil is to have MI take a small value. Ordinarily, the three parameters that have most influence on MI are gross vehicle weight (GVW), track length (TL), and track width (TW). With values of GVW, TL, and TW specified, values of the first three factors in MI are defined: contact pressure factor GVW/2(TL)(TW), weight factor, and track factor (see Table 4). The remaining five factors in Table 4 ordinarily have much less effect on MI than do the first three, particularly if values of the bogie factor and clearance factor fall within usual limits (about 1.0 to 2.0 for each).

193. Considering, in order, only the first three factors in MI, vehicle performance in fine-grained soil improves (i.e., MI decreases) as track contact pressure GVW/2(TL)(TW) decreases, as GVW decreases, and

as TW increases. Track length (TL) is fairly rigidly defined by the vehicle preliminary design guidelines in Table 3 once chassis length CL is specified and vehicle length VL* and track height TH are determined. For purposes of the analysis immediately following, the vehicle design guidelines of Table 3 will be used and TL for a given vehicle will be considered fixed, or constant. This leaves changing values of either TW or GVW as the major options for changing MI. Under these constraints, then, major interest centers on the influence that parameter TW has on GVW and, ultimately, on MI.

194. To illustrate the influence of TW on GVW and on MI according to the Table 3 guidelines, all vehicle parameters other than TW were held constant for the five example vehicles, and TW was varied so that TW/TL ranged from 0.1 to 0.5, which includes the range of TW/TL values ordinarily of practical interest in tracked vehicle design. Based on the design guidelines in Table 3, changes in TW produce corresponding changes in GVW. (The key relations here are $W_t = k \times TW \times TL$ and GVW = dry $W_{LC} + W_t$, where k increases with increasing ruggedness of tracked running gear and dry W_{LC} is constant for a specified vehicle chassis and payload.) For the five example vehicles, Figure 28a shows that GVW increases linearly with increasing TW/TL (where all vehicle parameters other than TW were held constant). The slope of a given line in Figure 28a depends on the combination of k and dry W_{LC} values for the vehicle that the line represents. Figure 28b shows that curves of the same general shape describe the relation of MI to TW/TL for all five example vehicles. MI increases as TW/TL decreases, and the rate of increase in MI becomes rather severe as TW/TL decreases below about 0.25. Overall, Figure 28 illustrates that increasing TW improves vehicle performance in soft soil (i.e., decreases MI), but at the expense of increasing gross vehicle weight.

195. The approach used in paragraphs 192-194 is only one of many that could be used to describe the influence of vehicle design parameters on MI. No matter what the approach, however, the factors in

---

* Or, for bulldozers, vehicle length without blade VLWOB.

Table 4 that ordinarily have most influence on MI are the first three. Also, whether the scheme used to lower MI is to decrease GVW, to increase TW, to increase TL, or to adjust the values of the last five factors of Table 4 up or down as appropriate, the overall aim must be to work toward a value of MI that is low enough to satisfy the combination of values of required vehicle performance, fine-grained soil strength, and supplied vehicle parameters that define the operating condition.

196. Analysis in paragraphs 192-194 constitutes a type "a" evaluation of the STAM trafficability submodel for vehicles operating nearshore in fine-grained soils. To make a corresponding type "b" evaluation, i.e., to define what constitutes an unrealistic grouping of values of vehicle design, vehicle performance, and nearshore environmental parameters relative to soil-related vehicle trafficability performance in fine-grained soils, requires examination of the influence that MI has on STAM-predicted vehicle ability to do three types of work--to negotiate soft soil, to develop DBP, and to develop TF.

197. If the only vehicle performance requirement relative to trafficking a fine-grained soil of known scenario cone index (CI_s) is that the vehicle be able to move under its own power, then required MI is determined from the relation in Figure 11 by solving for MI at $VCI_1 = CI_s$. A reasonable vehicle design is possible for this situation if the computed MI value is not so small as to require an unrealistic set of vehicle parameter values for its definition.

198. If, in addition to trafficking a fine-grained soil of known CI_s, the vehicle is required to develop a stated amount of drawbar pull, determination of the value of required MI depends on use of Equation 1 (paragraph 102) and the relations in Figures 15 and 11. The procedure is to:

a. Choose the appropriate curve in Figure 15 (on the basis of the value of VEW/2(TW)(TL) for the situation at hand).

b. Substitute (required DBP ÷ cos θ)/VEW for DBP_{20}/VEW as the ordinate variable of Figure 15 (because, from Equation 1, available DBP = DBP cos θ).

c. Solve for the smallest value of CI_x that corresponds to (required DBP ÷ cos θ)/VEW by using the appropriate curve in Figure 15.

d. Solve for VCI_1 by use of the relation $VCI_1 = CI_s - (CI_x$ from step c).

e. Use the relation in Figure 11 to solve for MI at the VCI_1 value from step d.

For the above procedure to be successfully implemented, specified values of required DBP, θ, and CI_s must be compatible. That is, the specified value of CI_s must be large enough and the computed value of CI_x small enough (where CI_x varies directly with required DBP ÷ cos θ, see steps b and c above) so that reasonable solutions (i.e., large enough values) can be obtained for VCI_1 and MI in steps d and e, respectively.

199. If the values of local slope θ and required tractive force TF are known, then the value of required MI depends on use of Equation 2 (paragraph 102) and the relations in Figure 29 and 11. (Figure 29 was obtained by summing the ordinate values from Figures 15 and 16 to obtain the relation $(DBP_{20} + SMR)/VEW$ versus CI_x.) The procedure is to:

a. Choose the appropriate curve in Figure 29 (on the basis of VEW/2(TW)(TL) value).

b. Substitute (required TF ÷ cos θ)/VEW for $(DBP_{20} + SMR)/VEW$ in the ordinate variable of Figure 29.

c. Determine the smallest CI_x that corresponds to (required TF ÷ cos θ)/VEW on the appropriate curve in Figure 29.

d. Solve for VCI_1 from $VCI_1 = CI_s - (CI_x$ from step c).

e. Use the relation in Figure 11 to solve for MI at the VCI_1 value from step d.

The above procedure can be successfully implemented only if values of required TF, θ, and CI_s, taken together, are not unrealistic.

200. Overall, the analyses in paragraphs 192-194 and 197-199 addressed the types "a" and "b" evaluations, respectively, of paragraph 184 relative to STAM predictions of soil-related vehicle trafficability performance in fine-grained soils. For coarse-grained soils relative to the type "a" evaluation, it is appropriate to deal not with mobility index MI, but with sand-track mobility number N_s (defined in paragraph 111). Paragraphs 109-115 showed that DBP_{20} and SMR are predicted by STAM for vehicle operation in coarse-grained soils by Equations 9-12, but that these equations should be used only if vehicle/

soil parameter N_s takes a value ≥ 50. For a given value of coarse-grained soil strength G, N_s is increased (i.e., vehicle performance is predicted to increase) by decreasing VEW, increasing TW, increasing TL, increasing track suspension flexibility, and moving the vehicle center of gravity forward. These first three actions agree precisely with those mentioned in paragraph 195 for decreasing MI (i.e., for increasing vehicle performance in fine-grained soils). The last two actions ordinarily can be accomplished within narrower ranges than can the first three, once the basic type of vehicle suspension and the general size/shape relations for a given vehicle have been decided.

201. Relative to the type "b" evaluation for coarse-grained soils, it is necessary again to address the three types of soil-related work considered by the STAM trafficability submodel--negotiation of soft soil, development of DBP, and development of TF. If the only vehicle performance requirement is that the vehicle be able to move under its own power (develop just over zero DBP), then this requirement is satisfied if the soil/vehicle situation of concern is defined by an N_s value of 1 or larger. A reasonable vehicle design is possible if the specified value of soil strength G is not so small as to require an unrealistic set of vehicle parameter values that, with this G value, define an N_s value ≥ 1.

202. Relative to STAM-predicted vehicle DBP and TF performance in coarse-grained soils, Equations 1-4 describe the relations for available DBP, available TF, and required TF. In the present version of STAM, values of DBP* and SMR to be used in the right side of Equations 1-4 are defined by Equations 9 and 10 for tracked vehicles with flexible suspensions and by Equations 11 and 12 for those with rigid suspensions. For the relations in Equations 9-12 to be used, N_s must be ≥ 50. The first check, then, as to the reasonableness of a specified G value in conjunction with a set of vehicle design parameter values is to determine whether the value of vehicle/soil parameter N_s is ≥ 50. Nearly always

---

* DBP, not required DBP.

this condition can be satisfied.* If $N_s \geq 50$, the next check is made by exercising Equations 1-4 in conjunction with Equations 9-12 and specified values of G, θ, required DBP, and required TF. The specified values are reasonable if this exercise shows that available DBP and available TF equal or exceed required DBP and required TF values for a design vehicle of acceptable parametric values.

203. STAM stability submodel evaluation. In evaluating the influence of vehicle design parameters on STAM-predicted stability performance, it is convenient to deal, in order, with the maintenance of forward motion, resistance to side sliding, lateral vehicle stability, and longitudinal vehicle stability subroutines. Exercise of these first two subroutines in the example problems produced no predictions of NOGO for any of the vehicle/operating condition combinations, although these problems included some extremely severe operating conditions. Accordingly, it is judged unnecessary to make the types "a" and "b" evaluations described in paragraph 184 relative to the maintenance of forward motion and resistance to side-sliding subroutines.**

204. In making an "a-type" evaluation of STAM-predicted lateral vehicle stability, the primary job is to evaluate how major vehicle design parameters influence predicted angle α, the angle between the bottom of a tracked vehicle and the horizontal (Figure 20). From paragraph 133, α is directly related to $\ddot{\alpha}$, and $\ddot{\alpha}$ is defined as $\ddot{\alpha} = M_o/J_o$. Thus, α decreases--i.e., resistance to lateral overturn improves--as M_o decreases and as J_o increases. Dealing first with overturning moment M_o, paragraphs 131 and 132 showed that the only vehicle design parameters explicitly included in Equations 13 and 14 to define overturning

---

* If $N_s < 50$, relations from Reference 59 for defining DBP and SMR can be used.

** To keep vehicle maintenance of forward motion and resistance to side-sliding problems to a minimum, the vehicle should be designed so that frontal and broadside water forces acting on the vehicle are minimized. This is done by a combination of streamlining the shape of the vehicle, using semi-open, flow-through vehicle containment areas wherever possible, and using exterior dimensions of the vehicle that are as small as practical.

moment M_o are VEW, j, and b (each illustrated in Figure 20 and defined in paragraph 131). M_o is decreased by increasing VEW and by decreasing j. Parameter b appears in each of Equations 13 and 14 for M_o in two places--in the first place increasing b increases M_o, and in the second place increasing b decreases M_o. Ordinarily, the second influence is much greater than the first, so that, generally, increasing b decreases M_o. To obtain maximum lateral stability from the design parameters of VEW, j, and b, a bottom crawler should be heavy, low (i.e., have a low center of gravity), and wide. The one other parameter in Equations 13 and 14 that is related to a vehicle design parameter is parameter a (defined in paragraph 131). The value of parameter a varies directly with vehicle height VH. M_o decreases as a decreases, again indicating that a nearshore bottom crawler should have a low profile.

205. Dealing next with the influence of vehicle mass moment of inertia J_o on α, J_o increases (and resistance to lateral overturn improves) with increasing values of VEW, j, b, VW, and VL (vehicle width and length, respectively).

206. Overall, the conclusions in paragraph 204 for decreasing α by decreasing M_o and those in paragraph 205 for decreasing α by increasing J_o agree that VEW and b should be made large, but are in direct conflict relative to j. (Paragraph 204 indicates that j should be small, paragraph 205, that j should be large.) Further, the analysis in paragraph 204 suggests that M_o decreases as vehicle size (at least VH) decreases, while the analysis in paragraph 205 suggests that J_o increases as vehicle size (at least VW and VL) increases--again, a direct conflict relative to what to do to decrease α.

207. Still considering only the lateral stability subroutine of STAM, another complication arises when water force parameters F, L, and B are evaluated. (The influence of all the other parameters in Equations 13 and 14 on M_o--and subsequently on α--was evaluated in paragraph 204.) Values of F, L, and B are predicted as functions of vehicle design parameters according to the complex relations that were alluded to in paragraphs 70-96 and that are defined in the copy of the computer

program of the water force calculations submodel mailed to the project sponsor. These relations predict values of F, L, and B to decrease as vehicle size decreases. The effect of decreasing each of F, L, and B is to decrease M_o, i.e., to decrease α and to improve vehicle lateral stability. Thus, in addition to the two separate and conflicting effects that changing vehicle size has on α already described in paragraph 206 (relative to M_o and J_o), there is now introduced a third, complex effect due to vehicle size that is related to F, L, and B.

208. Analysis in paragraphs 204-207 addressed the type "a" evaluation defined in paragraph 184 relative to the STAM lateral stability subroutine. Relative to the type "b" evaluation, the complications mentioned in paragraph 207 concerning the parameters that define F, L, and B (Equations 13 and 14) are further compounded when it is recognized that values of F, L, and B depend not only on values of vehicle design parameters, but also on values of vehicle operating parameters (vehicle heading angle, vehicle submergence, etc.) and nearshore environmental parameters (seafloor slope, obstacle height, current velocity, wave height, etc.). Therefore, a particular set of values of vehicle operational and nearshore environmental parameters must be specified to define a baseline or datum condition for evaluating whether or not the values of these parameters, together with the values of a particular set of vehicle design parameters, constitute an unrealistic grouping. That is, for the STAM lateral stability subroutine, a type "b" evaluation can be made only on an ad hoc basis, with each situation defined in terms of all three types of parameters--vehicle design, nearshore environmental, and vehicle operating.

209. Therefore, to illustrate a type "b" evaluation of the STAM lateral stability subroutine relative to the prediction of the peak value of angle α (i.e., α_{max}) produced during a wave period, it was necessary first to choose (a) a preliminary vehicle design, (b) a reasonable, yet difficult set of values for the nearshore environmental parameters, and (c) the worst anticipated vehicle operating conditions for the combinations of (a) and (b). Example vehicle 2 (the seafloor transport vehicle) was selected along with the following values for the

nearshore environmental parameters:*

Wave period: 8 sec
General slope: 8 percent
Local slope: 15 percent
Current velocity: 2.5 knots
Wave height: 6 ft
Ground material: hard rock
Obstacle height: 18 in.
Obstacle approach angle: 105 deg

210. Next, the STAM lateral stability subroutine was exercised to determine that the largest value of angle α_{max} was predicted to occur at a vehicle heading angle ϕ of 60 deg (illustrated by the solid curve in Figure 30) and at station 7 for example vehicle 2 and the nearshore environmental conditions described above. The next step was to determine the vehicle design parameters that appeared to have the most influence on α_{max}--VEW, j, b, VW, VL, and VH were mentioned in paragraphs 204-207. Parameter b was subsequently deleted since it changes value in direct proportion with parameter VW. Since the STAM subroutine of interest was concerned with lateral not longitudinal stability, parameter VW was surmised to have far greater influence on α_{max} than parameter VL, and parameter VL was also omitted from consideration.

211. Ultimately, then, it was judged useful to evaluate the patterns of α_{max} values that the STAM lateral stability subroutine would predict for design vehicle 2 (performing under the environmental conditions of paragraph 209 and the operating conditions of paragraph 210) as functions of VEW, j, VW, and VH. To do this, successive computer runs of the lateral stability subroutine were made with the values of all input parameters held constant except for VEW, which values were systematically varied between runs. The same procedure was then used for parameters j, VW, and VH. Figure 31 illustrates the results obtained. In Figure 31, α_{max} is the ordinate variable, and ratios VEW/VEW_2, j/j_2, etc., are the abscissa variables, with the denominator in each abscissa

* Values of the nearshore environmental parameters were supplied by the project sponsor.

variable set equal to its baseline value, i.e., to the value of the parameter of interest for example vehicle 2.*

212. Figure 31 shows that varying the separate values of VEW, j, and VH, from one half to twice their vehicle 2 baseline values caused only slight changes in predicted values of α_{max}. Values of α_{max} were reduced by increasing VEW and by decreasing VH (in agreement with conclusions drawn earlier in paragraphs 204-206) and were influenced least by changing the values of j (in agreement with the conclusion in paragraph 206). Varying vehicle width VW from one half to twice its baseline value caused much greater changes in predicted values of α_{max} in Figure 31 than did corresponding variations in the values of VEW, j, and VH. For the baseline conditions of Figure 31, then, VW has considerably more influence on α_{max} than do VEW, j, and VH.

213. Note that since the value of α_{max} at an abscissa value of 1.0 is only 0.29 rad (well under the nominal upper limit of 0.4 rad for α_{max}), this indicates that the baseline values established for example vehicle 2 are adequate to promote good resistance to lateral overturn. If this were not the case, i.e., if α_{max} took a value greater than 0.4 rad at an abscissa value of 1.0, then relations in Figure 31 indicate that the strongest action to take to lower the value of α_{max} would be to increase the value of VW. From a practical standpoint, VW can be increased from its baseline value by no more than about 10 to 20 percent (by increasing the value of chassis width, or track width, or both). Thus, the maximum value of VW/VW_2 of practical interest in Figure 31 is about 1.2. Since the value of α_{max} at $VW/VW_2 = 1.2$ is only slightly smaller than that of α_{max} at $VW/VW_2 = 1.0$, this indicates that little improvement in α_{max} would result from increasing VW. On the other hand, values of α_{max} increase rapidly as the value of VW/VW_2 lessens from 1.0, indicating that sizeable decreases in the width of

---

* Values of the ratio $\alpha_{start}/\alpha_{finish}$ were also predicted for every case where values of α_{max} were predicted. Hardly any NOGO's were predicted in terms of this ratio (i.e., hardly any values smaller than 1 were obtained), so the analysis described in paragraphs 209-214 was conducted only with respect to α_{max}.

example vehicle 2 from its baseline value would significantly worsen predicted vehicle lateral stability (for the conditions of Figure 31).

214. The same approach described in paragraphs 204-207 and 208-214 for making types "a" and "b" evaluations, respectively, of STAM-predicted lateral vehicle stability can also be made relative to longitudinal stability. Essentially the same conclusions reached in paragraphs 204-207 apply to the longitudinal stability situation if β is substituted for α, β for α, M_p for M_o, J_p for J_o, and ℓ_1 for b/2. Only one supporting comment need be added to this general statement. Relative to ℓ_1, and in direct correlation with the conclusion reached in paragraph 204 for parameter b relative to lateral stability, the value of ℓ_1 should be maximized. If it is considered possible that either the front end or the rear end of the vehicle can be tilted upwards (as in Figure 22), then ℓ_1 should be maximized when both of these situations are considered, i.e., ℓ_1 should equal 0.5 TL.

215. A type "b" evaluation of STAM-predicted longitudinal stability was made using the same approach and nearly the same baseline conditions as used in paragraphs 208-213 for lateral stability. These conditions included example vehicle 2 for the baseline vehicle design; the nearshore environmental conditions described in paragraph 209; and station 7 and vehicle heading angle ϕ = 15 deg for the vehicle operating conditions.* For these conditions, Figure 32 shows the relations obtained for β_{max} versus VEW/VEW_2, j/j_2, VL/VL_2, and VH/VH_2. Varying the separate values of VEW, j, and VH from one half to twice their baseline values influenced STAM-predicted β_{max} values only slightly. The curve for β_{max} versus VL/VL_2 in Figure 32 is much steeper on both sides of an abscissa value of 1.0 than are the other three curves in the figure, indicating that, relative to the Table 3 design guidelines, VL influences β_{max} much more strongly than do VEW, j, and VH.

---

* A plot of angle β_{max} versus vehicle heading angle ϕ showed that the largest value of β_{max} was obtained at ϕ = 15 deg (in essentially the same way that the plot in Figure 30 showed that the largest value of α_{max} was obtained at ϕ = 60 deg).

216. Since β_{max} = 0.42 rad in Figure 32 for an abscissa value of 1.0, this indicates that the Table 3 guidelines define a vehicle that is not well suited to resisting longitudinal overturn for the conditions of Figure 32. Because VL influences β_{max} much more than do VEW, j, and VH, the strongest action to reduce β_{max} would be to increase VL. Ordinarily, however, VL can be increased from its baseline value by only about 10 percent, since the baseline VL value is closely related to specified vehicle chassis length. From Figure 32, increasing VL/VL_2 from 1.0 to 1.1 decreases β_{max} only slightly.

217. Summary evaluation for the STAM trafficability and stability submodels. Let designations T-I, T-F, and T-C identify the trafficability subroutines for vehicle/obstacle geometric interference, for fine-grained soils, and for coarse-grained soils, respectively, and let designations S-Lat and S-Long identify the stability subroutines for resistance to lateral and to longitudinal overturn, respectively. Types "a" and "b" evaluations (defined in paragraph 184) for these subroutines were described in these paragraphs:

	Paragraph Numbers Wherein Evaluations Were Made				
Type Evaluation	Subroutine T-I	Subroutine T-F	Subroutine T-C	Subroutine S-Lat.	Subroutine S-Long
a	186-189	192-195	200	204-207	214
b	186-189	197-199	201-202	208-213	215

218. Major findings determined herein for the subroutines of the STAM trafficability and stability submodels relative to the type "a" evaluation of paragraph 184 are summarized in Figure 33. Entries under the first column heading name the parameters for which type "a" evaluations have been made herein. The remaining columns are paired, with the first column in each case identifying the paragraphs wherein a type "a" evaluation was made for a given parameter and subroutine, and the second column describing the conclusion reached in these paragraphs as to whether the parameter's value should be increased or decreased to cause STAM-predicted vehicle performance to improve.

219. The tabulation in Figure 33 illustrates that a sizeable number of conflicts exist among the STAM subroutines as to which type of change

(increase or decrease) in the value of a given design parameter will cause predicted vehicle performance to improve. This suggests that trade-offs in assigning values to a number of vehicle design parameters are a basic part of the design process for vehicles intended to perform in the nearshore environment. Thus, while it is important to recognize the patterns by which changes in vehicle design parameter values influence the performance predicted by individual STAM subroutines (as has been evaluated to this point), it is more important to evaluate trade-offs in parameter values that will lead to predicted optimum overall performance. It is necessary, then, to move from the "a" and "b" evaluations of paragraph 184 relative to individual vehicle design parameters and individual STAM subroutines to corresponding "a" and "b" evaluations relative to two or more vehicle design parameters and the STAM model as a whole.

220. Illustration of a trade-off in vehicle design parameter values. Recall that the influence of vehicle design parameter VW on STAM-predicted α_{max} was described in Figure 31 and paragraphs 208-213, the influence of VL on β_{max} in Figure 32 and paragraph 215. It is possible to demonstrate at least one type of trade-off in VW and VL values relative to both α_{max} and β_{max} based on the following three relations that exist between Figures 31 and 32: (a) all baseline conditions in Figures 31 and 32 were the same (i.e., identical values were used for the vehicle design, vehicle performance,* and nearshore environmental parameters); (b) the baseline VW and VL values of example vehicle 2 were VW_2 = 216 in., VL_2 = 225 in., so that VW_2/VL_2 = 0.96; and (c) the value of VL was held constant in Figure 31 as values of VW/VW_2 were varied, while VW value was held constant in Figure 32 as VL/VL_2 values were varied.

221. Because of the above three relationships, an increase in the value of VW/VW_2 from 1.0 to some value, e.g. 1.2, in Figure 31 causes the value of VW/VL to change from 0.96 to 0.96 × 1.2 = 1.15. A corresponding change in the value of VW/VL in Figure 32 results if VL/VL_2 is

---

* The fact that vehicle heading angle ϕ was 60 deg in Figure 31 and 15 deg in Figure 32 has no effect on the analysis in paragraphs 220-221.

changed from 1 to 1/1.2. That is, in terms of the ratio VW/VL, a change in VW/VW_2 value from 1 to n in Figure 31 corresponds to a change in VL/VL_2 value from 1 to 1/n in Figure 32. Because of this relationship, it is possible to determine that single value of VW/VL for which α_{max} in Figure 31 and β_{max} in Figure 32 are most nearly equal. This near-balance is achieved at $VW/VW_2 = 0.82$ in Figure 31, $VL/VL_2 = 1.22$ in Figure 32, where $\alpha_{max} = 0.35$ rad and $\beta_{max} = 0.34$ rad, respectively. Thus, for the one particular set of baseline conditions in Figures 31 and 32, vehicle resistance to lateral and to longitudinal overturn, considered together, would be improved by changing example vehicle 2's VW/VL value from 0.96 to $0.96 \times 0.82 = 0.79$.*

222. A general approach to making nearshore vehicle design trade-offs. The trade-off analysis described in paragraphs 220-221 illustrates just one of literally an infinite number of situations under which a balance might be sought in the values assigned to two or more vehicle design parameters to achieve STAM-predicted optimum overall vehicle performance. Here, a given "situation" is defined by the particular combination of (a) vehicle design parameters whose value trade-offs the vehicle designer desires to evaluate; (b) types of STAM-predicted performance the designer wishes to consider; and (c) values taken for the baseline parameters** of the STAM subroutines of interest. Generally, the situation in trade-off analysis will be much more complex than that in paragraphs 220-221 (where only two vehicle design parameters, two STAM subroutines, and one set of baseline parameter values were considered). Each situation should be manageable, however, if the approach taken in the trade-off analysis follows these steps:

---

* The value of VW/VL at which STAM predicts good balance between tracked vehicle ability to resist both lateral and longitudinal overturn changes as the nearshore environmental and vehicle operating conditions change--it is not constant at VW/VL = 0.79.

** Baseline parameters are the vehicle design, nearshore environmental, and vehicle operating parameters required as input values to the STAM subroutines.

1. Specify values of (a) the vehicle performance requirements (drawbar pull, vehicle payload, maximum vehicle speed, etc.) and (b) the baseline parameters that define each STAM subroutine of interest to the vehicle designer.

2. Designate, among all the vehicle design parameters, which ones will be treated as variables and which ones will have their values held constant.

3. Exercise STAM by systematically varying the values of those vehicle design parameters that are designated as variables (step 2) in the STAM subroutines of interest (step 1) until the best vehicle design is obtained that is capable of satisfying the specified vehicle performance requirements (step 1) in the specified nearshore environment (step 1).

223. Generally, all subroutines in all four blocks of STAM (Figure 9) should be exercised in a given vehicle design (trade-off) analysis. Step 1 in paragraph 222 requires value specification for (a) the vehicle design parameters listed in Table 2, (b) the nearshore environmental parameters listed in columns 3-9 of Table A1, and (c) vehicle operating parameter ϕ (vehicle heading angle). The two or more vehicle design parameters to be considered as variables in step 2 of paragraph 222 ordinarily should come from those parameters listed in the tabulation in Figure 33.* Finally, to obtain the final vehicle design an effective iterative procedure must be used, as outlined in step 3 in paragraph 222. As a building is structurally designed from top to bottom, so the design of a candidate nearshore, bottom-crawling tracked vehicle ordinarily should proceed from vehicle top to bottom. The starting point is to define the vehicle's payload body and cab (i.e., the vehicle upper structure) in terms of those dimensions, weights, shapes, center of gravity locations, etc., that are (a) pertinent to implementation of the STAM subroutines and (b) descriptive of the vehicle's upper structure for (at least) the empty and fully loaded payload conditions.

---

* In addition to the vehicle design parameters listed in the tabulation in Figure 33, a sizeable number of other design parameters are required by the STAM trafficability submodel--see Table 2, for instance. Parameters in Table 2 that do not appear in the Figure 33 tabulation, unless they are assigned unusually large or small values, ordinarily have much less influence on STAM-predicted vehicle trafficability performance than do the Figure 33 parameters.

224. Next, those vehicle chassis that are compatible with the characteristics of the vehicle's upper structure should be selected as candidate chassis. Each chassis considered ordinarily will include a crossover frame,* two tracks, and an individual power supply (probably a hydraulic motor) for each track. Often, a single track chassis offers choice among two or more track sizes (i.e., track widths) and among two or more track gauges (i.e., distances between track center lines of a vehicle). If a single chassis does not offer variations in both track size and gauge, then at least two different chassis should be included for evaluation. In any case, the one or more chassis selected as candidates should offer the possibility of varying conceptual values of both track width and track gauge (and, thus, vehicle width).

225. To this point, the candidate overall vehicle designs are defined by combinations of (a) one upper structure, both loaded and unloaded (paragraph 223), and (b) one or more candidate vehicle chassis (paragraph 224). Before exercising STAM in the vehicle design process, values must be computed for all of the vehicle design parameters required by STAM in terms of each overall candidate vehicle design. Also before employing STAM, it is advisable to make the following hand calculations for each candidate design:

a. Compute $TL/(VW - TW)$. The value of this term should lie between 1 and 2 to render the vehicle easily skid-steerable.

b. If the vehicle is to operate in fine-grained soils, compute the two extreme values of the vehicle's mobility index: MI_ℓ for the vehicle unloaded and submerged (lightest vehicle weight), and MI_h for the vehicle fully loaded in air (heaviest vehicle weight). Carry out, as appropriate, the procedures described in paragraphs 199, 198, and 197 to determine the largest acceptable values of MI that correspond to the vehicle's being able to provide

---

* The crossover frame connects the two tracks of the vehicle and provides the base upon which the upper structure (payload body and cab) of the vehicle are built.

required tractive force, provide required drawbar pull, and negotiate soft soil, repectively.* The candidate design is acceptable if its MI_f is smaller than the MI's computed from the procedures of paragraphs 199 and 198 and if its MI_h value is smaller than MI compute from the procedure of paragraph 197.

c. If the vehicle is to operate in coarse-grained soils, compute the value of sand-track mobility number N_s (defined in paragraph 111). It is advisable that the vehicle be designed such that $N_s \geq 50$; for even extremely small values of sand strength G, this requirement nearly always can be satisifed. With $N_s \geq 50$, Equations 9-12 can be used in conjunction with Equations 1-4 to evaluate predicted vehicle ability to satisfy drawbar pull and tractive force requirements. (If the value of G is such that $N_s \geq 50$, this always indicates that the vehicle can move under its own power.)

Preliminary check a is a general one, and checks b and c relate to the STAM trafficability submodel.** STAM's stability submodel depends, among other things, on the water force values predicted by block 2 of STAM (Figure 9). Thus, any preliminary checks relative to vehicle stability performance would be rather crude and would depend on gross estimates of the values of water forces to be encountered.

226. The next and final step in the vehicle trade-off analysis is to exercise STAM iteratively for each overall candidate vehicle design. Ordinarily, STAM should be exercised in successive runs starting with the most desirable concept vehicle (usually the smallest and least expensive one), then the second-most desirable, etc., until the best design is identified that STAM predicts can perform acceptably in a particular nearshore environment. Guidance as to whether the value of a given vehicle design parameter should be increased or decreased to

---

* TF requirements generally are more difficult to satisfy than are DBP requirements, and each of these is more difficult to satisfy than simply negotiating soft soil. Hence, if all three of these types of performance are to be considered, the procedures in paragraphs 201, 200, and 199 should be used in that order.

** At present, preliminary checks a, b, and c must be made by hand. Subsequent work to increase STAM's capabilities should include consideration of incorporating these checks within the structure of STAM.

improve predicted vehicle performance in successive STAM runs can be obtained from paragraphs 186-189, 192-195, and 200 for the STAM trafficability submodel and from paragraphs 204-207 and 214 for the STAM stability submodel (Figure 33).

227. The general approach to making nearshore vehicle design trade-offs described in paragraphs 221-226 will fit many, if not most, actual situations. While each particular design analysis will have its own peculiar set of restrictions, some common general points will be found among most designs. Vehicle cost will almost always be a primary consideration. Nearly always, the outer faces of the vehicle should be streamlined and as open to water flow as possible to promote the smallest possible water forces. The vehicle nearly always should be low, wide, and rugged. But beyond these general points, each particular vehicle design will focus on its own ordering of design parameters in terms of their importance to the design at hand. Thus, each actual nearshore vehicle design trade-off analysis must be pursued on an ad hoc basis (following a design procedure similar to that described in paragraphs 222-226). In this connection STAM is a first-generation computerized model that describes vehicle/soil/water force interactions quantitatively and in sufficient detail to allow this model to be used as the key part of analyses for the selection and preliminary design of a nearshore vehicle's running gear and chassis configuration.

Parametric Analysis of STAM

228. The analyses described under the previous center heading, "Evaluation of Vehicle Design Parameter Influence on Predicted Nearshore Vehicle Performance" (paragraphs 178-227), constitute a parametric analysis of STAM in the functional sense. That is, these analyses described (a) the influence of changes in vehicle design parameter values on STAM-predicted performance in individual STAM subroutines, (b) guidance as to how rational trade-offs can be made among values of vehicle design parameters to obtain predicted optimum vehicle performance for all STAM subroutines, and (c) methods by which evaluations can

be made as to what constitutes an unrealistic grouping of values of vehicle design, vehicle performance, and nearshore environmental parameters. The parametric analysis of STAM is completed by dealing with the question "What parameters are required to describe STAM?" This question was answered by supplying to the project sponsor a listing of all parameters included in STAM, where each parameter was described by (a) its symbol as used in STAM (i.e., its computer symbol), (b) the STAM submodel in which the parameter is used, (c) the parameter's definition, and (d) the units of the parameter as it is used in STAM. Finally, Appendix C presents definitions of all notations used in the text of this report, including all STAM parameters referred to in the report.

PART V: CONCLUSIONS AND RECOMMENDATIONS

Conclusions

229. The foregoing analysis is considered adequate basis for the following conclusions:

a. The environmental conditions that most strongly influence the trafficability and stability performance of a vehicle operating on the nearshore ocean bottom are: (1) water forces acting on the vehicle, (2) seafloor soil strength, (3) seafloor microrelief (local slope and obstacles), and (4) turbidity. Conditions 1-3 can now be described by parameters that are sufficiently quantifiable to permit these parameters' use in a mathematical model of nearshore vehicle performance. The state of the art does not allow the effects of turbidity to be included in such a model.

b. The ideal nearshore, bottom-crawling vehicle should: (1) be powered and steerable, (2) be streamlined, (3) be rugged, (4) be low and wide, with a low center of gravity, (5) have low-ground contact pressure, (6) have running gear outer faces configured to gain maximum available tractive force, and (7) have chassis and running gear configured to provide maximum obstacle override capability.

c. The chassis/running gear combination that appears most suitable for satisfying the criteria of b above in near-future applications is a single-unit chassis mounted on two wide, rugged tracks. This conclusion was reached by evaluating both (1) the anticipated nearshore performance capabilities of all types of chassis and running gears presently available and (2) reported experience in nearshore vehicle operation on a worldwide basis.

d. The Surfzone Transition Analytical Methodology (STAM) developed herein is a computerized mathematical model that requires detailed input descriptions of (1) the bottom-crawling vehicle's design characteristics, (2) the nearshore environment of concern, and (3) the vehicle's performance requirements. From this input, STAM can predict (1) the values of major water forces acting on the vehicle and (2) the vehicle's trafficability and stability performance.

e. In example selection problems that included nearshore environmental conditions from moderate to very severe, STAM predicted that five types of nearshore bottom crawlers, which were designed to satisfy the criteria of

b above, can perform well in terms of both trafficability and stability.

f. STAM uses rather complex subroutines to describe various aspects of nearshore trafficability performance (vehicle/obstacle interference and vehicle ability to negotiate soft soils, develop drawbar pull, and develop tractive force in fine- and coarse-grained soils) and vehicle stability performance (vehicle resistance to lateral and to longitudinal overturn, vehicle ability to maintain forward motion and to resist side sliding). Examination of the roles of all the vehicle design parameters included in STAM's trafficability and stability submodel showed that, for some design parameters, a change in the parameter's value (say, increasing track length) causes all aspects of STAM-predicted vehicle performance to improve. For a sizeable number of design parameters, however, a change in the parameter's value (say, an increase in gross vehicle weight) causes some aspects of predicted performance to improve, other aspects to worsen.

g. STAM can be utilized in a systematic approach to determine whether specified values of nearshore environmental parameters, vehicle performance requirements, and vehicle design parameters constitute a realistic or an unrealistic grouping relative to predicted vehicle trafficability and stability performance. Further, in vehicle design applications, STAM can be used to determine an optimum design that satisfies or comes closest to satisfying stated vehicle performance requirements for a specified nearshore environment and a given vehicle design envelope (i.e., a set of limits within which values of the vehicle design parameters can vary).

h. In the two types of STAM applications described in g, the user of STAM must exercise good judgment if he is to apply STAM efficiently to his particular vehicle performance evaluation or vehicle design problem. Detailed guidelines provided in this report relative to both of these types of STAM applications can be used directly as presented in the report or can be readily adapted to particular evaluation or design situations.

Recommendations

230. It is recommended that:

a. Study be undertaken to quantify turbidity and to develop a means for predicting its value as a function of pertinent nearshore environmental, vehicle design, and vehicle operational parameters.

b. Research be conducted to develop a proven methodology for predicting vehicle trafficability performance in submerged coarse-grained (sandy) soils. Further, the methodology now incorporated in STAM for this purpose should, at a minimum, be refined in the next-generation version of STAM to reflect performance predicted as a function of the sand-track mobility number.

c. Work be done to incorporate into STAM the capability to predict accurately the influence of pitch and yaw (steering) articulation on the trafficability and stability performance of multi-unit tracked vehicles.

d. In light of the difficulties in defining drag, inertial and lift coefficients for a variety of underwater vehicles in an oscillatory velocity field, carefully conceived scale model tests be conducted to evaluate these important coefficients. Further, scale model testing of breaking wave forces should be done to gain insight into vehicle overturning problems and other potential vehicle operational constraints in high force regions where analytical solutions are not obtainable.

e. The first-generation, desk-study version of STAM developed in this report be refined and verified to predict actual nearshore vehicle trafficability and stability performance accurately. This should be accomplished in stages--first by scale-model laboratory testing; next by carefully controlled prototype vehicle testing in a precisely described nearshore region; and finally by practical applications involving a broad range of bottom-crawling vehicles and nearshore environments.

REFERENCES

1. Wiendieck, K. W., "A Preliminary Study of Seafloor Trafficability and Its Prediction," Technical Report No. M-70-8, Jul 1970, U. S. Army Engineer Waterways Experiment Station, CE, Vicksburg, Miss.

2. Roren, E. M. Q. and Overvik, T., "Behavior of Structures and Structural Design," Behavior of Off-Shore Structures (BOSS '76), Proceedings of the First International Conference, Vol 1, Norwegian Institute of Technology, Trondheim, 1976, p 104.

3. Herrmann, H. G., III, "Classification of Sites and Their Environmental Characteristics Affecting Design/Performance of Nearshore/Surfzone Bottom Crawling Equipment," Technical Memorandum TM-42-77-15, Civil Engineering Laboratory, NCBC, Port Hueneme, Calif.

4. Demars, K. R. and Taylor, R. J., "Naval Seafloor Soil Sampling and In-Place Test Equipment: A Performance Evaluation," Technical Report R730, Jun 1971, U. S. Naval Civil Engineering Laboratory, Port Hueneme, Calif.

5. Izumi, H., Kawauchi, M., Terayama, T., and Yoneda, T., "Development of a Survey and Inspection Robot System for Underwater Construction Works," Proceedings of the Fourth International Symposium on Industrial Robots, Vol 1, Tokyo, Japan, 1974, pp 43-52.

6. Turnage, G. W., "Measuring Soil Properties in Vehicle Mobility Research; Effects of Velocity, Size, and Shape of Probes on Penetration Resistance of Fine-Grained Soils," Technical Report No. 3-652, Report 3, Nov 1970, U. S. Army Engineer Waterways Experiment Station, CE, Vicksburg, Miss.

7. Smith, J. L., "Strength-Moisture-Density Relations of Fine-Grained Soils in Vehicle Mobility Research," Technical Report No. 3-639, Jan 1964, U. S. Army Engineer Waterways Experiment Station, CE, Vicksburg, Miss.

8. Duncan, C. C., "Plowing Cables Under the Sea," International Conference on Communications of the Institute of Electrical and Electronic Engineers, Philadelphia, Pa., Jun 1968.

9. Rockwell, P. K., "Deep Ocean Cable Burial Concept Development," Technical Note N-1453, Aug 1976, Civil Engineering Laboratory, NCBC, Port Hueneme, Calif.

10. Bayles, J. J., "Trafficability on the Ocean Floor; Conquering the Benthos," Technical Note N-649, Jan 1965, U. S. Naval Civil Engineering Laboratory, Port Hueneme, Calif.

11. Nuttall, C. J., Jr., "Ground-Crawling: 1966, The State-of-the-Art of Designing Off-Road Vehicles," Contract Report 3-162, May 1967, U. S. Army Engineer Waterways Experiment Station, CE, Vicksburg, Miss.

12. Sunobe, K., Izumi, H., Kawasaki, H., Anazi, T., Murata, T., and Itami, Y., "Development of Underwater Bulldozer Systems," Second International Ocean Development Conference, Tokyo, Japan, Oct 1972, p 13.

13. Willoughby, W. E., "Low-Ground-Pressure Construction Equipment for Use in Dredged Material Containment Area Operations and Maintenance Performance Predictions," Technical Report D-77-7, Aug 1977, U. S. Army Engineer Waterways Experiment Station, CE, Vicksburg, Miss.

14. Hanamoto, B., "Cobra: Positive Pitch Controlled Articulated Testbed," Special Report 207, May 1974, U. S. Army Engineer Cold Regions Research and Engineering Laboratory, CE, Hanover, N.H.

15. Beck, R. R. and Kamm, I. O., "A Cybernetically Coupled Research Vehicle," Automotive Engineering Congress and Exposition, Detroit, Mich, Feb 24-28, 1975, Society of Automotive Engineers, Inc., Paper No. 750217.

16. Brackett, R. L., Tausig, W. R., and Herrmann, H. G., III, "Nearshore Trencher, Part II: Concept Development," Technical Memorandum No. 43-77-09, Mar 1977, Civil Engineering Laboratory, NCBC, Port Hueneme, Calif.

17. Banzoli, V., DiTella, V., Dossi, L., and Gava, P., (Italian), "New Concept of Underwater Remote Controlled Tracked Vehicle for Deep-Water Trenching Operations," Paper No. OTC 2587, Eighth Annual Offshore Technology Conference, May 1976, Houston, Tex.

18. Itami, Y., Fukubayashi, N., Izumi, H., and Murata, T., (Japanese), "Leveling Method of the Riprap Mound by the Underwater Bulldozer," Third International Ocean Development Conference, Tokyo, Japan Aug 1975, pp 343-357.

19. Daniell, F. (English), "A Heavy-Duty Sea Bed Work Vehicle," Ocean Industry Digest, Vol 4, No. 3, Mar 1969, pp 77-87.

20. Reidy, F. A. (American), "Vehicle Makes Ocean-Bottom Surveys," Ocean Industry Digest, Vol 2, No. 6, Jun 1967, pp 40-44.

21. Alexander, C. M., (American) "Seafloor Effectiveness of RUM II," SIO Reference 75-20, Jun 1975, Marine Physical Laboratory, Scripps Institution of Oceanography, San Diego, Calif.

22. Bracket, R., Tausig, W., Herrmann, H., III, Tucker, L., and Ward, C., "Nearshore Trencher, Part I: State-of-the-Art Assessment," Technical Memorandum No. 43-77-03, Oct 1976, Civil Engineering Laboratory, NCBC, Port Hueneme, Calif.

23. Moriya, H. and Ikeda, K., "Development and Undersea Test of Underwater Trencher (UT)," Third International Ocean Development Conference, Tokyo, Japan, Aug 1975, pp 381-399.

24. Ikeda, K. and Moriya, H., "Development and Practical Use of Submersible Dredger," Third International Ocean Development Conference, Tokyo, Japan, Aug 1975, pp 359-380.

25. Shimegi, M., "Designing an Underwater Tractor," Conference of Off-Highway Vehicles, Tractors, and Equipment, Institute of Mechanical Engineering of United Kingdom, Oct 1975, pp 135-142.

26. "The AMC-71 Mobility Model," Technical Report No. 11789 (LL 143), Vols I and II, Jul 1973, U. S. Army Tank-Automotive Command, Warren, Mich.

27. Jurkat, M. P., Nuttall, C. J., and Haley, P. W., "The AMC '74 Mobility Model," Technical Report No. 11921 (LL 149), May 1975, U. S. Army Tank-Automotive Command, Warren, Mich.

28. Green, C. E. and Rula, A. A., "Low-Ground-Pressure Construction Equipment for Use in Dredged Material Containment Area Operation and Maintenance-Equipment Inventory," Technical Report D-77-1, Apr 1977, U. S. Army Engineer Waterways Experiment Station, CE, Vicksburg, Miss.

29. Morison, J. R., O'Brien, M. P., Johnson, J. W., and Schaaf, S. A., "The Force Exerted by Surface Waves on Piles," Petroleum Transcripts, American Institute of Mining Engineers, Vol 189, 1950, pp 149-154.

30. Carr, J. H., "Breaking Wave Forces on Plane Barriers," Report No. E-11.3, Nov 1954, California Institute of Technology, Pasadena, Calif.

31. Beckman, H. and Thibodeaux, M. H., "Wave Force Coefficients for Offshore Pipelines," Journal of the Waterways and Harbors Division, American Society of Civil Engineers, Vol 88, No. WW2, May 1962, pp 125-138.

32. Brates, E. F. and Wallace, R., "Wave Forces on Submerged Pipelines," Proceedings of the 13th Coastal Engineering Conference, American Society of Civil Engineers, Vol III, 1972, pp 1703-1722.

33. Castiel, J., "Breaking Wave Forces on Submarine Pipelines, Experimental Investigation," Miscellaneous Report No. 13, University of Hawaii-Look Laboratory-76-m-13, Aug 1976, University of Hawaii, James K. K. Look Laboratory of Oceanographic Engineering, Hawaii.

34. Herbich, J. B. and Shank, G. E., "Forces Due to Waves on Submerged Structures," Journal of the Waterways and Harbors Division, American Society of Civil Engineers, Vol 97, No. WW1, Feb 1971, pp 57-77.

35. Hoerner, S. F., "Fluid Dynamic Drag," 1965 (Published by the author).

36. Riabouchinski, D., "Sur la resistance des Fluides," Comptes Rend Congress International des Mathematiciens, 1920, pp 568-585.

37. Goda, Y., "Wave Forces on a Vertical Circular Cylinder: Experiments and a Proposed Method of Wave Force Computation," Report 8, Port Harbor Technical Research Institute, 1964.

38. LeMéhauté, B., Divoky, D., Lin, A., "Shallow Water Waves: A Comparison of Theory and Experiment," Proceedings of the 11th Conference on Coastal Engineering, American Society of Civil Engineers, Vol I, 1968, pp 86-107.

39. Eagleson, P. S. and Dean, R. G., "Small Amplitude Wave Theory," Estuary and Coastal Hydrodynamics, A. T. Ippen, ed., McGraw-Hill, New York, 1966, pp 1-92.

40. Wiegel, R. L., Beebe, K. E., and Moon, J., "Ocean Wave Forces on Circular Cylindrical Piles," Journal of the Hydraulics Division American Society of Civil Engineering, Vol 83, No. HY2, Apr 1957, pp H99-1 to H99-36.

41. Wilson, B. W. and Reid, R. O., "Discussion of Wave Force Coefficient for Offshore Pipelines," by Beckman and Thibodeaux, Journal of Waterways and Harbors, American Society of Civil Engineers, Vol 89, No. WW1, Feb 1963, pp 61-65.

42. Gaillard, D. O., "Wave Action in Relation to Engineering Structures," reprinted 1935, Ft. Belvoir, Va., U. S. Army Corps of Engineers, The Engineer School, 1904.

43. Molitor, D. A., "Wave Pressures on Sea-Walls and Breakwaters," Transactions, American Society of Civil Engineers, Paper No. 1913, 1935, pp 984-1017.

44. Bognold, R. A., "Interim Report on Wave Pressure Research, " Journal, Institute of Civil Engineering, Vol 12, 1939, pp 201-226.

45. Denny, F. D., "Further Experiments on Wave Pressure," Journal, Institute of Civil Engieering, No. 4, Feb 1951, pp 330-345.

46. Minikin, R. R., Winds, Waves and Maritime Structures, "2nd ed," Griffin, London, 1963.

47. Miller, R. L. et al., "Field Measurements of Impact Pressures in Surf," Proceedings of the 14th Coastal Engineering Conference, American Society of Civil Engineers, Vol III, Chapter 103, 1974, pp 1761-1777.

48. Wiegel, R. L. and Beebe, K. E., "The Design Wave in Shallow Water," Journal of the Waterways Division, American Society of Civil Engineering, Vol 82, No. WWI (Paper 910) Mar 1956.

49. Silvester, R., Coastal Engineering, I, Elsevier, Amsterdam, 1974.

50. Horikawa, K. and Kuo, C. T., "A Study on Wave Transformation Inside the Surf Zone," Proceedings of the 10th Conference on Coastal Engineering, Vol 1, 1966, pp 217-233.

51. Nakamura, M., Sheraeshi, H., and Susaki, Y., "Wave Decaying Due to Breaking," Proceedings of the 10th Conference on Coastal Engineering, Vol 1, 1966, pp 234-253.

52. Iwagaki, Y., "Hyperbolic Waves and Their Shoaling," Proceedings of the 11th Conference on Coastal Engineering, Vol 1, 1968, pp 214-244.

53. Hayashi, T. and Hattori, M., "Pressure of the Breaker Against a Vertical Wall," Proceedings, Coastal Engineering in Japan, Vol 1958, pp 25-37.

54. LeMehauté, B. and Koh, R. C. Y., "On the Breaking of Waves Arriving at an Angle to the Shore," Journal of Hydraulic Research, 5, 1967, pp 67-80.

55. Collins, I. A., "Probabilities of Breaking Wave Characteristics," Proceedings of the 12th Conference on Coastal Engineering, Vol 1, 1970, pp 399-414.

56. Galvin, C. J., Jr., "Breaker Travel and Choice of Design Wave Height," Journal of the Waterways and Harbors Division, American Society of Civil Engineers, Vol 95, No. WW2, Paper 6569, 1969.

57. Jurkat, M. P., Nuttall, C. J., Jr., and Haley, P. W., "The U. S. Army Mobility Model (AMM-75)," Proceedings of the Fifth International Conference, The International Society for Terrain-Vehicle Systems, Inc., Detroit, Mich, Vol 4, Jun 1975.

58. Nuttall, C. J., Jr., and Randolph, D. D., "Mobility Analysis of Standard-and High-Mobility Tactical Support Vehicles (HIMO Study)," Technical Report No. M-76-3, Feb 1976, U. S. Army Engineer Waterways Experiment Station, CE, Vicksburg, Miss.

59. Turnage, G. W., "Performance of Soils Under Track Loads; Track Mobility Number for Coarse-Grained Soils," Technical Report M-71-5, Report 3, May 1976, U. S. Army Engineer Waterways Experiment Station, CE, Vicksburg, Miss.

60. Dugoff, H. and Ehrlich, I. R., "Model Tests in Submerged Soils," Journal of Terramechanics, Vol 3, No. 4, 1966, pp 53-70.

61. Baladi, G. Y. and Rohani, B., "Liquefaction Potential of Dams and Foundations; Development of an Elastic-Plastic Constitutive Relationship for Saturated Sand," Research Report S-76-2, Report 3, Feb 1977, U. S. Army Engineer Waterways Experiment Station, CE, Vicksburg, Miss.

Table 1

Values of Vehicle Basic Design and Performance Parameters

Specified for the Five Example Vehicles

Parameter Symbol	Parameter Name	Parameter Unit	Value of Parameter for Vehicle No. 1	2	3	4	5
	Vehicle Basic Design Parameters						
Dry W_{LC}	Dry weight of loaded chassis	lb	5,500	18,000	20,000	50,000	40,000
Wet W_{LC}	Submerged weight of loaded chassis	lb	3,000	13,000	14,000	35,000	35,000
CW	Chassis width	in.	48	84	72	83*	96
CH	Chassis height	in.	36	60	24	42*	72
CL	Chassis length	in.	180	180	192	220	192
Dry W_p	Dry payload weight	lb	1,000	7,500	10,000	0	0
PW_{max}	Maximum payload width	in.	0	72	60	0	0
PH_{max}	Maximum payload height	in.	0	48	72	0	0
PL_{max}	Maximum payload length	in.	0	120	120	0	0
	Vehicle Performance Parameters						
V_{max}	Maximum vehicle speed	ft/sec	3.4	2	2	0.083**	2
$DBP_{req'd}$	Required drawbar pull	lb	100	0	0	4,500	30,000

* For example vehicle 4, the seafloor trencher, take the chassis cross-sectional area from the front to be 0.4 (60 sq ft) = 24 sq ft, and from side to be 0.8 (80 sq ft) = 64 sq ft. Take CH to be 3.5 ft. Then CW = 24 sq ft ÷ 3.5 ft = 6.9 ft = 83 in. And CL = 64 sq ft ÷ 3.5 ft = 18.3 ft = 220 in.

** Also, for example vehicle 4, the "V_{max}" value of 0.083 ft/sec listed above is the maximum operational (working) speed of the vehicle. For vehicle 4 traveling to and from the work site under tractive force requirements much less than those at the work site, the vehicle can be geared to travel at much higher speed--e.g., on the order of 1-2 ft/sec.

Table 2

Computed and Assigned Values of Vehicle Design Parameters Used by STAM in the Example Selection Problems

Parameter Symbol*	Parameter Unit	Parameter Value for Example Vehicle No. 1	2	3	4	5
		Water Force Calculations Submodel				
VL	in.	180	225	240	275	336
VHF	ft	5.50	7.50	9.50	6.67	8.67
VFW	ft	10.83	18.00	17.67	20.25	19.67
DRYWT	lb	16,990	63,360	71,460	138,090	106,890
SUBWT	lb	10,810	45,760	57,170	96,660	93,530
		Trafficability Submodel				
VT^{a}*	-	0**	0	0	0	0
GVW	lb	16,990	63,360	71,460	138,090	106,890
VL	in.	180	225	240	275	336
VW	in.	130	216	212	243	236
HLE†	in.	34	22.5	24	27.5	24
HAA^{b}	in.	34	22.5	24	27.5	24
GC†	in.	15	15	16	19	16
DS	in.	54	90	96	110	96

Note: Parameter symbols not defined in Table 2 can be found in Appendix D: Notation.

* In the first column, superscript a indicates that the value of the parameter was assigned to notify the trafficability submodel of some particular vehicle characteristic; superscript b indicates that a value was assigned for a parameter; and no superscript indicates that the parameter value was computed using the guidelines of Table 3.

** For vehicle type VT, 0 = tracked vehicle and 1 = wheeled vehicle.

† Values of height of leading edge HLE and ground clearance GC were assigned for example vehicle 1 and computed for example vehicles 2-5.

(Continued)

Table 2 (Continued)

Parameter Symbol	Parameter Unit	Parameter Value for Example Vehicle No. 1	2	3	4	5
		Trafficability Submodel (Continued)				
DCG_b	in.	90.1	111.8	117.4	143.3	126.2
VAA^b	deg	45	90	90	90	90
ACG	deg	3.2	8.5	7.6	6.8	10.4
FLEW	lb	33,980	126,720	142,920	276,180	213,870
TLC	in.	111	183	195	223	195
TL	in.	108	180	192	220	192
TW	in.	38	63	67	77	67
ATS	sq in.	217	595	673	889	673
BN_b	-	12	9	10	11	10
GH^a	in.	1.0	1.0	2.0	2.0	2.0
TT^b	-	0*	1	1	1	1
TN	-	2	2	2	2	2
RWR	in.	10.6	23.3	24.8	28.7	25.0
RISR	in.	10.6	23.3	24.8	28.7	25.0
HRIS	in.	25	23.3	24.8	28.7	25.0
$DRISCG_b$	in.	79.1	89.3	93.4	115.8	102.2
XBC	-	0.8	0.8	0.8	0.8	0.8
CGF	in.	54	91.7	99.4	105.0	91.5
CGH	in.	19.2	13.1	12.5	13.7	18.5
REC**	in.	36	22.5	24	27.5	25.0
RWW_b	in.	10.6	23.3	24.8	28.7	25.0
VDA^b	deg	45	90	90	90	90

* For track type TT, 0 = flexible and 1 = girderized.

** The value of height of vehicle trailing edge REC was assigned for example vehicle 1 and computed for example vehicles 2-5.

(Continued)

Table 2 (Continued)

Parameter Symbol	Parameter Unit	Parameter Value for Example Vehicle No. 1	2	3	4	5
		Trafficability Submodel (Concluded)				
$TVAR^{a}$*	-	0	0	0	0	0
EFF^{b}	-	0.95	0.95	0.95	0.95	0.95
FDR^{b}	-	1	1	1	1	1
$FDREF^{b}$	-	0.98	0.98	0.98	0.98	0.98
HPT	hp/ton	12.4	7.3	7.2	0.30	7.3
VLWOB**	in.	-	-	-	-	240
W_t	lb	11,490	45,360	51,460	88,090	66,890
TH	in.	36	45	48	55	48
RGCH	in.	15	15	16	19	16

Coordinates of drive sprocket speed (DDS) versus tractive force (TF) curve		1 DSS	1 TF	2 DSS	2 TF	3 DSS	3 TF	4 DSS	4 TF	5 DSS	5 TF
	mph versus lb	-0	98,542	-0	430,849	0	485,929	0	781,575	0	726,851
		0.4	98,542	0.2	430,849	0.2	485,929	0.010	781,575	0.2	726,851
		0.6	65,694	0.4	215,424	0.4	242,964	0.015	521,050	0.4	363,426
		0.8	49,271	0.6	143,616	0.6	161,976	0.020	390,788	0.6	242,284
		1.0	39,417	0.8	107,712	0.8	121,482	0.025	312,630	0.8	181,713
		1.2	32,847	1.0	86,170	1.0	97,186	0.030	260,525	1.0	145,370
		1.4	28,155	1.2	71,808	1.2	80,988	0.035	223,307	1.2	121,142
		1.6	24,635	1.36	63,360	1.36	71,460	0.040	195,394	1.36	106,890
		1.8	21,898	1.36	0	1.36	0	0.045	173,683	1.36	0
		2.0	19,708					0.050	156,315		
		2.2	17,917					0.055	142,105		
		2.32	16,990					0.0566	138,090		
		2.32	0					0.0566†	0		

* For TVAR, 0 = automatic and 1 = manual transmission.

** Parameters VLWOB, W_t, TH, and RGCH are not required as input by the trafficability submodel per se. For the five example vehicles, values of these parameters were computed as part of the scheme outlined in Table 3 for defining the values of those preliminary design parameters that are required to implement STAM.

† See second footnote of Table 1 regarding the difference between maximum operational speed (0.083 ft/sec or 0.0566 mph) and maximum travel speed of example vehicle 4.

(Continued)

Table 2 (Concluded)

Parameter Symbol	Parameter Unit	Parameter Value for Example Vehicle No. 1	2	3	4	5
		Stability Submodel				
j	in.	29.8	36.4	37.3	42.4	43.5
b	in.	92	153	145	166	169
ℓ_1	in.	54.0	88.3	92.6	105.0	91.5
J_o*	lb-sec^2-in.	315,600; 201,400	3,063,700; 2,218,400	3,276,300; 2,626,700	8,276,400; 5,816,800	6,302,000; 5,520,400
J_p*	lb-sec^2-in.	534,200; 341,100	5,268,700; 3,816,800	5,936,400; 4,760,200	14,992,800; 10,494,600	10,444,000; 9,150,700

* J_o and J_p are used in STAM subroutines that describe vehicle resistance to lateral and to longitudinal overturn, respectively. For each combination of J and example vehicle number, the first J value listed is for the vehicle in-air; the second, for the vehicle fully submerged. Values of J_o and J_p decrease as vehicle effective weight (VEW) decreases.

Table 3

Guidelines Used to Define Vehicle Preliminary Design Parameter Values for the Five Example Vehicles*

Vehicle Parameter Symbol	Vehicle Parameter Unit	Equation	Equation Applies to Vehicle No.	Range of Coefficient Values**	STAM Sub-models†	Comments
TH	in.	TH = 0.2 VL = 0.2 CL	1	0.15-0.25	-	
		= 0.2 VL = 0.25 CL	2, 3, 4	0.15-0.25	-	
		= 0.2 VLWOB	5	0.15-0.25	-	
VLWOB	in.	VLWOB = CL + TH = 1.25 CL	5	1.20-1.30	-	
VL	in.	VL = CL	1		W	
		= CL + TH = 1.25 CL	2, 3, 4	1.20-1.30	W	
		= 1.4 VLWOB	5	1.3-1.5	W	
TL	in.	TL = 0.6 VL	1	0.55-0.7	T	Track ramped at each end
		= VL - TH	2, 3, 4		T	Track semi-circular at each end.
		= VLWOB - TH	5		T	Track semi-circular at each end

Note: Parameter symbols not defined in Table 3 can be found in Appendix D: Notation.

* The five example vehicles are named in paragraph 55.

** In the equations listed, each underlined number represents a coefficient for which any of a range of values might be selected. The range of coefficient values listed in the fifth column is considered to be reasonable and to lead to definition of a vehicle with attributes like those mentioned in paragraphs 52, 53, and 56.

† The "STAM Submodels" are those submodels in which the vehicle design parameters appear. In this table, "W" stands for the water force calculations submodel (block 2 in Figure 9); "T", for the trafficability submodel (block 3); and "S", for the stability submodel (block 4).

(Continued)

Table 3 (Continued)

Vehicle Parameter Symbol	Vehicle Parameter Unit	Equation	Equation Applies to Vehicle No.	Range of Coefficient Values	STAM Sub-models	Comments
VH	in.	$VH = CH + GC + RGCH$ $= GC + TGCH + PH_{max} + 10$	1, 2, 4, 5 3		W*	
TW	in.	$TW = \underline{0.35}\ TL$	1-5	0.2-0.4	T	
VW	in.	$VW = CW + 2\ TW + \underline{6}$	1-5	4-12	W*	6 and 4-12 are not coefficients, but values of clearance between vehicle chassis and running gear (total for both sides of vehicle)
W_t**	lb	$W_t = \underline{2.8} \times TW \times TL$	1	2.2-3.2	-	Rugged tracked running gear
		$= \underline{4.0} \times TW \times TL$	2, 3	3.4-4.4	-	Very rugged tracked running gear
		$= \underline{5.2} \times TW \times TL$	4, 5	4.6-5.6	-	Extremely rugged tracked running gear
GVW	lb	$GVW = \text{dry } W_{LC} + W_t$	1-5		W†, T	

* The water force calculations submodel uses VHF and VWF, vehicle height and vehicle width, respectively, each in ft.

** For $W_t = k \times TW \times TL$, the value of k increases directly with the degree of ruggedness and the load-carrying capability required of the tracked vehicle. For example, the fully loaded in-air weight (excluding running gear and connections thereto) of example vehicle 1 was 5,500 lb (with k = 2.8); the weight of example vehicles 2 and 3 were 18,000 and 20,000 lb, respectively (with k = 4.0), and of example vehicles 4 and 5, 50,000 and 40,000 lb, respectively (with k = 5.2).

† The water force calculations submodel uses DRYWT in place of GVW.

(Continued)

Table 3 (Continued)

Vehicle Parameter Symbol	Vehicle Parameter Unit	Equation	Equation Applies to Vehicle No.	Range of Coefficient Values	STAM Sub-model	Comments
t	in.	$t = VW - TW$	1-5		-	
c	in.	$c = VW - 2TW$	1-5		-	
ATS	sq in.	$ATS = 0.15\ TW \times TW = 0.15\ TW^2$	1-5		T	
BN	-	$BN = \frac{TL}{20}$	1-5		T	Round answer to next larger whole number
HLE	in.	$HLE = 0.5\ TH$	2-5		T	The value of HLE was assigned for vehicle 1
DS	in.	$DS = 0.5\ TL$	1-5		T	
FLEW	lb	$FLEW = 2\ GVW$	1-5		T	
TLC	in.	$TLC = TL + 3$	1-5		T	
RWR	in.	$RWR = \{TL - [(BN - 1) \times 2]\} \div [2\ (BN - 1)] +$ track thickness	1		T	The tracked running gear of vehicle 1 is ramped at each end
		$= \frac{TH}{2}$ + track thickness	2-5		T	The tracked running gears of vehicles 2-5 are semicircular at each end
RISR	in.	$RISR = RWW +$ track thickness	1		T	
		$= \frac{TH}{2}$ + track thickness	2-5		T	
HRIS	in.	$HRIS =$ track height - track thickness - rear sprocket radius	1		T	
		$= \frac{\text{track height}}{2}$ + track thickness	2-5		T	

(Continued)

Table 3 (Continued)

Vehicle Parameter Symbol	Vehicle Parameter Unit	Equation	Equation Applies to Vehicle No.	Range of Coefficient Values	STAM Sub-model	Comments
CGF	in.	$CGF = \frac{TL}{2} + FCG - \frac{VL}{2}$	1-4		T	
		$= VLWOB - (VL - FCG) - \frac{TH}{2}$	5		T	
CGH	in.	CGH = HCG - RWR	1-5		T	
GC	in.	CG = 15	1		T	Value of CG was assigned for vehicle 1
		$GC = \frac{1}{3}TH$	2-5		T	
RGCH	in.	RGCH = 0.4 TH	1		-	
		$= \frac{1}{3}TH$	2-5		-	
REC	in.	REC = 36	1		T	Value of REC was assigned for vehicle 1
		= 0.5 TH	2-5		T	
RWW	in.	RWW = RISR - track thickness	1-5		T	
DRISCG	in.	$DRISCG = \sqrt{a^2 + b^2}$, where	1-5		T	
		a = (CGH + RWR) - HRIS	1-5		T	
		$b = \frac{VL}{2} - RISR$	1		T	
		= VL - CGF	2-5		T	
ACG	in.	$ACG = \sin^{-1}\frac{a}{DRISCG}$	1-5		T	
DCG	in.	DCG = DRISCG + RISR	1		T	
		$= DRISCG + \frac{TH}{2}$	2-5		T	
TF	lb	$TF = \frac{375\ HP}{V}$	1-5		T	V is vehicle translational velocity in mph, measured at the drive sprocket (DSS)*

* See paragraphs 63 and 64 for the scheme used to define TF and DSS for the five example vehicles.

(Continued)

Table 3 (Concluded)

Vehicle Parameter Symbol	Vehicle Parameter Unit	Equation	Equation Applies to Vehicle No.	Range of Coefficient Values	STAM Sub-model	Comments
HPT	hp/ton	HPT = hp/GVW (in tons)	1-5		T	
DRYWT	lb	DRYWT = GVW	1-5		W	
SUBWT	lb	SUBWT = DRYWT × R*	1-5		W	
j	in.	j = CGH + RWR	1-5		S	
b	in.	b = VW - TW	1-5		S	b = t
ℓ_1	in.	ℓ_1 = CGF or TL - CGF, whichever is smaller	1-5		S	
J_o	$lb\text{-}in_2\text{-}sec$	$J_o = \frac{VEW}{g} r_1^2$	1-5		S	r_1 is radius of gyration of the vehicle about point 0 in Figure 20
J_p	$lb\text{-}in_2\text{-}sec$	$J_p = \frac{VLW}{g} r_2^2$	1-5		S	r_2 is radius of gyration of the vehicle about point P in Figure 22

* R = the ratio, submerged weight/dry weight, for a given seafloor vehicle fully loaded but excluding running gear and connections thereto. For each of the five example vehicles, values of R can be determined from information presented in Appendix A.

Table 4

Mobility Index, VCI_1 and VCI_{50} Equations for Self-Propelled Tracked Vehicles

$$\text{Mobility index} = -\left(\frac{\text{contact pressure}}{\text{track factor}} \times \text{weight factor} \times \text{grouser factor} + \text{bogie factor} - \text{clearance factor}\right) \times \text{engine factor} \times \text{transmission factor}$$

wherein

$$\text{contact pressure} = \frac{\text{gross vehicle weight, lb.}}{\text{area of tracks in contact with ground, sq in.}}$$

weight factor: less than 50,000 lb = 1.0
50,000 to 69,999 lb = 1.2
70,000 to 99,999 lb = 1.4
100,000 lb or greater = 1.8

$$\text{track factor} = \frac{\text{track width, in.}}{100}$$

grouser factor: grousers less than 1.5 in. high = 1.0
grousers more than 1.5 in. high = 1.1

$$\text{bogie factor} = \frac{\text{gross weight in lb divided by 10}}{(\text{total number of bogies on tracks in contact with ground}) \times (\text{area of 1 track shoe in sq. in.})}$$

$$\text{clearance factor} = \frac{\text{clearance, in.}}{10}$$

engine factor: 10 or greater hp per ton of vehicle wt = 1.0
less than 10 hp per ton of vehicle wt = 1.05

transmission factor: automatic = 1.0; manual = 1.05

$$VCI_1 = 7.0 + 0.2\,MI - \left(\frac{39.2}{MI + 5.6}\right)$$

$$VCI_{50} = 19.27 + 0.43\,MI - \left(\frac{125.79}{MI + 7.08}\right)$$

Table 5

Environmental Conditions

Scenario	General Slope, %	Seafloor Survey Vehicle		Seafloor Trans-Vehicle		Seafloor Work Platform		Seafloor Trencher Vehicle		Underwater Bulldozer		Distance From Shore to 150-ft Depth, ft
		Current Velocity fps	Wave Height ft	Current Velocity fps	Wave Height ft	Current Velocity fps	Wave Height ft	Current Velocity fps	Wave Height ft	Current Velocity fps	Wave Height ft	
A	0.2	0.5	4.0	0.5	4.0	0.5	4.0	0.5	5.0	0.5	4.5	75,000
B	0.6	0.5	4.0	0.5	4.0	0.5	4.0	0.5	5.0	0.5	4.5	25,000
C	1.0	0.5	4.0	0.5	4.0	0.5	4.0	0.5	5.0	0.5	4.5	15,000
D	3.0	2.0	6.2	2.0	8.0	2.0	7.0	2.0	15.5	2.0	12.0	5,000
E	5.0	4.0	7.5	4.0	9.5	4.0	8.5	4.0	17.5	4.0	13.4	3,000
F	8.0	4.0	7.5	4.0	10.5	4.0	9.0	4.0	17.5	4.0	13.5	1,875
G	10.0	5.0	7.5	5.0	12.5	5.0	10.0	5.0	20.0	5.0	16.5	1,500
H	15.0	6.0	9.1	6.0	16.5	6.0	12.5	6.0	25.1	6.0	21.0	1,000

Table 6

Vehicle Coefficients

Vehicle	Drag Coefficients			Inertial Coefficients			Lift Coefficient
	Front	Oblique	Side	Front	Oblique	Side	
Survey	0.50	0.50	0.50	1.40	2.80	4.20	0.20
Transport	1.25	1.10	1.50	1.50	2.50	3.50	0.05
Work Platform	1.35	1.10	1.50	1.70	2.35	3.00	0.10
Trencher	1.40	1.05	1.60	1.80	2.20	2.60	0.10
Bulldozer	1.50	1.20	1.50	1.70	2.35	3.00	0.20

Table 7

Seafloor Soil Strength and Geometry

File for Trafficability Submodel

Example Vehicle 2--Seafloor Transport Vehicle

Terrain Unit No.	Terrain Unit Distance, ft	Surface Type	Surface Strength	Slope, %	Obstacle Angle, deg	Obstacle Vertical Magnitude, in.	Obstacle Base Width, in.	Obstacle Length, ft	Obstacle Spacing, ft	Obstacle Spacing Type
(1)	(2)	(3)	(4)	(5)	(6)	(7)	(8)	(9)	(10)	(11)
A	300	1	2	2	105	6	9	72	25	2
B	300	1	4	4	105	6	9	72	25	2
C	300	1	8	5	105	6	9	72	25	2
D	300	2	30	10	105	12	18	72	25	2
E	300	1	3000	25	105	24	36	72	25	2
F	300	1	4000	25	105	24	36	72	25	2
G	300	1	5000	25	105	36	48	72	25	2
H	300	1	5000	60	105	60	90	72	25	2

(1)	(2)	(3)	(4)	(5)	(6)	(7)	(8)	(9)	(10)	(11
				Summary of Maximum Water Force Values						
		Vehicle Weight lb		Broadside Force		Frontal Force		Lift Force		
Operation Condition	Scenario	In-Air	Sub-merged	Maximum Value, lb	Station, Wave Period,* Heading Angle	Maximum Value, lb	Station, Wave Period, Heading Angle	Maximum Value, lb	Station, Wave Period, Heading Angle	Scena Cor Ind
I	D	16,900	10,810	164	4, 15, 90	56,025	6, 8, 90	6,896	7, 15, 90	
	E	↓	↓	657	4, 15, 90	75,515	6, 8, 90	8,049	7, 15, 90	3,(
	F			657	4, 15, 90	88,673	6, 8, 90	7,989	7, 15, 90	4,(
	G			1,026	5, 15, 90	94,931	6, 8, 90	7,915	7, 15, 90	5,(
II	A			10	5, 15, 90	24,824	6, 8, 90	3,754	7, 15, 90	
III	C			10	5, 15, 90	31,969	6, 8, 90	4,567	7, 15, 90	
	H			1,478	7, 15, 90	112,180	6, 8, 90	8,932	7, 15, 90	5,(
I	B	63,360	45,760	53	7, 15, 0	72,865	6, 8, 15	2,182	7, 15, 15	
	D	↓	↓	840	4, 15, 0	161,342	6, 8, 15	4,220	7, 15, 15	
II	D			840	4, 15, 0	161,342	6, 8, 15	4,220	7, 15, 15	
	E			3,358	4, 15, 0	214,000	6, 8, 15	4,857	7, 15, 15	3,(
	F			3,358	5, 15, 0	270,267	6, 8, 15	5,197	7, 15, 15	4,(
III	H			7,556	7, 15, 0	411,353	6, 8, 15	7,054	7, 15, 15	5,(
I	A	71,460	57,170	71	8, 15, 0	63,918	6, 15, 15	4,808	7, 15, 15	
II	B	↓	↓	71	8, 15, 0	96,983	7, 8, 15	5,528	7, 15, 15	
III	D			1,134	5, 15, 0	216,525	6, 8, 15	9,672	7, 15, 15	
	G			7,089	7, 15, 0	409,963	6, 8, 15	12,575	7, 15, 15	5,(
I	D	138,090	96,660	973	2, 15, 0	254,263	6, 8, 15	14,121	7, 15, 15	
	E	↓	↓	3,892	2, 15, 0	327,915	6, 8, 15	15,650	7, 15, 15	3,(
	F			3,892	3, 15, 0	381,287	6, 8, 15	15,534	7, 15, 15	4,(
	G			6,081	3, 15, 0	450,846	6, 8, 15	17,011	7, 15, 15	5,(
II	C			61	5, 15, 0	86,007	6, 8, 15	5,561	7, 15, 15	
III	H			8,756	5, 15, 0	547,507	6, 8, 15	19,690	7, 15, 15	5,(
IV	A			61	5, 15, 0	66,849	6, 8, 15	4,571	7, 15, 15	
I	D	106,890	93,530	1,449	3, 15, 90	338,850	6, 8, 90	33,284	7, 15, 90	
	E	↓	↓	5,795	4, 15, 90	431,107	6, 8, 90	36,586	7, 15, 90	3,
II	D			1,449	3, 15, 90	338,850	6, 8, 90	33,284	7, 15, 90	
	F			5,795	5, 15, 90	509,134	6, 8, 90	36,516	7, 15, 90	4,(
	G			9,055	5, 15, 90	629,368	6, 8, 90	42,053	7, 15, 90	5,(
III	H			13,039	7, 15, 90	770,241	6, 8, 90	49,192	7, 15, 90	5,(

* Values of wave periods are in seconds, vehicle heading angles in degrees.

** The longitudinal overturn subroutine was not exercised and no entries were made in columns 34-39 for those example v

had scenario obstacle heights larger than $OH_{max} = \ell_1 (\sin \delta - \frac{j}{\ell_1} \frac{\sin^2 \delta}{\cos \delta})$. This practice was conservative because

accurate for seafloor local slope = 0 (see Figure 18a, where $\delta = \sin^{-1} [OH/(\ell_1 - j \tan \delta)]$, but overestimates OH

θ increases from zero.

Table 8

Summary of Results of STAM Application

(9)	(10)	(11)	(12)	(13)	(14)	(15)	(16)	(17)	(18)	(19)	(20)	(21)	(22)	(23)	(24)	(25)
alues		Summary of Check on Seafloor Trafficability Performance														
Lift Force											Required TF_1 lb		Required TF_2 lb		Available	
Maximum Value, lb	Station, Wave Period, Heading Angle	Scenario Cone Index	One Pass VCI In-Air	One Pass VCI Sub-merged	NOGO Sta	Geo-metric Inter-ference	Required DBP lb	Available DBP_{20}, lb In-Air	Available DBP_{20}, lb Sub-merged	NOGO Sta	In-Air	Sub-merged	In-Air	Sub-merged	In-Air	Sub-merge
															Example Vehicle 1 - Seafl	
6,896	7, 15, 90	30	--	--	--	No	100	12,024	7,691	--	3,472	2,257	7,870	5,070	13,705	8,76
8,049	7, 15, 90	3,000	4	3	--	No		7,207	4,495	--	4,381	2,838	16,160	10,370	8,263	8,19
7,989	7, 15, 90	4,000			--	No		7,029	4,496	--	4,378	2,836	16,155	10,368	8,262	8,19
7,915	7, 15, 90	5,000			--	Yes		7,030	4,497	--	4,376	2,835	--	--	8,261	8,19
3,754	7, 15, 90	2			DL	No		--	--	DL	--	--	--	--	--	--
4,567	7, 15, 90	8			--	No		3,568	3,057	--	4,951	2,883	6,947	4,162	8,641	8,09
8,932	7, 15, 90	5,000			--	Yes		6,214	3,975	--	8,972	5,775	--	--	7,302	7,24
															Example Vehicle 2 - Seafloor	
2,182	7, 15, 15	4	4	3	--	No	0	5,796	4,186	--	21,493	15,522	25,712	18,569	32,405	23,40
4,220	7, 15, 15	30	--	--	--	No		37,071	26,773	--	10,993	7,940	19,946	14,405	41,736	30,14
4,220	7, 15, 15	30	--	--	--	No		37,071	26,773	--	10,993	7,940	19,946	14,405	41,736	30,14
4,857	7, 15, 15	3,000	4	3	--	No		26,345	19,027	--	16,049	11,591	35,552	25,670	30,818	30,64
5,197	7, 15, 15	4,000			--	No		26,352	19,032	--	16,037	11,582	35,536	25,660	30,813	30,61
7,054	7, 15, 15	5,000			--	No		23,296	16,825	--	33,261	24,022	269,719	194,800	27,233	27,05
															Example Vehicle 3 - Seafl	
4,808	7, 15, 15	2	4	3	DL	No	0	--	--	DL	--	--	--	--	--	--
5,528	7, 15, 15	4			--	No		4,454	3,563	--	5,579	20,463	30,259	24,207	33,805	27,04
9,672	7, 15, 15	30	--	--	--	No		41,810	33,449	--	12,399	9,919	22,011	17,609	47,072	37,65
12,575	7, 15, 15	5,000	4	3	--	No		29,726	23,781	--	18,079	14,464	53,729	42,995	34,749	34,66
															Example Vehicle 4 - Seaflo	
14,121	7, 15, 15	80	--	--	--	No	4,500	80,794	56,554	--	28,459	21,271	43,239	31,617	90,962	63,67
15,650	7, 15, 15	3,000	6	4	--	No		51,593	40,191	--	39,479	28,984	70,515	50,718	58,260	66,71
15,534	7, 15, 15	4,000			--	No		51,604	40,202	--	39,452	28,966	70,481	50,699	58,246	66,71
17,011	7, 15, 15	5,000			--	No		51,611	40,208	--	39,436	28,955	89,601	64,054	58,237	66,73
5,561	7, 15, 15	8			--	No		15,833	23,569	--	49,846	30,891	57,116	35,976	59,614	63,71
19,690	7, 15, 15	5,000			--	No		45,618	35,540	--	76,991	55,242	209,521	148,008	51,475	58,90
4,571	7, 15, 15	2			DL	No		--	--	DL	--	--	--	--	--	--
															Example Vehicle 5 - Unde	
33,284	7, 15, 90	30	--	--	--	No	30,000	62,539	54,723	--	33,546	31,228	46,679	42,720	70,410	61,62
36,586	7, 15, 90	3,000	7	5	--	No		39,936	38,890	--	42,076	38,692	70,322	63,411	45,097	51,83
33,284	7, 15, 90	30	--	--	--	No		62,539	54,723	--	33,546	31,228	46,679	42,720	70,410	61,62
36,516	7, 15, 90	4,000	7	5	--	No		39,945	38,900	--	42,055	38,674	70,294	63,391	45,086	51,83
42,053	7, 15, 90	5,000			--	No		39,950	38,906	--	42,043	38,663	89,926	80,573	45,079	51,83
49,192	7, 15, 90	5,000			--	No		35,311	34,389	--	71,113	64,099	470,038	413,147	39,845	45,83

mns 34-39 for those example vehicle/scenario combinations that

ice was conservative because this definition of OH_{max} is

$\delta)]$, but overestimates OH_{max} by increasingly large amounts as

Table 8

Summary of Results of STAM Application to the Example Vehicle Problems

(21)	(22)	(23)	(24)	(25)	(26)	(27)	(28)	(29)	(30)	(31)	(32)	(33)	(34)	(35)	(36)	
r Performance																
β_1	Required TF_2, lb		Available TF, lb				Summary of Check on Lateral Overturn						Summary of Check on L			
lb-ged	In-Air	Sub-merged	In-Air	Sub-merged	NOGO TF_1 Sta	NOGO TF_2 Sta	Case	α_{max} radians	Station, Wave Period, Heading Angle	Case	$\frac{\alpha_{start}}{\alpha_{finish}}$	Station, Wave Period, Heading Angle	Case	β_{max} radians	Station, Wave Period, Heading Angle	C
Example Vehicle 1 - Seafloor Survey Vehicle																
257	7,870	5,070	13,705	8,766	--	--	B	0.246	8, 8, 90	B	1.0	8 8, 90	2	0.430	6, 8, 15	
838	16,160	10,370	8,263	8,199	--	DL	B	0.937	8, 15, 90	B	0.690	8, 15, 90	**			
836	16,155	10,368	8,262	8,199	--	DL	B	0.979	8, 15, 90	B	0.635	8, 15, 90				
835	--	--	8,261	8,199	--	NOGO	B	1.499	8, 15, 90	B	0.432	8, 15, 90				
-	--	--	--	--	DL	DL	B	0.085	8, 15, 90	B	1.0	7, 8, 15	2	0.148	6, 8, 15	
883	6,947	4,162	8,641	8,097	--	--	B	0.115	8, 15, 90	B	1.0	8, 8, 90	2	0.181	6, 8, 15	
775	--	--	7,302	7,247	--	NOGO	B	4.305	8, 15, 90	B	0.291	8, 15, 90				
Example Vehicle 2 - Seafloor Transport Vehicle																
522	25,712	18,569	32,405	23,403	--	--	B	0.079	8, 15, 90	B	1.0	7, 8, 15	2	0.119	8, 15, 90	
940	19,946	14,405	41,736	30,143	--	--	B	0.178	8, 15, 90	B	1.0	4, 8, 15	2	0.275	6, 8, 15	
940	19,946	14,405	41,736	30,143	--	--	B	0.178	8, 15, 90	B	1.0	4, 8, 15	2	0.275	6, 8, 15	
591	35,552	25,670	30,818	30,643	--	DL	B	0.411	8, 15, 90	B	1.0	8, 8, 90	2	0.673	6, 8, 15	
582	35,536	25,660	30,813	30,633	--	DL	B	0.436	8, 15, 90	B	1.0	8, 8, 90	2	0.705	6, 8, 15	
022	269,719	194,800	27,233	27,057	DL	DL	B	2.242	8, 15, 90	B	0.421	8, 15, 90				
Example Vehicle 3 - Seafloor Work Platform																
-	--	--	--	--	DL	DL	B	0.061	8, 15, 90	B	1.0	8, 8, 90	2	0.087	8, 15, 90	
463	30,259	24,207	33,805	27,044	--	--	B	0.081	8, 15, 90	B	1.0	8, 8, 90	2	0.107	8, 15, 90	
919	22,011	17,609	47,072	37,659	--	--	B	0.183	8, 15, 90	B	1.0	8, 8, 90	2	0.255	6, 8, 15	
464	53,729	42,995	34,749	34,604	--	DL	B	0.731	8, 15, 90	B	0.976	8, 8, 90	2	0.984	8, 15, 15	
Example Vehicle 4 - Seafloor Trencher Vehicle																
271	43,239	31,617	90,962	63,671	--	--	B	0.172	8, 15, 90	B	1.0	8, 8, 90	2	0.222	6, 8, 15	
984	70,515	50,718	58,260	66,734	--	DL	B	0.390	8, 15, 90	B	1.0	8, 8, 90	2	0.504	8, 15, 90	
966	70,481	50,699	58,246	66,731	--	DL	B	0.391	8, 15, 90	B	1.0	8, 8, 90	2	0.504	8, 15, 90	
955	89,601	64,054	58,237	66,729	--	DL	B	0.531	8, 15, 90	B	1.0	8, 8, 90	2	0.746	8, 15, 90	
891	57,116	35,976	59,614	63,759	--	--	B	0.086	8, 15, 90	B	1.0	5, 8, 15	2	0.109	8, 8, 90	
242	209,521	148,008	51,475	58,981	DL	DL	B	1.665	8, 15, 90	B	0.547	8, 15, 90				
	--	--	--	--	DL	DL	B	0.056	8, 15, 90	B	1.0	7, 8, 15	2	0.079	8, 15, 90	
Example Vehicle 5 - Underwater Bulldozer																
228	46,679	42,720	70,410	61,610	--	--	B	0.171	8, 15, 90	B	1.0	8, 8, 90	2	0.235	6, 8, 15	
992	70,322	63,411	45,097	51,851	--	DL	B	0.498	8, 15, 90	B	1.0	8, 8, 90	2	0.567	8, 15, 15	
228	46,679	42,720	70,410	61,610	--	--	B	0.171	8, 15, 90	B	1.0	8, 8, 90	2	0.235	6, 8, 15	
974	70,294	63,391	45,086	51,846	--	DL	B	0.524	8, 15, 90	B	1.0	8, 8, 90	2	0.579	8, 15, 15	
963	89,926	80,573	45,079	51,842	--	DL	B	0.800	8, 15, 90	B	0.754	8, 15, 90	2	0.966	8, 15, 15	
999	470,038	413,147	39,845	45,823	DL	DL	B	2.362	8, 15, 90	B	0.382	8, 15, 90				

(32)	(33)	(34)	(35)	(36)	(37)	(38)	(39)	(40)	(41)	(42)	(43)
Lateral Overturn		Summary of Check on Longitudinal Overturn						Summary of Check on Motion and Position			
α_{start} / α_{finish}	Station, Wave Period, Heading Angle	Case	β_{max} radians	Station, Wave Period, Heading Angle	Case	β_{start} / β_{finish}	Station, Wave Period, Heading Angle	G/T	Station, Wave Period, Heading Angle	I/U	Station, Wave Period, Heading Angle
1.0	8 8, 90	2	0.430	6, 8, 15	1	0.795	6, 8, 15	0.267	6, 8, 15	0.229	8, 8, 90
0.690	8, 15, 90	**						0.373	6, 8, 15	0.449	8, 8, 90
0.635	8, 15, 90							0.429	6, 8, 15	0.463	8, 8, 90
0.432	8, 15, 90							0.605	6, 8, 15	0.469	8, 8, 90
1.0	7, 8, 15	2	0.148	6, 8, 15	1	1.0	7, 8, 15	0.141	7, 8, 15	0.139	8, 8, 90
1.0	8, 8, 90	2	0.181	6, 8, 15	1	1.0	6, 8, 15	0.141	6, 8, 15	0.142	8, 8, 90
0.291	8, 15, 90							0.496	6, 8, 15	0.209	8, 8, 90
1.0	7, 8, 15	2	0.119	8, 15, 90	2	1.0	7, 8, 15	0.073	6, 8, 15	0.087	8, 8, 90
1.0	4, 8, 15	2	0.275	6, 8, 15	2	1.0	6, 8, 15	0.156	6, 8, 15	0.176	8, 8, 90
1.0	4, 8, 15	2	0.275	6, 8, 15	2	1.0	6, 8, 15	0.156	6, 8, 15	0.176	8, 8, 90
1.0	8, 8, 90	2	0.673	6, 8, 15	1	0.990	6, 8, 15	0.208	6, 8, 15	0.339	8, 8, 90
1.0	8, 8, 90	2	0.705	6, 8, 15	1	0.888	6, 8, 15	0.263	6, 8, 15	0.383	8, 8, 90
0.421	8, 15, 90							0.402	6, 8, 15	0.229	8, 8, 90
1.0	8, 8, 90	2	0.087	8, 15, 90	1	1.0	7, 8, 15	0.041	7, 8, 15	0.098	8, 8, 90
1.0	8, 8, 90	2	0.107	8, 15, 90	1	1.0	7, 8, 15	0.071	7, 8, 15	0.098	8, 8, 90
1.0	8, 8, 90	2	0.255	6, 8, 15	1	1.0	6, 8, 15	0.189	6, 8, 15	0.180	8, 8, 90
0.976	8, 8, 90	2	0.984	8, 15, 15	2	0.869	8, 15, 15	0.326	6, 8, 15	0.424	8, 8, 90
1.0	8, 8, 90	2	0.222	6, 8, 15	2	1.0	8, 8, 15	0.119	6, 8, 15	0.176	8, 8, 90
1.0	8, 8, 90	2	0.504	8, 15, 90	2	1.0	8, 8, 15	0.154	6, 8, 15	0.320	8, 8, 90
1.0	8, 8, 90	2	0.504	8, 15, 90	2	1.0	8, 8, 0	0.178	6, 8, 15	0.341	8, 8, 90
1.0	8, 8, 90	2	0.746	8, 15, 90	2	1.0	8, 8, 0	0.211	6, 8, 15	0.380	8, 8, 90
1.0	5, 8, 15	2	0.109	8, 8, 90	2	1.0	5, 8, 15	0.039	6, 8, 15	0.064	8, 8, 90
0.547	8, 15, 90							0.257	6, 8, 15	0.204	8, 8, 90
1.0	7, 8, 15	2	0.079	8, 15, 90	1	1.0	7, 8, 15	0.036	6, 8, 15	0.062	8, 8, 90
1.0	8, 8, 90	2	0.235	6, 8, 15	2	1.0	8, 8, 15	0.164	6, 8, 15	0.250	8, 8, 90
1.0	8, 8, 90	2	0.567	8, 15, 15	2	1.0	8, 8, 15	0.211	6, 8, 15	0.457	8, 8, 90
1.0	8, 8, 90	2	0.235	6, 8, 15	2	1.0	8, 8, 15	0.164	6, 8, 15	0.250	8, 8, 90
1.0	8, 8, 90	2	0.579	8, 15, 15	1	1.0	6, 8, 15	0.247	6, 8, 15	0.481	8, 8, 90
0.754	8, 15, 90	2	0.966	8, 15, 15	2	0.812	8, 15, 15	0.309	6, 8, 15	0.580	8, 8, 90
0.382	8, 15, 90							0.384	6, 8, 15	0.290	8, 8, 90

Table 9

Tally Summary of Results of STAM Application to the Example Vehicle Problems

(1) Operating Condition	(2) Scenario	(3) Scenario CI Less Than One-Pass VCI	(4) Geometry Interference	(5) Avail DBP_{20} Less Than Req'd	(6) Avail. TF Less Than Req'd TF_1	(7) Avail. TF Less Than Req'd TF_2	(8) α_{max} Greater Than 0.4 Rad	(9) $\frac{\alpha_{start}}{\alpha_{finish}}$ Less Than 1	(10) β_{max} Greater Than 0.4 Rad	(11) $\frac{\beta_{start}}{\beta_{finish}}$ Less Than 1	(12) G/T Greater Than 1	(13) I/U Greater Than 1	(14) Total NOGO's
					Example Vehicle 1 - Seafloor Survey Vehicle								
I	D	GO	GO	GO	GO	GO	GO	GO	NOGO	NOGO	GO	GO	2
	E	GO	GO	GO	GO	NOGO	NOGO	NOGO	NOGO	NOGO	GO	GO	5
	F	GO	GO	GO	GO	NOGO	NOGO	NOGO	NOGO	NOGO	GO	GO	5
	G	GO	NOGO	GO	GO	NOGO	NOGO	NOGO	NOGO	NOGO	GO	GO	6
II	A	NOGO	GO	NOGO	NOGO	NOGO	GO	GO	GO	GO	GO	GO	4
III	C	GO	GO	GO	GO	GO	GO	GO	GO	GO	GO	GO	0
	H	GO	NOGO	GO	GO	NOGO	NOGO	NOGO	NOGO	NOGO	GO	GO	6
					Example Vehicle 2 - Seafloor Transport Vehicle								
I	B	GO	GO	GO	GO	GO	GO	GO	GO	GO	GO	GO	0
	D	GO	GO	GO	GO	GO	GO	GO	GO	GO	GO	GO	0
II	D	GO	GO	GO	GO	GO	GO	GO	GO	GO	GO	GO	0
	E	GO	GO	GO	GO	NOGO	NOGO	GO	NOGO	NOGO	GO	GO	4
	F	GO	GO	GO	GO	NOGO	NOGO	GO	NOGO	NOGO	GO	GO	4
III	H	GO	GO	GO	NOGO	NOGO	NOGO	NOGO	NOGO	NOGO	GO	GO	6
					Example Vehicle 3 - Seafloor Work Platform								
I	A	NOGO	GO	NOGO	NOGO	NOGO	GO	GO	GO	GO	GO	GO	4
II	B	GO	GO	GO	GO	GO	GO	GO	GO	GO	GO	GO	0
III	D	GO	GO	GO	GO	GO	GO	GO	GO	GO	GO	GO	0
	G	GO	GO	GO	GO	NOGO	NOGO	NOGO	NOGO	NOGO	GO	GO	5
					Example Vehicle 4 - Seafloor Trencher Vehicle								
I	D	GO	GO	GO	GO	GO	GO	GO	GO	GO	GO	GO	0
	E	GO	GO	GO	GO	NOGO	GO	GO	NOGO	GO	GO	GO	2
	F	GO	GO	GO	GO	NOGO	GO	GO	NOGO	GO	GO	GO	2
	G	GO	GO	GO	GO	NOGO	NOGO	GO	NOGO	GO	GO	GO	3
II	C	GO	GO	GO	GO	GO	GO	GO	GO	GO	GO	GO	0
III	H	GO	GO	GO	NOGO	NOGO	NOGO	NOGO	NOGO	NOGO	GO	GO	6
IV	A	NOGO	GO	NOGO	NOGO	NOGO	GO	GO	GO	GO	GO	GO	4
					Example Vehicle 5 - Underwater Bulldozer								
I	D	GO	GO	GO	GO	GO	GO	GO	GO	GO	GO	GO	0
	E	GO	GO	GO	GO	NOGO	NOGO	GO	NOGO	GO	GO	GO	3
II	D	GO	GO	GO	GO	GO	GO	GO	GO	GO	GO	GO	0
	F	GO	GO	GO	GO	NOGO	NOGO	GO	NOGO	GO	GO	GO	3
	G	GO	GO	GO	GO	NOGO	NOGO	NOGO	NOGO	NOGO	GO	GO	5
III	H	GO	GO	GO	NOGO	NOGO	NOGO	NOGO	NOGO	NOGO	GO	GO	6
TOTAL NOGO's		3	2	3	6	19	14	9	17	12	0	0	85

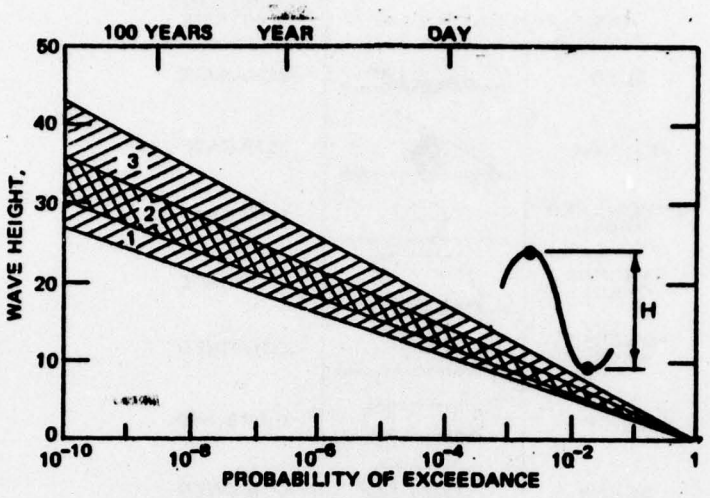

Figure 1. Long-term distribution of wave heights H at three ocean locations (after Reference 2)

SLOPE (θ) - THE ANGULAR DEVIATION OF A SURFACE FROM THE HORIZONTAL.

OBSTACLE APPROACH ANGLES (A) - THE ANGLES FORMED BY THE INCLINES AT THE BASE OF A POSITIVE VERTICAL OBSTACLE (MOUND) OR AT THE TOP OF A NEGATIVE VERTICAL OBSTACLE (DEPRESSION).

OBSTACLE BASE WIDTH (WB) - THE DISTANCE ACROSS THE BOTTOM OF THE OBSTACLE.

OBSTACLE SPACING (OBS) - THE HORIZONTAL DISTANCE BETWEEN INITIAL CONTACT EDGES OF VERTICAL OBSTACLES.

OBSTACLE HEIGHT (H) - THE VERTICAL DISTANCE FROM THE BASE OF A VERTICAL OBSTACLE TO THE CREST OF THE OBSTACLE.

OBSTACLE LENGTH (OBL) - THE LENGTH OF THE LONG AXIS OF THE OBSTACLE, MEASURED PERPENDICULAR TO THE PLANE OF THE PAPER.

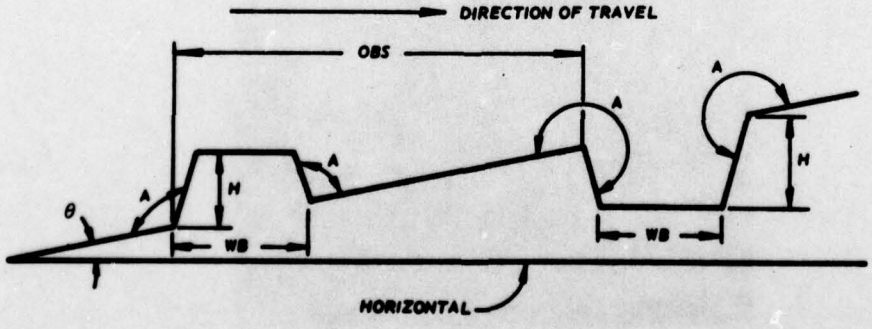

Figure 2. Stylized description of seafloor microrelief

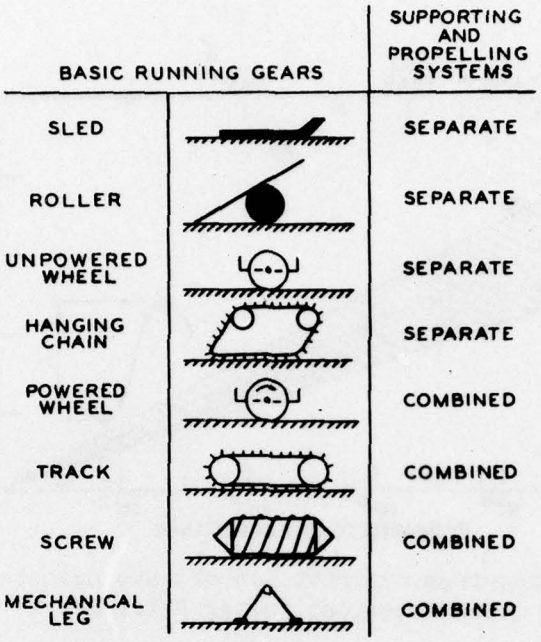

Figure 3. Basic running gears (from Reference 1)

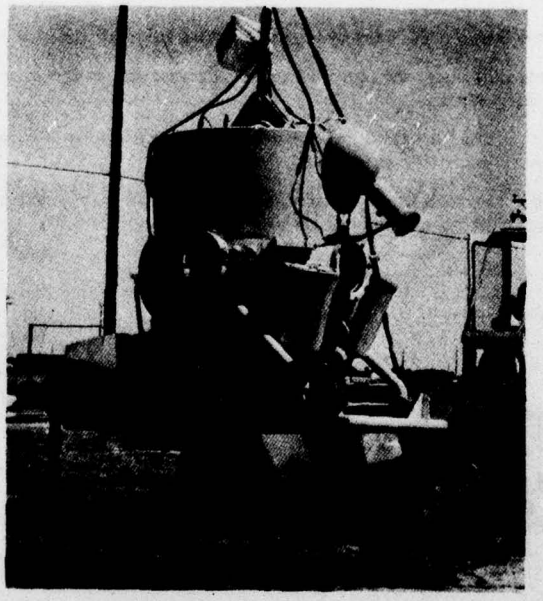

Figure 4. Tracked diving bell (from Reference 1)

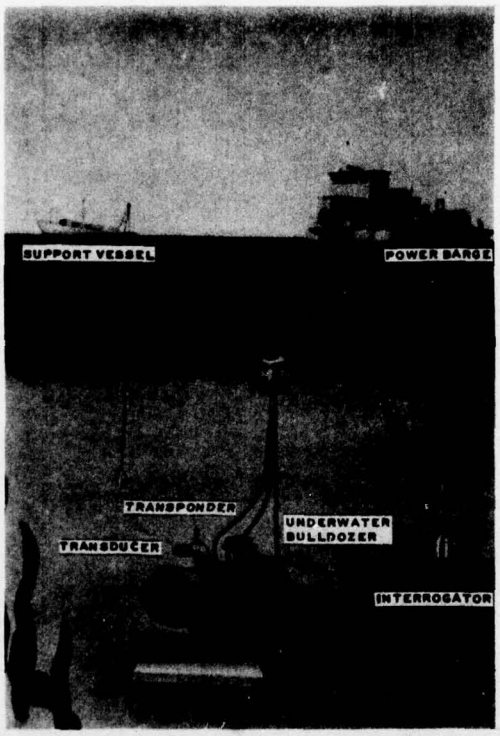

Figure 5. Underwater bulldozer, surface-controlled

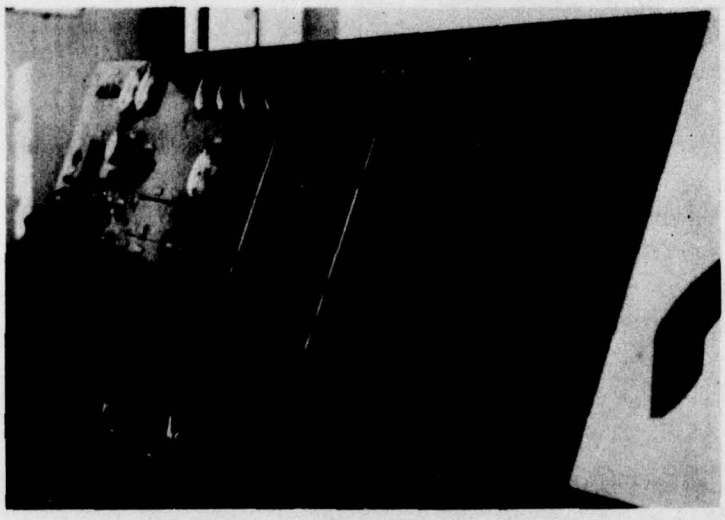

Figure 6. Control desk for underwater bulldozer

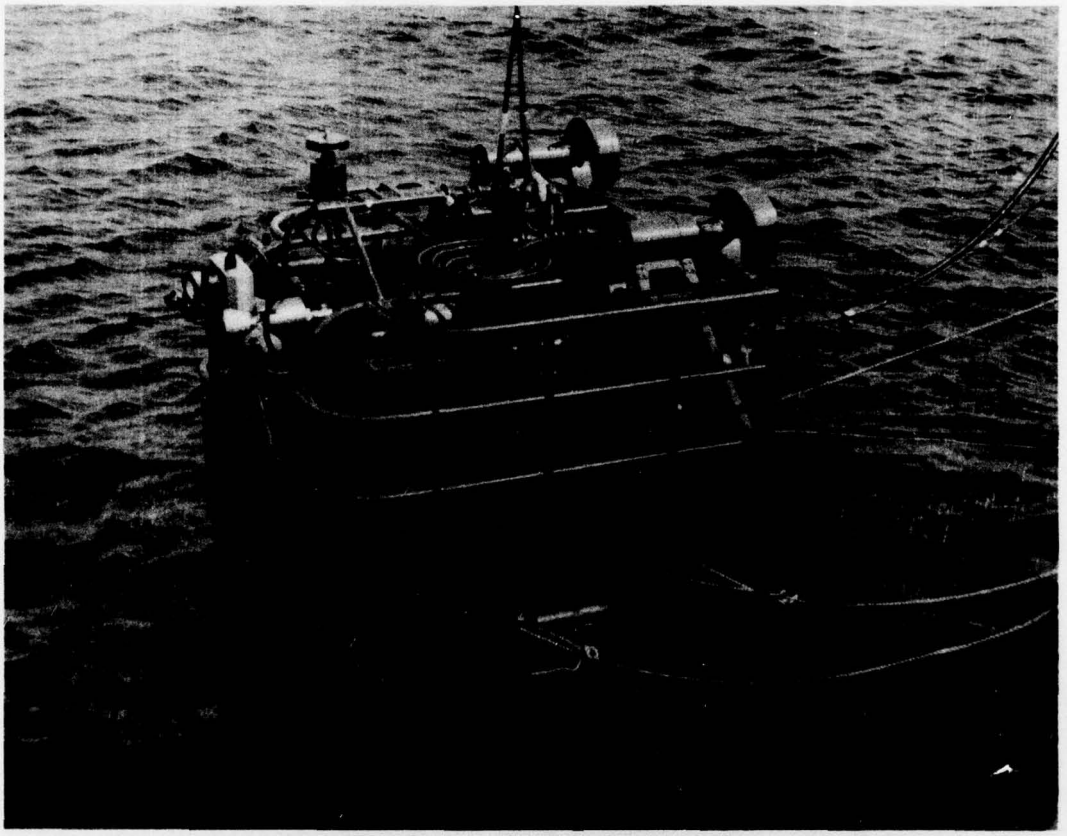

Figure 7. Seafloor crawler of the Survey and Inspection Robot (SIR) System

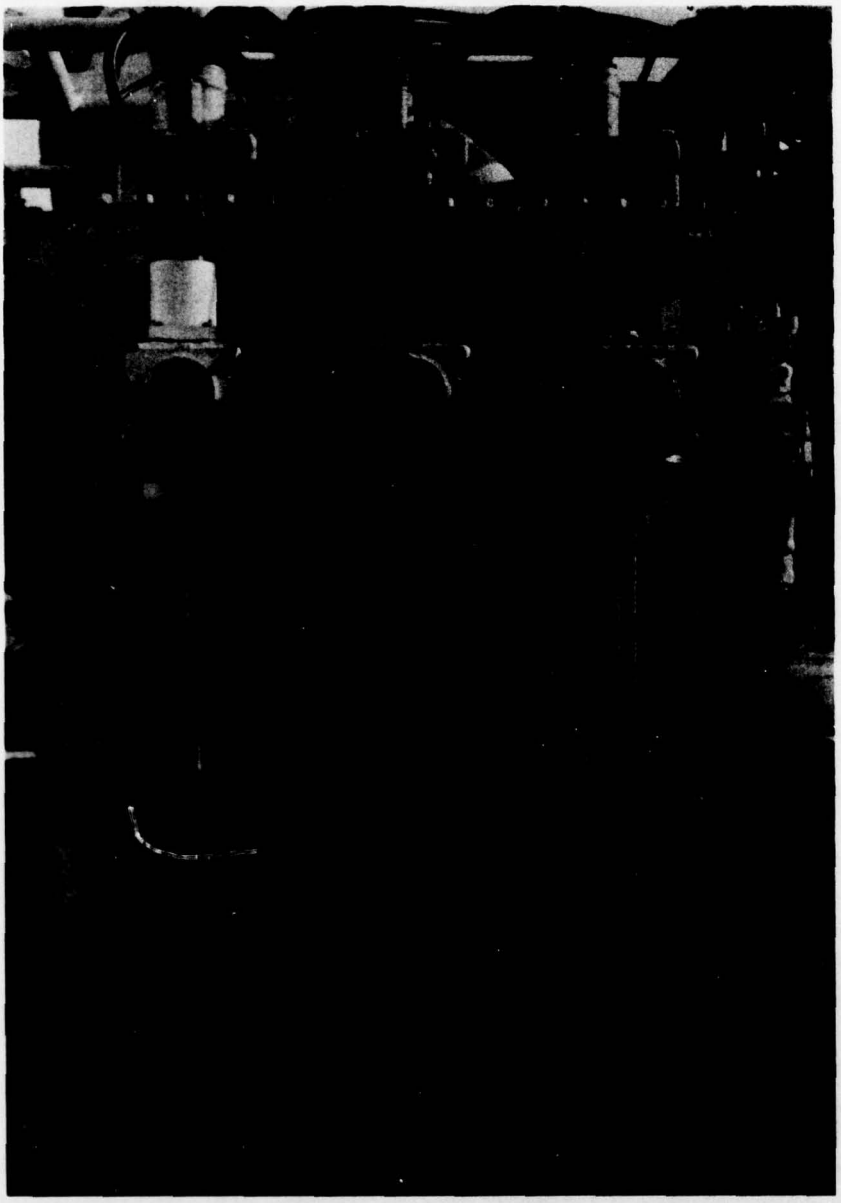

Figure 8. In situ soil testing devices of the SIR System

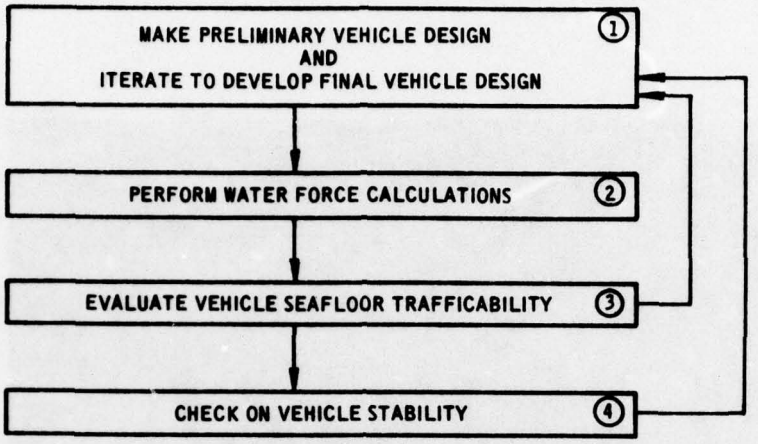

Figure 9. Overall structure of STAM

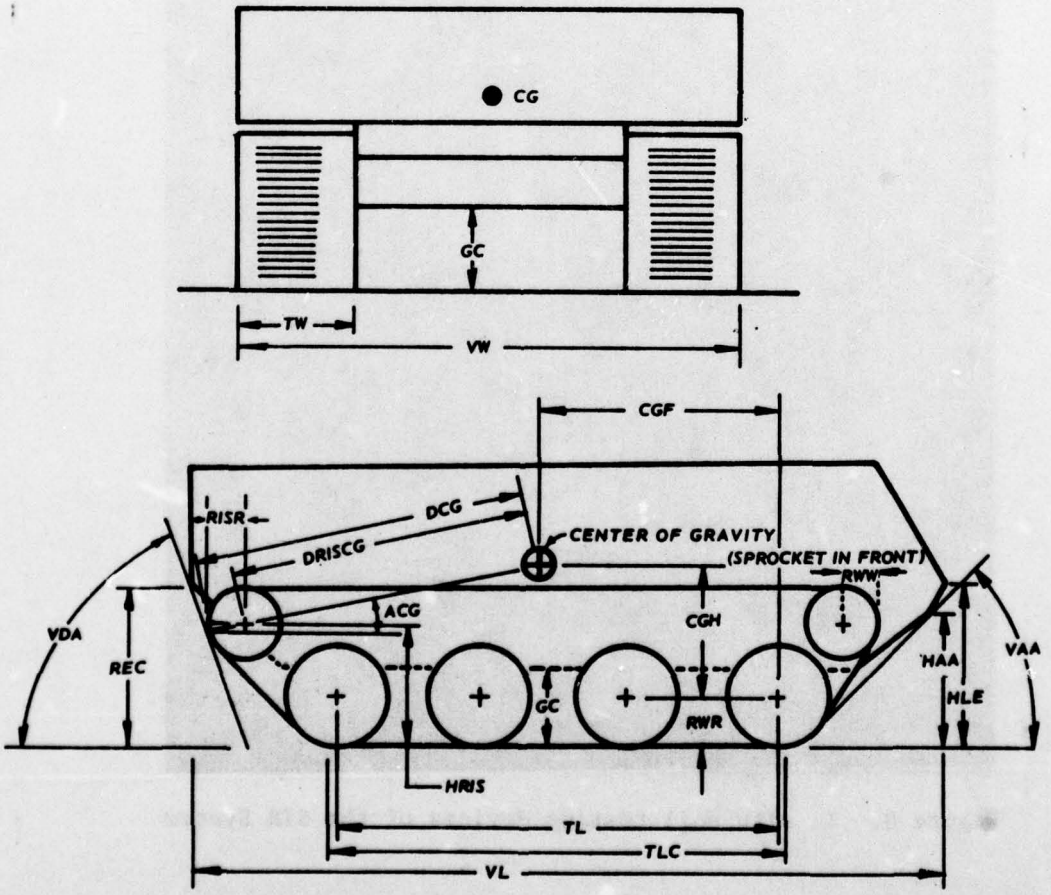

Figure 10. Tracked vehicle description in terms of STAM trafficability submodel vehicle geometry parameters

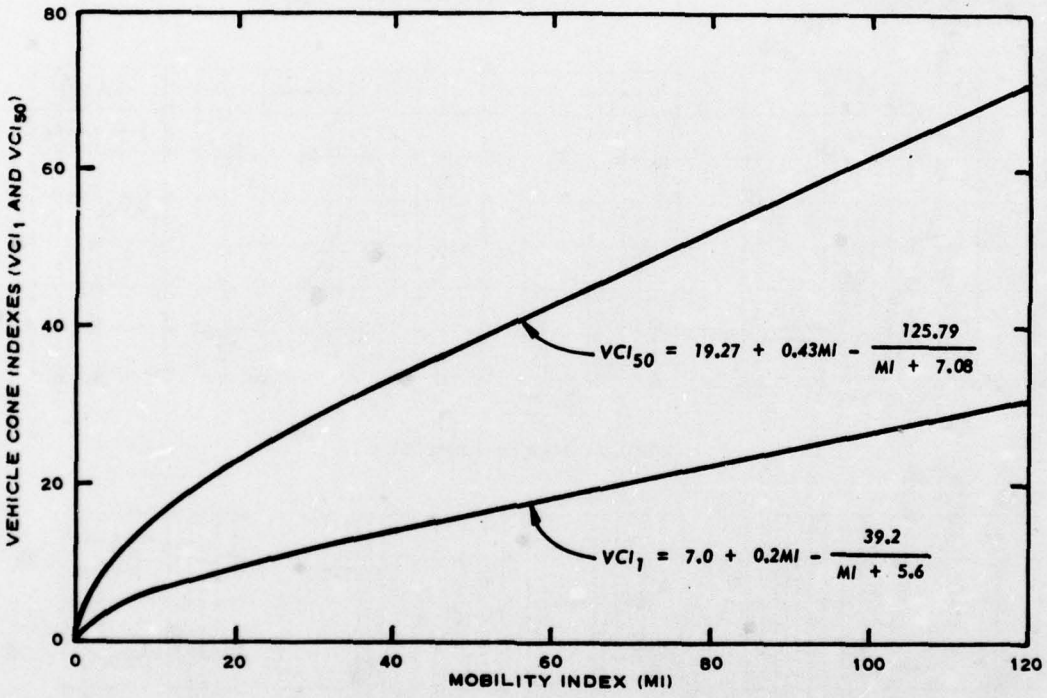

Figure 11. Relations of VCI_1 and VCI_{50} to MI for self-propelled tracked vehicles in clay

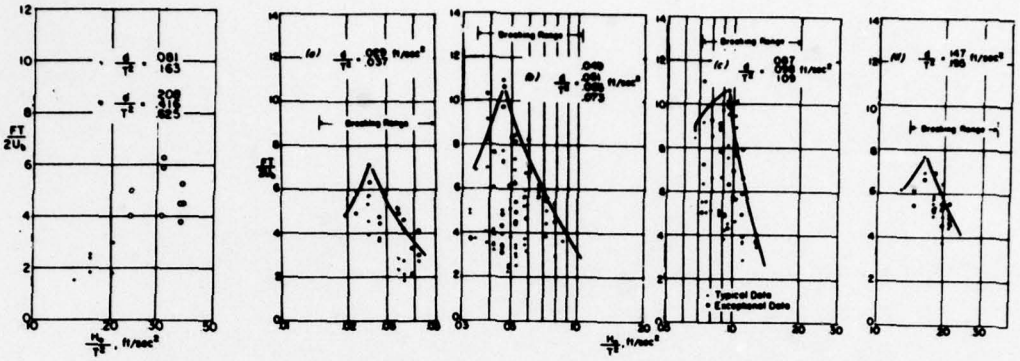

a. VERTICAL BARRIER, 1:3 SLOPE

b. VERTICAL BARRIER, 1:10 SLOPE

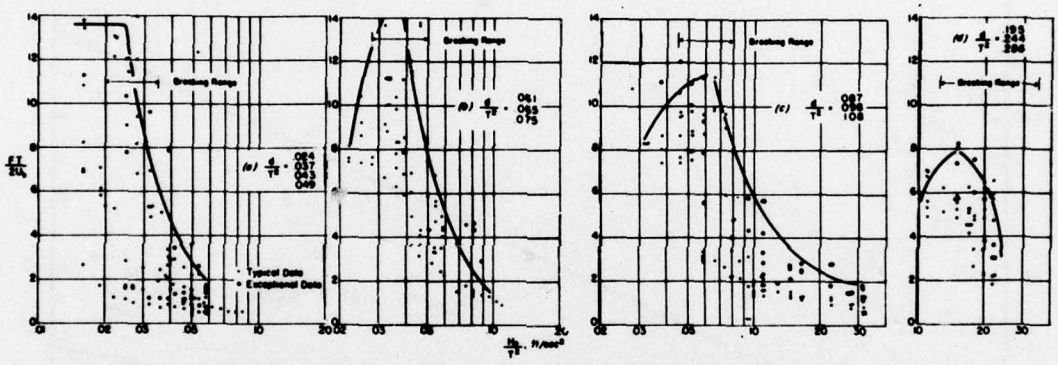

c. VERTICAL BARRIER, 1:30 SLOPE

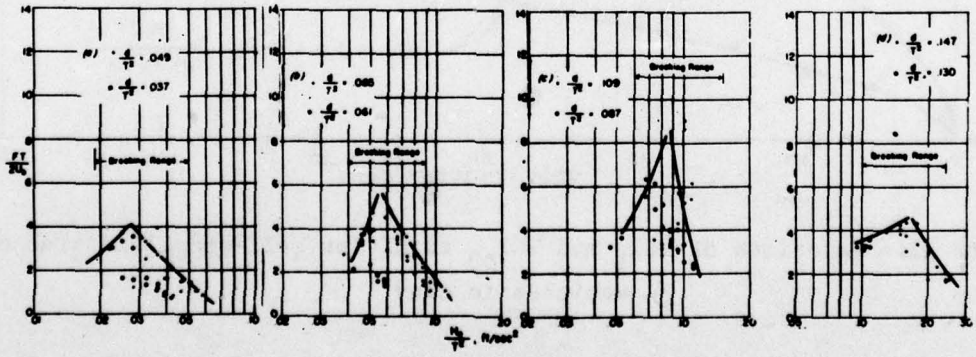

d. 30-DEG SLOPING BARRIER, 1:10 SLOPE

Figure 12. Dimensionless representation of water force data (after Reference 30)

VEHICLE NO. 2 - SEAFLOOR TRANSPORT VEHICLE

VEHICLE DRY WEIGHT 63360.0 LB

VEHICLE SUBMERGED WEIGHT 45760.0 LB

VEHICLE HEADING ANGLE 0. DEG

WAVE PERIOD 8. SEC WAVE HEIGHT 8.0 FT

CURRENT VELOCITY 2.0 FPS GENERAL SLOPE 3.0 %

SCENARIO D

(1) STA	(2) WATER DEPTH (FT)	(3) VEH. EFFEC. WEIGHT (LB)	(4) B'SIDE FORCE (LB)	(5) FRONTAL FORCE (LB)	(6) LIFT FORCE (LB)
1	1.6	59662.0	176.4	3574.5	0.
2	3.2	55964.0	352.8	12256.3	0.
3	4.7	52266.0	529.2	25081.7	0.
4	6.3	48568.0	705.6	33438.5	0.
5	7.9	45760.0	839.5	34890.9	681.6
6	9.5	45760.0	839.5	130585.4	2363.2
7	10.5	45760.0	839.5	118589.0	2494.2
8	24.4	45760.0	839.5	48658.6	391.2
9	38.4	45760.0	839.5	29905.5	159.1
10	52.3	45760.0	839.5	20746.7	79.7
11	66.3	45760.0	839.5	15090.3	43.2
12	80.2	45760.0	839.5	11210.9	24.3
13	94.2	45760.0	839.5	8532.0	14.3
14	108.1	45760.0	839.5	6489.0	8.3
15	122.1	45760.0	839.5	4938.2	4.9
16	136.0	45760.0	839.5	3787.8	2.9
17	150.0	45760.0	839.5	2902.9	1.7

a. Forces on seafloor transport vehicle 2

VEHICLE NO. 2 SCENARIO D WAVE PERIOD 8. ANGLE 0.

WAVE HT 8.0 FT SLOPE 3.0 %

DRY WEIGHT 63360. SUBMERGED WEIGHT 45760.

(1) WD	(2) VMAX	(3) AMAX	(4) WH	(5) WL
150.0	0.355	0.279	8.06	325.68
136.0	0.463	0.363	8.10	324.34
122.1	0.601	0.472	8.15	322.17
108.1	0.787	0.618	8.23	318.59
94.2	1.030	0.809	8.36	312.99
80.2	1.345	1.056	8.54	304.69
66.3	1.794	1.409	8.82	291.82
52.3	2.435	1.913	9.23	273.29
38.4	3.442	2.703	9.85	246.79
24.4	5.397	4.239	10.92	207.13

b. Associated velocities, accelerations, wave heights, and wave lengths

Figure 13. Example of STAM-computed (a) forces on seafloor transport vehicle 2, and (b) associated sea-state conditions

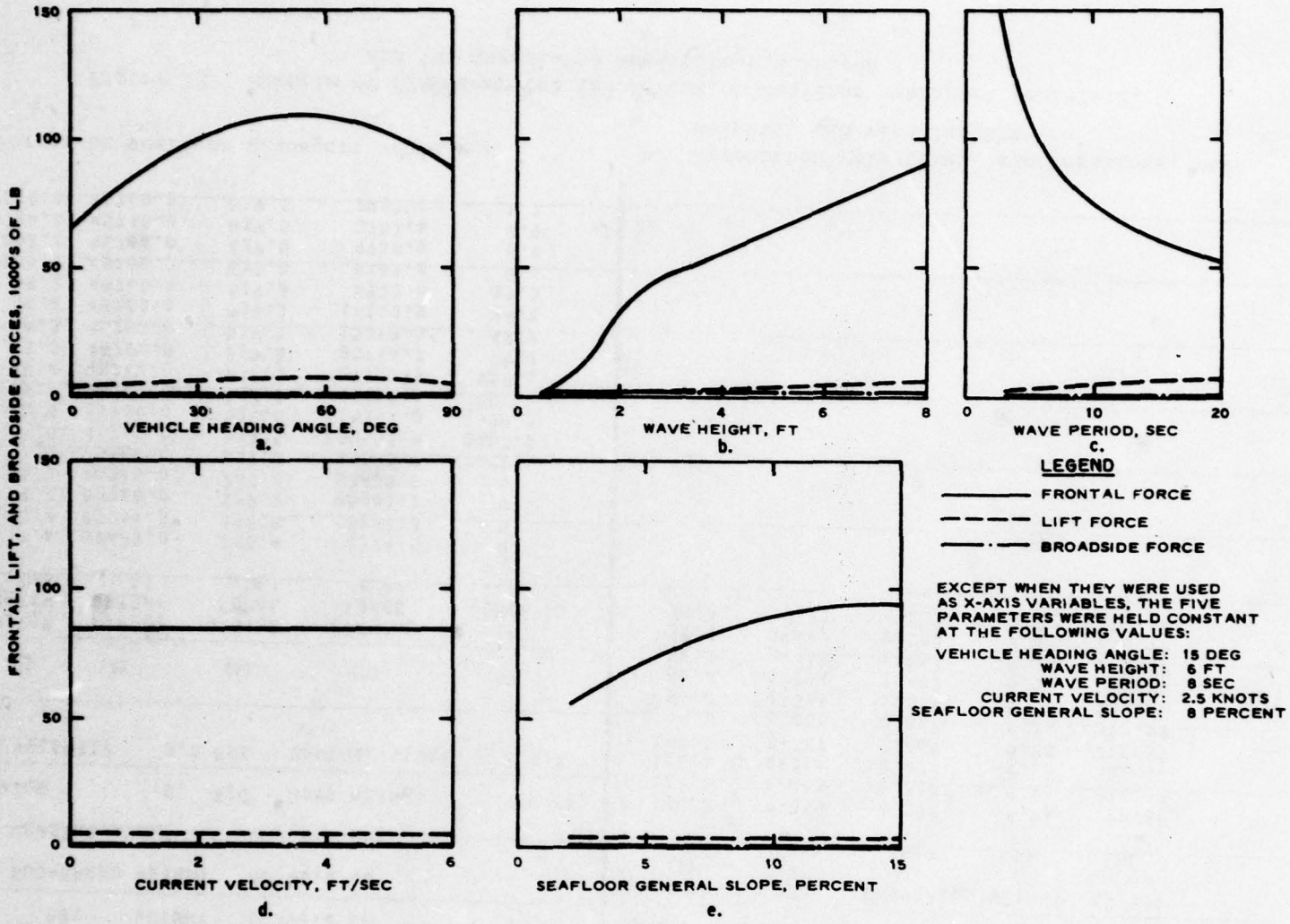

Figure 14. Predicted relations of frontal, lift, and broadside forces to vehicle heading angle and four nearshore environmental parameters for the survey vehicle

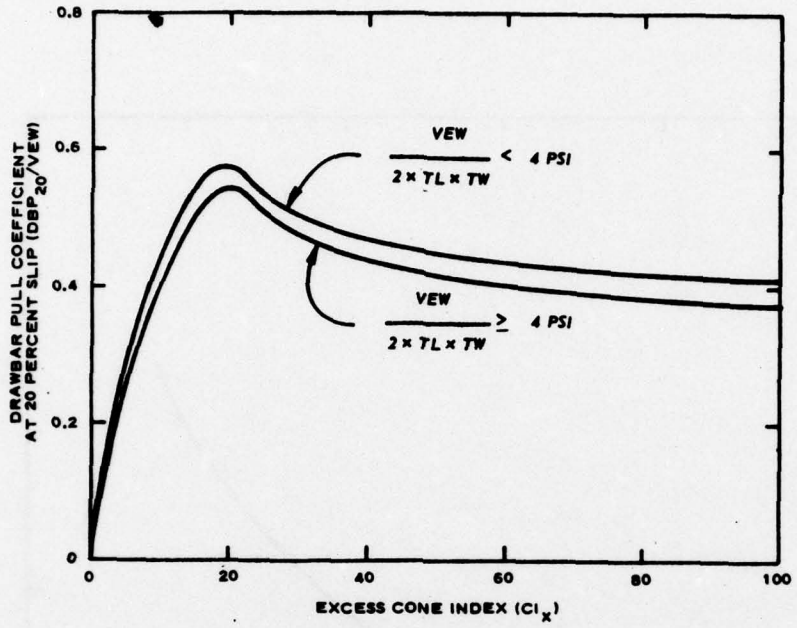

Figure 15. Predicted relation of DBP_{20}/VEW to CI_x for a tracked vehicle with grousers operating in wet-wet clay

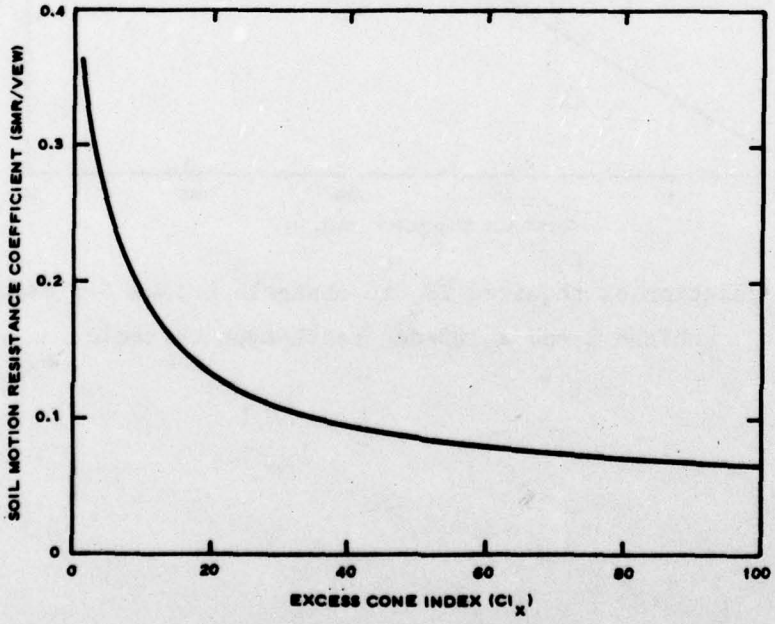

Figure 16. Predicted relation of SMR/VEW to CI_x for a tracked vehicle with grousers operating in clay

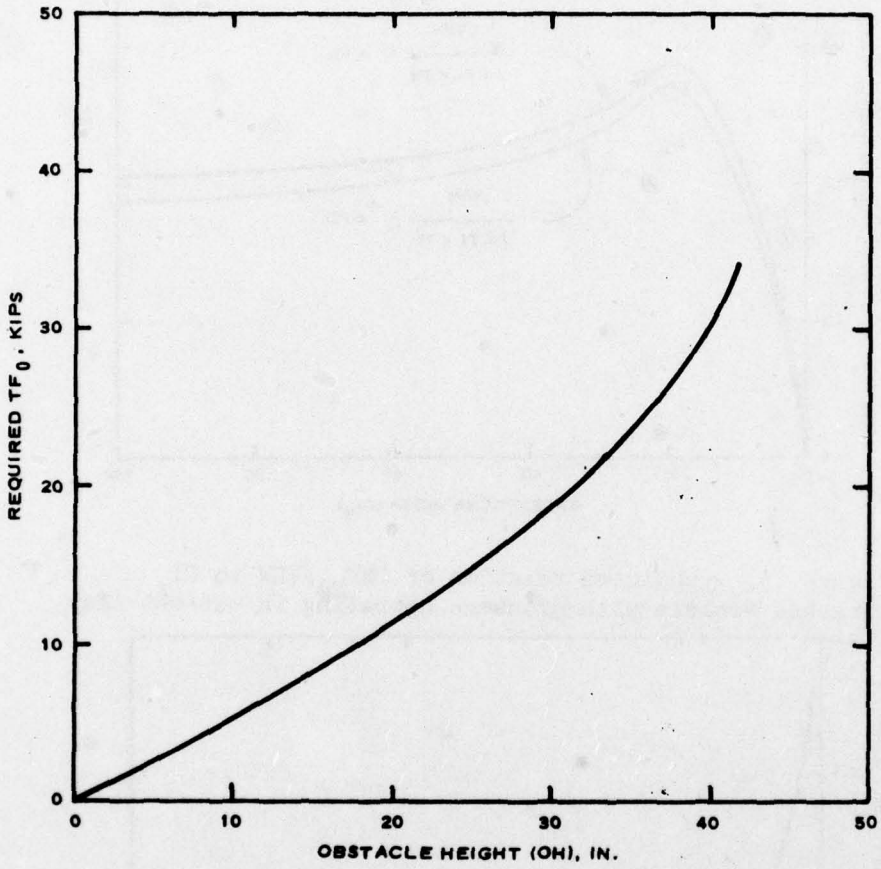

Figure 17. Relation of required TF_o to obstacle height for example vehicle 2 and a 105-deg bench-type obstacle

VEHICLE NO. 2 - SEAFLOOR TRANSPORT VEHICLE

VEHICLE DRY WEIGHT = 63360.0 LB

VEHICLE SUBMERGED WEIGHT = 45760.0 LB

SOIL STRENGTH (CONE INDEX) = 3000.0

OBSTACLE HEIGHT = 2.0 FT

REQUIRED DRAWBAR PULL = 0. LB

LOCAL SEAFLOOR SLOPE 25. %

WAVE PERIOD = 9. SEC

VEHICLE HEADING ANGLE = NA

SCENARIO E

(1)	(2)	(3)	(4)	(5)	(6)	(7)	(8)	(9)	(10)	(11)	(12)	(13)
STA	WATER DEPTH (FT)	VEHICLE EFFECTIVE WEIGHT (LB)	ONE PASS VCI	AVAIL. SOIL STRENGTH SUFF.	GO/NO GO OBSTACLE GEOM. INTERFERENCE	AVAIL. DBP20 (LB)	AVAIL. DBP20 SUFF.	REQUIRED TF1 (LB)	REQUIRED TF2 (LB)	AVAILABLE TF (LB)	AVAIL. TF REQ'D FOR TF1 SUFF.	AVAIL. TF REQ'D FOR TF2 SUFF.
DL	0.	63360.0	4.1	YES	GO	26345.2	YES	16049.4	35551.6	30818.1	YES	NO
1	1.6	59688.3	3.9	YES	GO	24818.5	YES	15119.3	33481.2	30779.8	YES	NO
2	3.1	56016.6	3.7	YES	GO	23291.8	YES	14189.2	31429.0	30741.4	YES	NO
3	4.7	52344.8	3.4	YES	GO	21765.0	YES	13259.1	29364.0	30703.0	YES	YES
4	6.3	48673.1	2.7	YES	GO	20238.4	YES	12329.1	27301.9	30644.7	YES	YES
5	7.8	45760.0	2.5	YES	GO	19027.1	YES	11591.2	25659.7	30634.2	YES	YES

Figure 18. Example application of STAM trafficability submodel

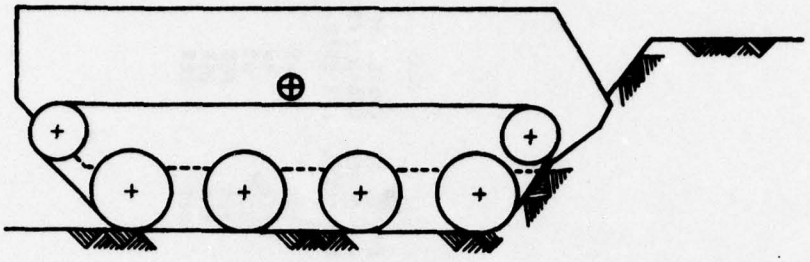

Figure 19. Type 40 geometric interference between tracked vehicle and obstacle

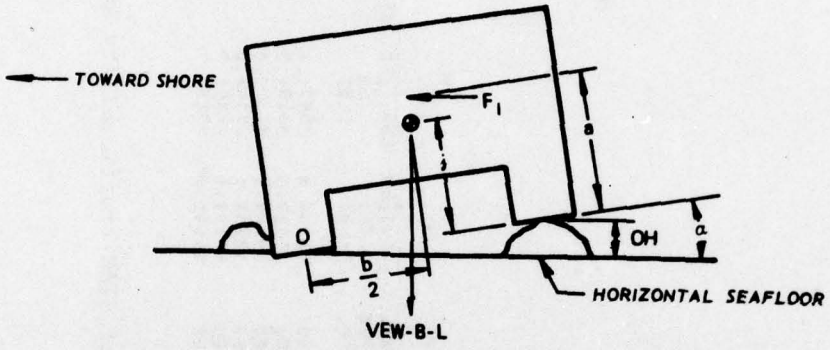

a. CASE A: LOCAL SLOPE = 0, IMPACT PART OF WATER FORCE CYCLE

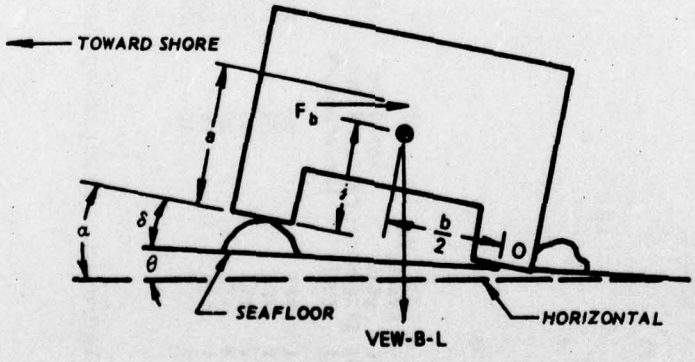

b. CASE B: LOCAL SLOPE = θ, BACKWASH PART OF WATER FORCE CYCLE

Figure 20. Sketch of tracked vehicle for two worst cases relative to lateral overturn

(1) VEH NO.	(2) SENA-ARIO	(3) WAVE HEIGHT FT	(4) OBSTACLE HEIGHT IN	(5) VEHICLE HEADING ANGLE DEG.	(6) WAVE PERIOD SEC.	(7) CASE	(8) STARTING VALUE FOR A RADIANS	(9) LOCAL SLOPE %	(10) STATIONS 1-7 ALL GO	(11) AMAX (STA) AFINISH(STA) RADIANS	(12) LOCAL SLOPE %	(13) STATIONS 8-17 ALL GO	(14) AMAX (STA) AFINISH(STA) RADIANS
2	E	9.5	24.0	0.	8.	A	0.158	0.	YES	0.158 (4) -0.104 (4)	0.	YES	0.157 (8) -0.140 (8)
						B	0.402	25.0	NO	0.402 (1) 0.145 (1)	25.0	NO	0.402 (8) 0.147 (8)
2	E	9.5	24.0	15.	8.	A	0.158	0.	YES	0.158 (6) -0.092 (6)	0.	YES	0.157 (8) -0.132 (8)
						B	0.402	25.0	NO	0.402 (1) 0.146 (1)	25.0	NO	0.402 (8) 0.183 (8)
2	E	9.5	24.0	30.	8.	A	0.158				0.	YES	0.157 (8) -0.103 (8)
						B	0.402	2			25.0	NO	0.402 (8) 0.218 (8)
2	E	9.5	24.0	45.	8.	A	0.158				0.	YES	0.157 (8) -0.080 (8)
						B	0.402	2			25.0	NO	0.402 (8) 0.248 (8)
2	E	9.5	24.0	60.	8.	A	0.158				0.	YES	0.157 (8) -0.063 (8)
						B	0.402	2			25.0	NO	0.402 (8) 0.269 (8)
2	E	9.5	24.0	75.	8.	A	0.158				0.	YES	0.157 (8) -0.055 (8)
						B	0.402	2			25.0	NO	0.405 (8) 0.280 (8)
2	E	9.5	24.0	90.	8.	A	0.158				0.	YES	0.157 (8) -0.046 (8)
						B	0.402	2			25.0	NO	0.411 (8) 0.291 (8)

Figure 21. Example application of STAM lateral overturn subroutine

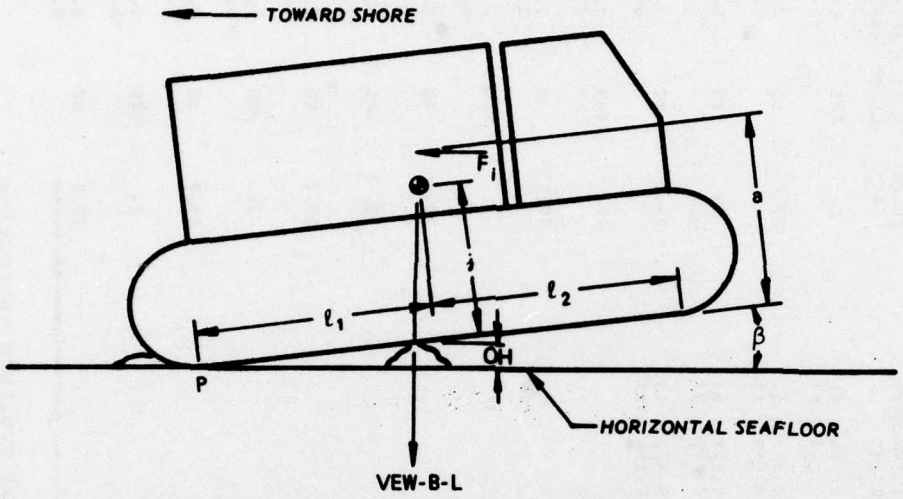

a. CASE 1: LOCAL SLOPE = 0, IMPACT PART OF WATER FORCE CYCLE

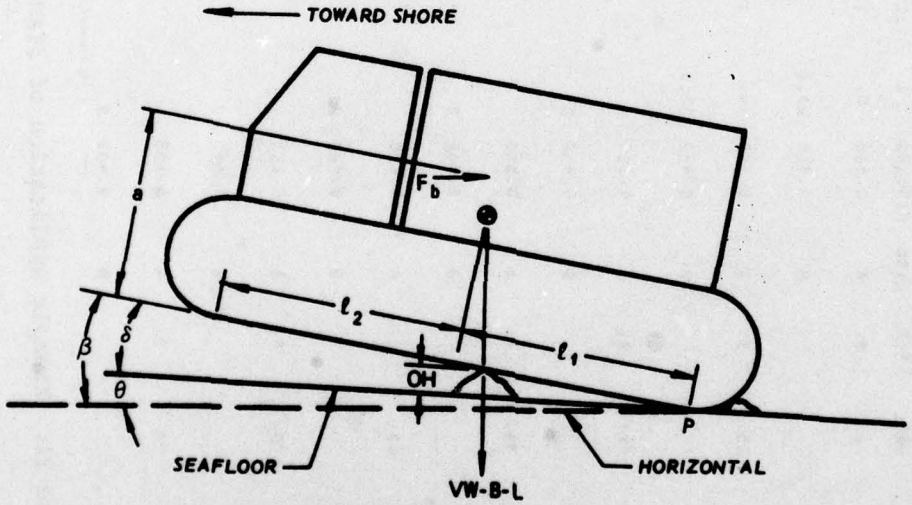

b. CASE 2: LOCAL SLOPE = θ, BACKWASH PART OF WATER FORCE CYCLE

Figure 22. Sketch of tracked vehicle for two worst cases relative to longitudinal overturn

(1)	(2)	(3)	(4)	(5)	(6)	(7)	(8)	(9)	(10)	(11)	(12)	(13)	(14)
VEH NO.	SCEN-ARIO	WAVE HEIGHT FT	OBSTACLE HEIGHT IN	VEHICLE HEADING ANGLE DEG.	WAVE PERIOD SEC.	MAXIMUM OBSTACLE HEIGHT NEGOTIABLE IN	STARTING VALUE FOR B RADIANS	LOCAL SLOPE %	STATIONS 1-7 ALL GO	BMAX (STA) BFINISH(STA) RADIANS	LOCAL SLOPE %	STATIONS 8-17 ALL GO	BMAX (STA) BFINISH(STA) RADIANS
2	E	9.5	24.0	0.	8.	31.4	0.380	0.	NO	0.402 (6) 0.394 (6)	0.	YES	0.380 (8) 0.293 (8)
							0.625	25.0	NO	0.625 (1) 0.506 (1)	25.0	NO	0.647 (8) 0.599 (8)
2	E	9.5	24.0	15.	8.	31.4	0.380	0.	NO	0.415 (6) 0.384 (6)	0.	YES	0.380 (8) 0.293 (8)
							0.625	25.0	NO	0.625 (1) 0.507 (1)	25.0	NO	0.647 (8) 0.600 (8)
2	E	9.5	24.0	30.	8.	31.4	0.380				0.	YES	0.380 (8) 0.287 (8)
							0.625				25.0	NO	0.642 (8) 0.593 (8)
2	E	9.5	24.0	45.	8.	31.4	0.380				0.	YES	0.380 (8) 0.275 (8)
							0.625				25.0	NO	0.632 (8) 0.578 (8)
2	E	9.5	24.0	60.	8.	31.4	0.380				0.	YES	0.380 (8) 0.257 (8)
							0.625				25.0	NO	0.625 (8) 0.557 (8)
2	E	9.5	24.0	75.	8.	31.4	0.380				0.	YES	0.380 (8) 0.236 (8)
							0.625				25.0	NO	0.625 (8) 0.533 (8)
2	E	9.5	24.0	90.	8.	31.4	0.380				0.	YES	0.380 (8) 0.214 (8)
							0.625				25.0	NO	0.625 (8) 0.507 (8)

Figure 23. Example application of STAM longitudinal overturn subroutine

(1)	(2)	(3)	(4)	(5)	(6)	(7)	(8)	(9)	(10)	(11)	(12)	(13)	(14)	(15)
					VEHICLE HEADING ANGLE = 0.0 DEG.					VEHICLE HEADING ANGLE = 15.0 DEG.				
VEH NO.	SCEN-ARIO	LOCAL SLOPE %	WAVE HEIGHT FT	WAVE PERIOD SEC.	STA	G	T	G/T	FORWARD MOTION MAINTAINED	STA	G	T	G/T	FORWARD MOTION MAINTAINED
2	E	0.0	9.5	8.	1	2.1	696.6	0.003	YES	1	2.5	696.6	0.004	YES
					2	7.6	672.2	0.011	YES	2	9.2	672.2	0.014	YES
					3	15.8	644.5	0.025	YES	3	19.2	644.5	0.030	YES
					4	21.9	612.5	0.036	YES	4	26.5	612.5	0.043	YES
					5	24.3	712.9	0.034	YES	5	29.4	711.7	0.041	YES
					6	120.4	698.1	0.173	YES	6	144.2	693.4	0.208	YES
					7	102.2	696.1	0.147	YES	7	122.4	691.0	0.177	YES
2	E	0.0	9.5	15.	1	5.1	1201.9	0.004	YES	1	6.2	1201.9	0.005	YES
					2	17.5	1130.2	0.015	YES	2	21.1	1130.2	0.019	YES
					3	26.8	1043.6	0.026	YES	3	32.3	1043.6	0.031	YES
					4	28.0	1250.9	0.022	YES	4	33.8	1248.2	0.027	YES
					5	27.6	1248.1	0.022	YES	5	32.7	1244.7	0.026	YES
					6	87.5	1207.4	0.072	YES	6	104.8	1194.5	0.088	YES
					7	74.8	1202.1	0.062	YES	7	89.8	1188.0	0.076	YES

Figure 24. Example application of STAM maintenance of forward motion subroutine

(1)	(2)	(3)	(4)	(5)	(6)	(7)	(8)	(9)	(10)	(11)	(12)	(13)	(14)	(15)	(16)	(17)	(18)
						CASE 1 STATIONS 1-7							CASE 2 STATIONS 8-17				
VEH NO.	SCEN-ARIO	WAVE WEIGHT FT	WAVE PERIOD SEC.	LOCAL SLOPE %	VEHICLE HEADING ANGLE DEG.	STA	I	U	I/U	POSITION MAINTAINED	LOCAL SLOPE %	VEHICLE HEADING ANGLE DEG.	STA	I	U	I/U	POSITION MAINTAINED
2	E	9.8	8.	0.0	0.	7	2.3	348.1	0.007	YES	25.0	0.	8	1.4	76.1	0.018	YES
					15.	6	40.2	346.7	0.116	YES		15.	8	7.3	76.1	0.096	YES
												30.	8	13.3	76.1	0.174	YES
												45.	8	18.3	76.1	0.241	YES
												60.	8	22.0	76.1	0.289	YES
												75.	8	23.9	76.1	0.314	YES
												90.	8	25.8	76.1	0.339	YES
2	E	9.8	15.	0.0	0.	7	2.3	601.1	0.004	YES	25.0	0.	8	0.8	76.1	0.010	YES
					15.	6	29.6	597.3	0.050	YES		15.	8	3.6	76.1	0.047	YES
												30.	8	6.5	76.1	0.086	YES
												45.	8	9.0	76.1	0.118	YES
												60.	8	10.7	76.1	0.141	YES
												75.	8	11.9	76.1	0.156	YES
												90.	8	12.9	76.1	0.169	YES

Figure 25. Example application of STAM resistance to side sliding subroutine

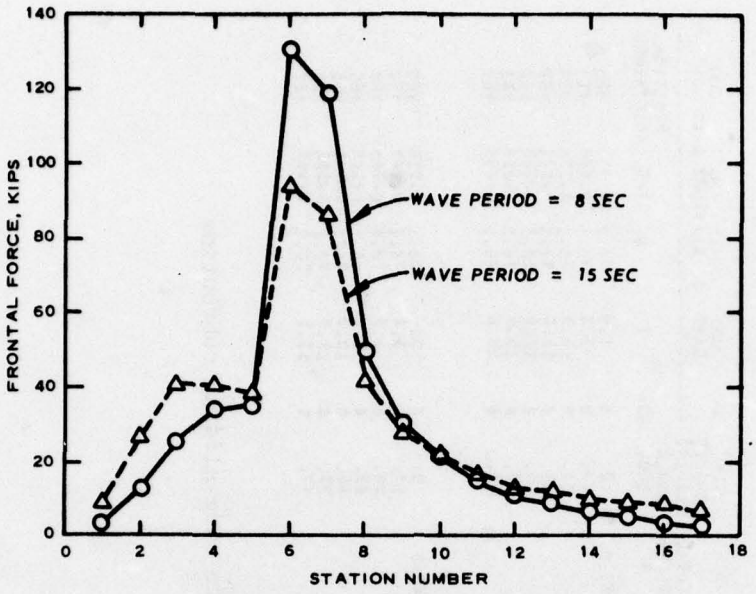

Figure 26. Relation of frontal force to station number for example vehicle 2, scenario D, 0-deg heading angle, and wave periods of 8 and 15 sec

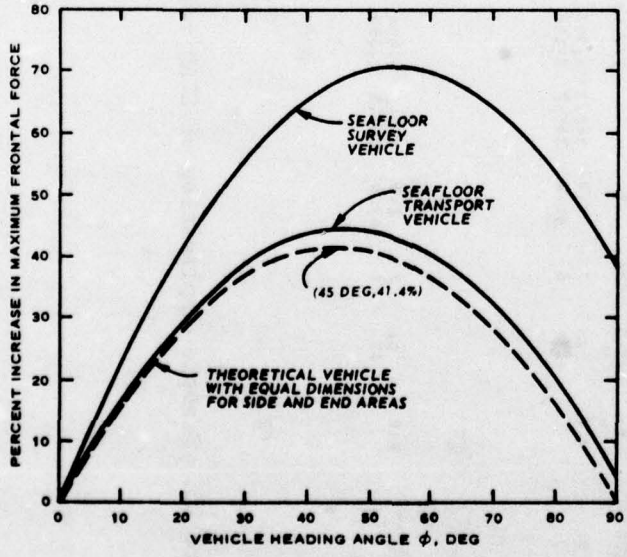

Figure 27. Relation of percent increase in maximum frontal force to vehicle heading angle for scenario C, wave period of 15 sec, and example vehicles 1 and 2

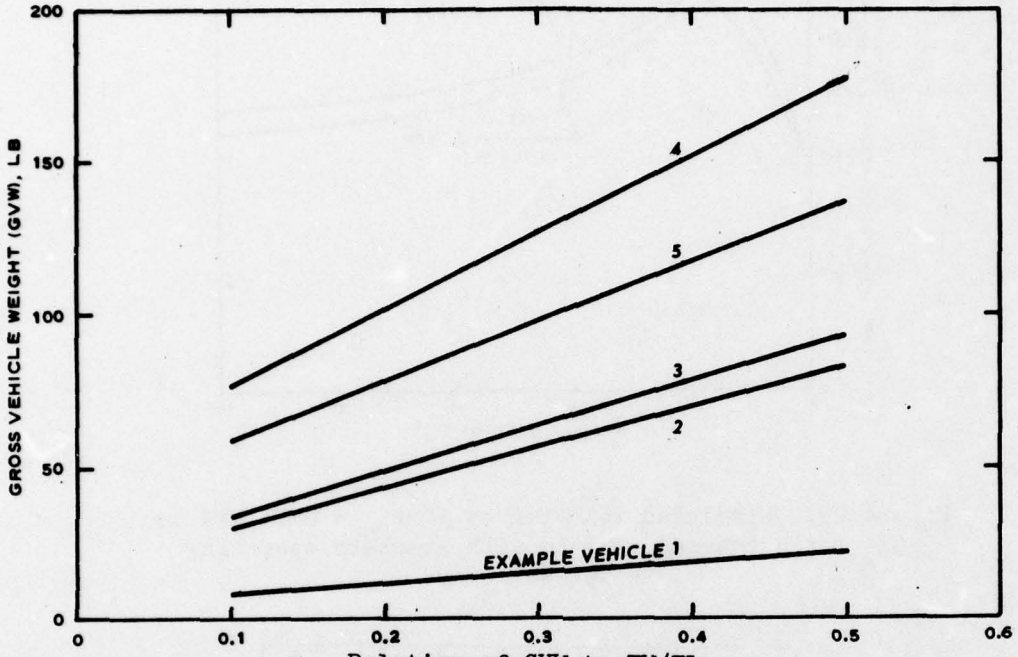

a. Relation of GVW to TW/TL

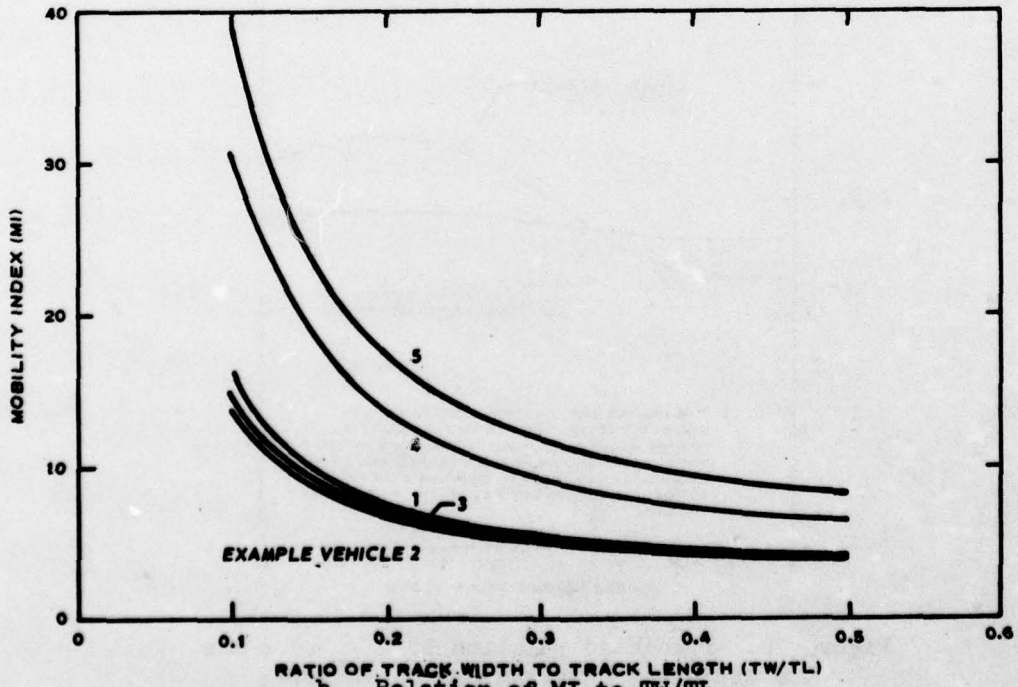

b. Relation of MI to TW/TL

Figure 28. Relations of GVW and MI to TW/TL for the five example vehicles

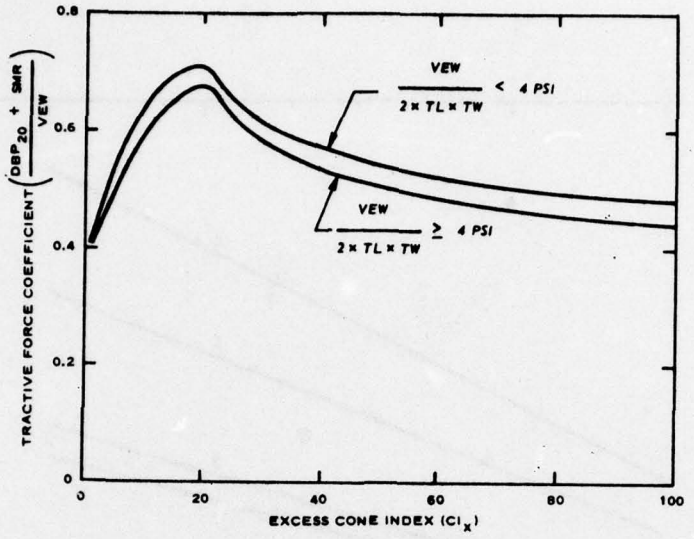

Figure 29. Predicted relation of $(DBP_{20} + SMR)/VEW$ to CI_x for a tracked vehicle with grousers operating in wet-wet clay

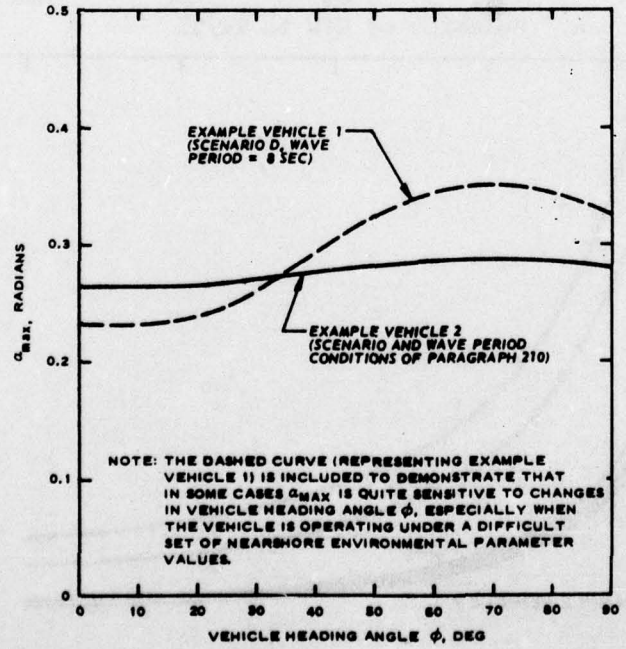

Figure 30. Predicted relation of α_{max} to ϕ for two different combinations of vehicle, scenario, and wave period

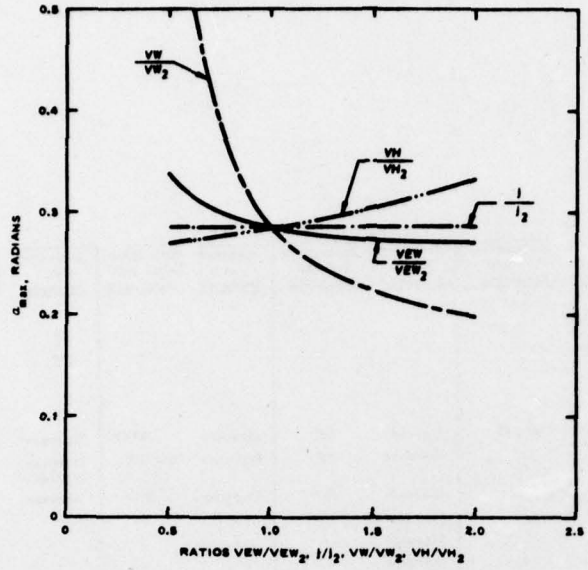

Figure 31. Predicted relations of α_{max} to four vehicle design parameter ratios for example vehicle 2 (under the environmental and operating conditions of paragraphs 209 and 210, respectively)

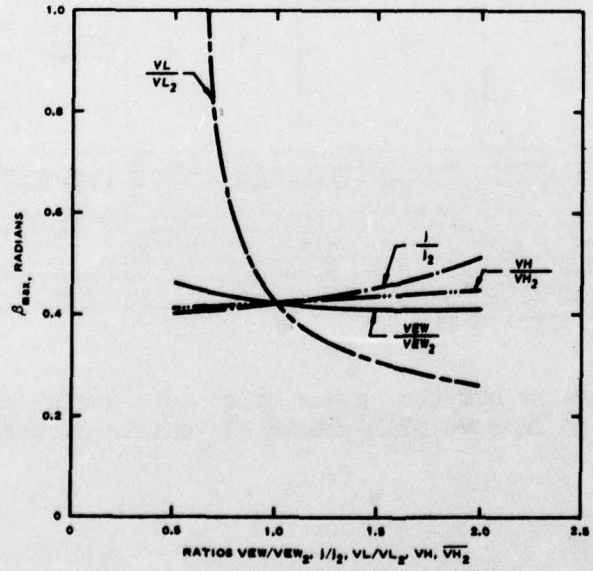

Figure 32. Predicted relations of β_{max} to four vehicle design parameter ratios for example vehicle 2 (under the environmental and operating conditions of paragraphs 209 and 215, respectively)

Vehicle Design Parameter	Subroutine T-I and Paragraph	Increase or Decrease	Subroutine T-F and Paragraph	Increase or Decrease	Subroutine T-C and Paragraph	Increase or Decrease	Subroutine S-Lat and Paragraph	Increase* or Decrease	Subroutine S-Lat and Pargraph	Increase* or Decrease
TH	187	Increase	-	-	-	-	-	-	-	-
CGH	187	Decrease	-	-	-	-	-	-	-	-
VAA, VDA	187-189	Depends on obstacle size and approach angle	-	-	-	-	-	-	-	-
TW	-	-	192-195	Increase	200	Increase	205**	Increase	214**	Increase
GVW(or VEW)	-	-	195	Decrease	200	Decrease	204,205	Increase, Increase	214	Increase, Increase
TL	-	-	195	Increase	200	Increase	205**	Increase	214	Increase
GH†	-	-	195	Increase	-	-	-	-	-	-
BH x ATS†	-	-	195	Increase	-	-	-	-	-	-
GC†	-	-	195	Increase	-	-	-	-	-	-
HPT†	-	-	195	Increase	-	-	-	-	-	-
Suspension flexibility	-	-	-	-	200	Increase	-	-	-	-
J	-	-	-	-	-	-	204,205	Decrease, Increase	214	Decrease, Increase
b	-	-	-	-	-	-	204,205	Increase, Increase	-	-
VH	-	-	-	-	-	-	204	Decrease	214	Decrease
VW	-	-	-	-	-	-	205	Increase	214	Increase
VL	-	-	-	-	-	-	205	Increase	214	Increase
Vehicle Size	187-189	Increase	-	-	-	-	206	Decrease, Increase	214	Decrease, Increase
							207	Decrease	214	Decrease, Increase, Decrease
t_1	-	-	-	-	-	-	-	-	214	Increase, Increase

* Where two or three entries appear under "Increase or Decrease" for either the S-Lat or S-Long subroutine and a given vehicle design parameter, the first entry relates to improving vehicle performance by decreasing either M_o or M_p, and the second (or second and third) to improving performance by increasing either J_2 or J_3.

** While TW and TL were not mentioned in paragraphs 204-207 and 214 as vehicle design parameters influencing vehicle S-Lat and S-Long performance, respectively, TW is directly related to VW and TL to VL. It was judged reasonable, then, to make the same entries for TW and TL for the S-Lat and S-Long subroutines as were made for VW and VL, respectively.

† The four vehicle design parameters GH, BH x ATS, GC, and HPT are the major parameters included in factors 4-7 of mobility index MI--the grouser, bogie, clearance, and engine factors, respectively. The information provided above relative to these four parameters complements the information above on TW, GVW (or VEW), and TL and the analysis in paragraphs 192-195, both of which pertain to factors 1-3 of MI. No "Increase or Decrease" question can be applied to factor 8 of MI (its last factor), but use of an automatic transmission is favored over a manual one.

Figure 33. Findings as to how the values of vehicle design parameters should be changed to improve STAM-predicted vehicle performance

APPENDIX A: DESCRIPTION OF VEHICLE MISSIONS AND VEHICLE DESIGN/PERFORMANCE/ENVIRONMENTAL REQUIREMENTS FOR FIVE EXAMPLE NEARSHORE, BOTTOM-CRAWLING VEHICLES

1. The descriptions in this appendix are considered useful because (a) the five example vehicles considered are representative of the broad range of bottom-crawling vehicles that ultimately will be employed in nearshore work, and (b) the descriptions illustrate the type of information required to design a nearshore crawler by the methods developed in this report--in particular, the quantitative information required by STAM.

Example Vehicle Mission and Performance/Design Requirements

2. The following paragraphs provide narrative descriptions of the missions of five example nearshore, bottom-crawling vehicles, together with information on some of the vehicle design, performance, and environmental requirements.

Seafloor survey vehicle (example vehicle 1)

3. This is a diver-operated vehicle (two SCUBA divers carrying their own life support equipment, 500/0 lb*) with self-contained power supply (2000/1500-lb interchangeable package of lead-acid batteries). Thus, power conservation is a concern. The vehicle surveys/runs along primarily preselected parallel routes carrying a maximum of 1000/500 lb of electronic survey equipment (acoustic positioning system, subbottom sounding acoustic system, video equipment, and data recording equipment, occupying less than 15 cu ft of space). The vehicle will typically operate off-the-beach for 1-hr sorties. Most work will be done in water depths less than 60 ft but beyond the surf zone. For one application there will be a requirement for the vehicle to develop a 100-lb drawbar pull in excess of that required to move the vehicle, for towing a small sled.

---

* Weights are given as dry weight/submerged weight.

4. Surveys will be of two types: (a) the assessment and selection of routes for cables or pipelines that typically run outward from the beach, and (b) the assessment and selection of locations for offshore foundations or anchorages. Maximum operating vehicle speed will be 2 knots (3.4 ft/sec).

5. The vehicle, exclusive of running gear and connections thereto, will likely have a semienclosed body measuring 4 ft wide by 3 ft high by 15 ft long. Its estimated weights, fully loaded but excluding running gear and connections thereto, are 5500/3500 lb.

Seafloor transport vehicle
(example vehicle 2)

6. The transport vehicle is designed strictly to transport a cargo (anchor blocks, a portable power supply, structural component, etc.) across the beach and out to a shallow-water (less than 100-ft water depth) site. The vehicle will be driven by a pair of SCUBA divers. Their precise route is selectable. The vehicle will operate at a speed of less than 2 ft/sec using self-contained storage batteries as the power source; thus, power conservation is a major concern. No drawbar pull is required in excess of that needed for vehicle mobility. The cargo may be as large as 6 ft wide by 4 ft high by 10 ft long and weigh as much as 7500/6000 lb.

7. The vehicle, exclusive of running gear will be 7 ft wide by 5 ft high and 15 ft long. It will be an open structure except for the forward driver's area, which will be semiclosed. Its fully loaded weights, exclusive of running gear, will be 18,000/13,000 lb.

Seafloor work platform
(example vehicle 3)

8. This vehicle is a chassis to which pieces of construction equipment (backhoes, rock drills, crane-manipulators, winches, chambers for dry seafloor work, etc.) are attached. It transports the equipment from the beach to the work site at low speeds (less than 2 ft/sec). There is no requirement for drawbar pull in excess of that required for mobility. However, when the vehicle is parked at the work site, the running gear may have to be relatively rigid and resist large loads due to the operation of the equipment. Some maneuvering/repositioning may

be required at the site between equipment operations. Transit to the site will utilize SCUBA divers and self-contained power. Operation on-site will utilize umbilical-supplied power, divers, or remote control.

9. The payload equipment will attach to a 5- by 10-ft bed on the vehicle. The equipment will weigh a maximum of 10,000/8,000 lb and may have a solid side area as large as 10 ft wide by 6 ft high.

10. The vehicle, exclusive of running gear and payload equipment, will be an open-frame structure 6 ft wide by 16 ft long and only 2 ft high except for a few small elements. The maximum fully loaded weights of the vehicle, exclusive of the running gear and connecting elements, will be 20,000/14,000 lb.

Seafloor trencher
vehicle (example vehicle 4)

11. This vehicle follows a predetermined path from the beach out to water depths of 80 ft and operates remotely via an umbilical. The trencher traverses slowly (0.5 to 5 ft/min) and must develop a drawbar pull of 4500 lb in excess of that required for mobility in order to operate the rock-saw or soil-plow trencher system. The vehicle is described in Reference 16 of the main text; however, the running gear selection should be reconsidered.

12. The vehicle weight, exclusive of running gear is 50,000/35,000 lb. Its cross-sectional area is 80 sq ft on the side and 60 sq ft on the front. The trencher mechanism requires a fairly rigid chassis/running gear system to resist the dynamic loads it generates.

Underwater bulldozer
(example vehicle 5)

13. This vehicle is designed to clear or level an area/route or to develop high drawbar for pulling pipelines and cables. The vehicle will operate remotely outward from the beach using umbilical-supplied power. It will operate for long periods of time in the surf zone. Drawbar pull of 30,000 lb will be required in excess of that required for mobility of the vehicle. The vehicle will operate primarily in preselected areas and routes, at a maximum speed of 2 ft/sec.

14. The vehicle, exclusive of running gear, will be 8 ft wide by 6 ft high by 16 ft long with a semiclosed structure and will weigh 40,000/35,000 lb.

Nearshore Environment Requirements for the Five Example Vehicles

15. Table A1 summarizes the extreme environmental parameter values for the five example vehicles.

Table A1

Extreme Values of Nearshore Environmental Parameters for the Five Types of Bottom-Crawling Vehicles* Considered in the Example Selection Problems

		Extreme Values of Nearshore Environmental Parameters						
Scenario**	Ground Material	Soil Strength	Slope, Percent General	Slope, Percent Local	Obstacle Height ft	Current Velocity fps	Wave Height, ft †	Maximum Water Depth ft ††
A	Weak cohesive soil (mud)	S_u = 0.2 psi (CI = 2)	0.2	2	0.5	0.5	4.0, 4.0, 4.0, 5.0, 4.5	150
B	Weak cohesive soil (mud)	S_u = 0.4 psi (CI = 4)	0.6	4	0.5	0.5	4.0, 5.0, 4.0, 5.0, 4.5	150
C	Weak cohesive soil (mud)	S_u = 0.8 psi (CI = 8)	1.0	5	0.5	0.5	4.0, 4.0, 4.0, 5.0, 4.5	150
D	Loose sand	G = 10 psi/in. (CI = 30)	3.0	10	1.0	2.0	6.2, 8.0, 7.0, 15.5,12.0	150
E	Coral	CI = 3000	5.0	25	2.0	4.0	7.5, 9.5, 8.5, 17.5,13.4	150
F	Cobbles and boulders	CI = 4000	8.0	25	2.0	4.0	7.5, 10.5,9.0, 17,5,13.5	150
G	Hard rock	CI = 5000	10.0	25	3.0	5.0	7.5, 12.5,10.0,20.0,16.5	150
H	Hard rock	CI = 5000	15.0	60	5.0	6.0	9.1, 16.5,12.5,25.1,21.0	150

* The vehicles of concern are: Vehicle No. 1 - Seafloor Survey Vehicle
Vehicle No. 2 - Seafloor Transport Vehicle
Vehicle No. 3 - Seafloor Work Platform Vehicle
Vehicle No. 4 - Seafloor Trencher Vehicle
Vehicle No. 5 - Underwater Bulldozer

** The following combinations of scenarios (called operating conditions) are of particular interest in the present study.

Vehicle No.	Operating Condition (Roman No.) and Scenario (Letter)			
1	I: D,E,F,G	II: A	III: C,H	IV: none
2	I: B,D	II: D,E,F	III: H	IV: none
3	I: A	II: B	III: D,G	IV: none
4	I: D,E,F,G	II: C	III: H	IV: A
5	I: D,E	II: F,G	III: H	IV: none

† Except for wave height, the extreme value of each environmental parameter is the same for all five vehicles under a given scenario. For wave height, the five values listed for each scenario apply, in order, to vehicles 1-5.

†† A maximum water depth of 150 ft for vehicle operation is used for all vehicle/scenario combinations, thus matching or exceeding the water depth values mentioned in pages A1-A4.

APPENDIX B: ABILITY OF TRACKED VEHICLES TO MAINTAIN FORWARD MOTION AND TO RESIST SIDE SLIDING WHILE OPERATING ON THE NEARSHORE OCEAN BOTTOM

1. Two important aspects of bottom-crawling vehicle stability in the nearshore region are vehicle ability to maintain forward motion and to resist side sliding. Mathematical modeling of both these aspects of vehicle performance centers on analyzing the pertinent free-body systems, as described in the following paragraphs.

Mathematical Description of Vehicle Ability to Maintain Forward Motion While Operating on the Nearshore Ocean Bottom

2. Figure B1 illustrates the major vehicle, soil, and water forces that act on a tracked vehicle attempting to maintain forward motion up a seafloor of slope θ. The sign convention and x, y reference frame that will be used relative to these forces are shown in the upper right part of the figure. The basic intent of this analysis is to develop a means for predicting whether vehicle forward distance moved x will be greater than zero over the course of a full wave period. A full wave period is taken to occupy time from 0 to WP, with the impact cycle of the full wave period occupying time 0 to IT and the backwash cycle time IT to WP.

3. Dealing first with the impact cycle, the sum of forces in the x direction in Figure B1 can be described by

$$F_x = F_i - (VEW - L - B) \sin \theta + T_e \tag{B1}$$

where $T_e = \mu N_e$ (B2)

and $N_e = (VEW - B - L) \cos \theta$ (B3)

In the above equations, VEW is vehicle effective weight, θ is seafloor slope; T_e is vehicle effective forward thrust; μ is coefficient of traction between the vehicle and the seafloor; and N_e is the resultant of soil forces normal to angle θ. In agreement with paragraph 131 of

the main text, F_i, L, and B are defined as follows:

$$F_i = F \sin \frac{\pi T}{IT} = F \sin \frac{\pi T}{\lambda WP} = F \sin kT, \tag{B4}$$

where $F = MFF \cos \phi + MBF \sin \phi$ and T is time starting at T = 0.

With $\lambda = IT/WP$ and $k = \pi/\lambda WP$, (B4a)

$$L = MLF \sin kT, \tag{B5}$$

and $$B = MB \sin kT. \tag{B6}$$

Then, $$F_x = F \sin kT - [VEW - (MLF + MB) \sin kT] \sin \theta + \mu [VEW - (MLF + MB) \sin kT] \cos \theta$$

$$= F \sin kT + (\mu \cos \theta - \sin \theta) [VEW - (MLF + MB) \sin kT] \tag{B7}$$

Let $\cos \theta - \sin \theta = H$

and $MLF + MB = M$.

Then, $$F_x = F \sin kT + H (VEW) - H(M) \sin kT \tag{B8}$$

$$= (F - HM) \sin kT + H(VEW) \tag{B9}$$

4. The acceleration of a tracked vehicle in the x direction caused by force F_x during the impact cycle is

$$\ddot{x} = \frac{F_x}{VEW/g}$$

$$= g \left[\frac{(F - HM) \sin kT}{VEW} + H \right]$$

Let $$\frac{F - HM}{VEW} = P. \tag{B10}$$

Then, $$\frac{\ddot{x}}{g} = P \sin kT + H, \tag{B11}$$

$$\frac{\dot{x}}{g} = - \frac{P}{k} \cos kT + HT + \dot{x}_o, \tag{B12}$$

and $$\frac{x}{g} = - \frac{P}{k} \sin kT + \frac{HT^2}{2} + \dot{x}_o T + x_o \tag{B13}$$

5. Having dealt to this point only with the impact cycle of a wave period, it is important next to consider the backwash cycle. During backwash (i.e., from time IT to WP),

$$F_x = - F_b \ (VEW - L - B) \sin \theta + \mu \ (VEW - B) \cos \theta$$

$$= - F_b + H \ (VEW - L - B). \tag{B14}$$

To define force F_b, recognize that there is a balance between the total energy expended during the impact and backwash cycles of a wave period,

which can be described by

$$\int_0^{IT} F_i \, dT = F_b \, BT$$

Then,
$$F_b = \frac{F}{BT} \int_0^{IT} \sin kT \, dT$$

$$= \frac{F}{kBT} \left| - \cos kT \right|_0^{IT}$$

$$= \frac{F}{kBT} \quad (1 - \cos kIT)$$

From Equation B4a, $kIT = \pi$ and $k = \frac{\pi}{\lambda WP}$.

So,
$$F_b = \frac{2F}{kBT} = \frac{2F \ (\lambda WP)}{\pi \ (1 - \lambda WP)} = \frac{2F}{\pi} \cdot \frac{\lambda}{1 - \lambda} \tag{B15}$$

6. During the backwash cycle, x is defined as $\ddot{x} = \frac{F_x}{VEW/g}$, with F_x defined in Equation B14. Then,

$$\frac{\ddot{x}}{g} = \frac{\left[-F_b + H(VEW - L - B)\right]}{VEW} = R, \tag{B16}$$

$$\frac{\dot{x}}{g} = R(T) + \frac{\dot{x}_1}{g}, \tag{B17}$$

and
$$\frac{x}{g} = \frac{R(T^2)}{2} + \frac{\dot{x}_1(T)}{g} + \frac{x_1}{g} . \tag{B18}$$

7. In describing the cumulative effects of F on x during one full wave period, let $\dot{x}$ and x in Equations B17 and B18 at the beginning of the backwash cycle (i.e., at time T = IT) be equal to $\dot{x}$ and x in Equations B12 and B13 at the end of the impact cycle (at the same time T = IT). Let $\dot{x}_o$ and x_o in Equations B12 and B13 each be assumed equal to 0 (with little resulting error). At time T = IT, then,

$$\dot{x} = g \left[H(IT) - \frac{P}{k} \cos k(IT)\right] \tag{B19}$$

and
$$x = g \left[\frac{H(IT)^2}{2} - \frac{P}{k} \sin k(IT)\right] \tag{B20}$$

Then, x_1 in Equations B17 and B18 equals x in Equation B19, and x_1 in Equation B18 equals x in Equation B20.

8. Evaluating distance x at the end of a full wave period, i.e., at time T = WP, with T in Equation B18 covering the time IT to WP, or $(1 - \lambda)WP$, and noting that IT = λWP produces

$$x = g \left\{ \frac{R(1 - \lambda)^2 (WP)^2}{2} + \left[H(\lambda WP) - \frac{P}{k} \cos k(\lambda WP) \right] \cdot (1 - \lambda)WP + \left[\frac{H(\lambda WP)^2}{2} - \frac{P}{k} \sin k(\lambda WP) \right] \right\} \quad \text{(B21)}$$

Then, $$\frac{x}{g(WP)^2} = \frac{R(1 - \lambda)^2}{2} + H\,\lambda(1 - \lambda) + \frac{H\lambda^2}{2}$$

$$\frac{-P}{k} \left[(1 - \lambda) \cos k(\lambda WP) + \sin k(\lambda WP) \right] \quad \text{(B22)}$$

Using $k\lambda WP = \pi$ (from Equation B4a) and simplifying produces

$$\frac{x}{g(WP)^2} = \frac{H - (1 - \lambda)^2 (H - R)}{2} \quad \text{(B23)}$$

From Equations B16 and B15, $R = \left[-\left(\frac{2F}{\pi} \cdot \frac{\lambda}{1 - \lambda} \right) + H\,(VEW - L - B) \right] \div VEW$

or $$R = H \left(1 - \frac{L + B}{VEW} \right) - \left(\frac{2\lambda}{\pi(1 - \lambda)} \cdot \frac{F}{VEW} \right)$$

and $$H - R = H \left(\frac{L + B}{VEW} \right) + \left(\frac{2\lambda}{\pi(1 - \lambda)} \cdot \frac{F}{VEW} \right)$$

From Equation B23, for $\frac{x}{g(WP)^2}$ to be greater than zero, then $(1 - \lambda)^2 \cdot (H - R)$ must be less than H. That is, for x > 0,

$$\left[(1 - \lambda)^2 \cdot H \left(\frac{L + B}{VEW} \right) \right] + \left[\frac{2\lambda(1 - \lambda)}{\pi} \cdot \frac{F}{VEW} \right] < H$$

or $$(1 - \lambda) \left[(1 - \lambda) \cdot \left(\frac{L + B}{VEW} \right) + \left(\frac{2\lambda}{\pi} \cdot \frac{F}{(VEW)(H)} \right) \right] < 1 \quad \text{(B24)}$$

Let $G = \frac{F}{VEW}$. Then, for x > 0,

$$(1 - \lambda) \cdot \frac{L + B}{VEW} + \frac{2\lambda}{\pi} \cdot \frac{G}{H} < \frac{1}{1 - \lambda}$$

and $$G < \frac{H}{2\lambda} \cdot \frac{1 - \left[\left(\frac{L + B}{VEW} \right) \cdot (1 - \lambda)^2 \right]}{1 - \lambda} \quad \text{(B25)}$$

or $$G < T \quad \text{(B26)}$$

The same result is shown in paragraph 153 of the main text. The proper interpretation of Equation B25 is that for a bottom-crawling vehicle to make a net gain in forward movement of distance x over the course of a full wave period, then the requirement G < T must be satisfied, where G is the ratio of maximum water force acting on the sides of the vehicle to the vehicle's effective weight, and T is a dimensionless term that reflects pertinent vehicle, seafloor, and sea-state conditions.

Mathematical Description of Vehicle Ability to Resist Side Sliding While Operating on the Nearshore Ocean Bottom

9. The second important aspect of bottom-crawling vehicle stabilty considered in this appendix is the ability of the vehicle to resist side sliding. Figure B2 illustrates the major vehicle, soil, and water forces acting on a tracked vehicle attempting to maintain position, i.e., to resist side sliding, on a seafloor of slope θ.

10. The force system in Figure B2 is essentially equivalent to that in Figure B1. In fact, the analysis of the Figure B2 system translates directly from that of the Figure B1 system (described in paragraphs 2-8) if F is defined as $F = MFF \sin \phi + MBF \cos \phi$ (instead of $F = MFF \cos \phi + MBF \sin \phi$, as in paragraph 2). With this difference noted, the equivalents of G and T in paragraph 8 (for maintenance of forward motion) are I and U, respectively, for resistance to side sliding, where

$$I = \frac{F}{VEW} \tag{B27}$$

and

$$U = \frac{\pi H}{2\lambda} \cdot \frac{1 - \left[\left(\frac{L + B}{VEW}\right) \cdot (1 - \lambda)^2\right]}{1 - \lambda} \tag{B28}$$

If $I < U$, vehicle side sliding is predicted not to occur; if $I \geq U$, it is predicted to occur.

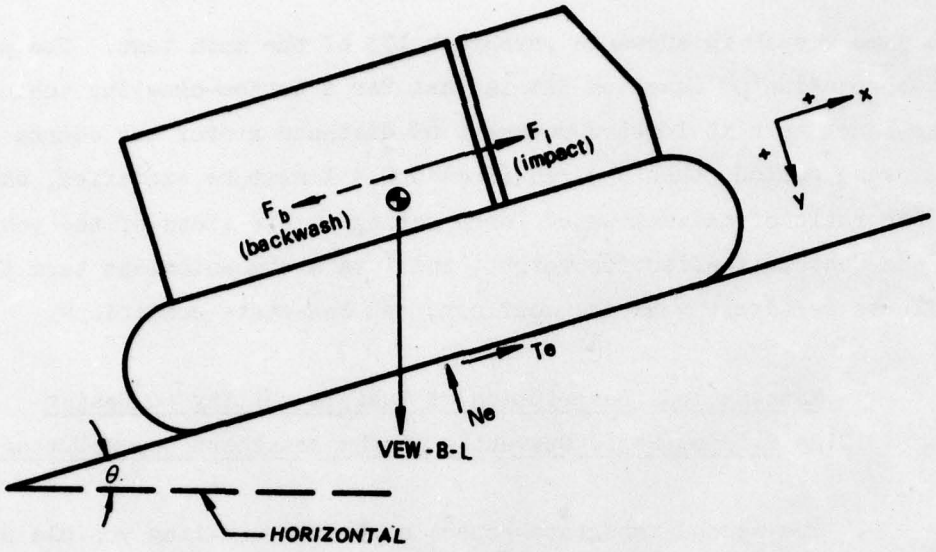

Figure B1. Free-body diagram of a tracked vehicle attempting to maintain forward motion on a seafloor of slope θ

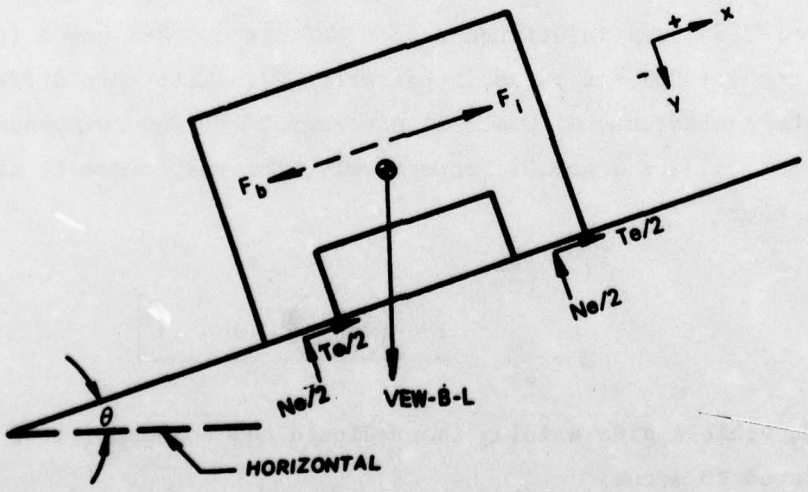

Figure B2. Free-body diagram of a tracked vehicle attempting to maintain position, i.e., resist side sliding on a seafloor of slope θ

APPENDIX C: IMPLEMENTATION OF STAM

1. Examples of outputs of the three submodels of STAM are included in the main body of this report in Figure 13 (for the water force calculations submodel), in Figure 18 (for the trafficability submodel), and in Figures 21 and 23-25 (for the four subroutines of the stability submodel). A detailed description of the computer program that comprises STAM was supplied to the project sponsor, including (a) a line-by-line listing of all computer instructions included in STAM, (b) a full set of computer cards that reflect these instructions, and (c) a listing of all the variables (and their definitions) that are included in the computer instructions. Pertinent parts of this description of the STAM computer program can be obtained by written request to: Civil Engineering Laboratory, U. S. Naval Construction Battalion Center, Port Hueneme, California 93041.

2. To assist the potential user of STAM, this appendix completes the STAM description in terms of the major features of (a) the physical requirements that a computer must satisfy for STAM to be implemented and (b) the input data format that STAM utilizes. At the WES, STAM is run on a Honeywell 635 computer that has 256k core memory of 36-bit words. STAM can be implemented on a considerably smaller computer, however--down to one of 25k core memory of 36-bit words.

3. STAM is written in Honeywell Series 6000 FORTRAN computer language and was developed to accept input in terms of data statements, constants, and data files. All data files are in free field format with line numbers. Brief descriptions of the major input requirements of STAM follow:

a. Vehicle data. The bulk of the vehicle description data is input through data file 02 of the STAM trafficability submodel which includes the dummy parameters listed in paragraph 62 and the vehicle design parameters listed under "trafficability submodel" in Table 2. Vehicle submerged weight is input to the trafficability submodel as a data statement, and vehicle effective weight as part

of data file 04.* The vehicle design parameters listed in Table 2 for the water force calculations and stability submodels are input as either data statements or constants.

b. Nearshore environment data. For a given bottom-crawling vehicle, the trafficability submodel receives input nearshore environment information by means of data statements, constants, and two data files, 01 and 04. File 01 inputs a description of seafloor soil strength and geometry in terms of the parameters listed in Table 7. For a given combination of vehicle, scenario, and wave period, file 04 inputs vehicle effective weight computed at each water depth of interest. The water force calculations submodel accepts all of its nearshore environment data through data statements and constants, and outputs its force calculations in printed form (if desired) and as a data file for input to the trafficability and stability submodels. (The computer format used is system standard binary write.) In the four subroutines of the stability submodel, nearshore environment data are input from data statements (for local slope and, as needed, for obstacle height), from constants, and from the output data file of the water force calculations submodel.

c. Vehicle performance requirement data. In the trafficability submodel, maximum drawbar pull and maximum vehicle operational speed are input by means of data statements. In the water force calculations and stability submodels, vehicle heading angle is input through data statements.

Taken together, the information in paragraph 3 describes the major features of input data requirements of the trafficability, water force calculations, and stability submodels of STAM.

---

* Trafficability submodel data file 04 is described under b.

APPENDIX D: NOTATION

1. A listing was compiled of the definitions and units of all symbols used in the computer subroutines developed in this study for the submodels of STAM. This listing was judged too lengthy to be included in this report, but copies of the listing have been supplied to the project sponsor.

2. The following listing includes all notations used in the text of this report, except for a few notations included in paragraphs 78-88 and in Appendix B. Those notations not included in the following listing are defined in context and are used no more than a few times within a very limited part of the report.

a	Height above bottom of vehicle at which water forces F_i and F_b can be taken to be concentrated
A	Obstacle approach angle
ACG	Angle formed at the vehicle pivot point by one line parallel to bottom of track and a second line that passes through the vehicle's center of gravity.
ATS	Area of one track shoe
b	Distance between center lines of vehicle tracks
B	Buoyancy
BN	Number of track bogies in contact with a single vehicle track over nominal track-ground contact length, ℓ
BT	Backwash time, that part of a total wave period during which the wave is moving away from shore
c	Distance between inner sides of vehicle tracks
CG	Center of gravity
CGF	Horizontal distance from vehicle CG to center line of front road bogie
CGH	Vertical distance from vehicle CG to center line of road bogie
CH	Chassis height
CI	Cone index
CI_s	Scenario cone index
CI_x	Excess cone index

CL	Chassis length
CW	Chassis width
d	Distance from the center of the vehicle rear road wheel to a vertical line through the vehicle's CG (with the vehicle resting on a flat, level, unyielding surface)
DBP, DBP_{20}, DBP_{40}, $DBP_{req'd}$	Vehicle drawbar pull; vehicle drawbar pull at 20 and 40 percent slip, respectively; and drawbar pull required of vehicle
DCG	Distance from vehicle CG to pivot point on back end of vehicle track
DL	Dry land
DRISCG	Direct distance from vehicle CG to center of rear idler or sprocket
dry W_{LC}, dry W_p	Dry (in-air) weight of loaded chassis and of payload, respectively
DRYWT	Dry weight of the vehicle (equals in-air gross vehicle weight)
DS	Distance vehicle spans over a ditch before significant vertical motion of the vehicle begins
DSS	Drive sprocket speed
EFF	Transmission efficiency (use 0.95 if not given)
F	Force acting on a vehicle due to water action
F_b	Backwash water force
F_i	Impact water force
FCG	Horizontal distance from leading edge of vehicle to vehicle CG when the vehicle rests on a flat, level, unyielding surface
FDR	Final drive ratio
FDREF	Final drive efficiency
FLEW	Maximum force that leading edge of vehicle can withstand
g	Acceleration due to gravity, 32.2 ft/sec^2
G*	Cone index gradient
GC	Vehicle ground clearance
GH	Grouser height

---

* G has a different meaning in the ratio G/T defined in paragraph 153.

GVW	Gross vehicle weight
H	$\mu \cos \phi - \sin \phi$ (used in the definition of T in paragraph 153)
HAA	Height of rigid point at front of tracked vehicle used in the determination of the vehicle approach angle VAA
HCG	Height of vehicle (G above ground when the vehicle rests on a flat, level, unyielding surface)
HLE	Height of leading edge of vehicle
hp	Horsepower
HPT	Horsepower per ton GVW
HRIS	Vertical distance from ground to center of rear idler or sprocket
I	Numerator in the ratio I/U, which is used by STAM to evaluate vehicle ability to resist side sliding on the nearshore ocean bottom
IT	Impact time, that part of a total wave period during which the wave is moving toward shore
j	Vertical distance from vehicle CG to the ground when the vehicle rests on a flat, level, unyielding surface
J_o	Moment of inertia of the vehicle above a point O at the center of the bottom of one of the vehicle's tracks, when the vehicle is viewed from the end.
J_p	Moment of inertia of the vehicle about a point P at the bottom, rearmost point of the vehicle's tracks, when the vehicle is viewed from the side
k	The parameter that, when multiplied by TW x Tl, yields an estimate of W_t
k_1	Energy dissipated by F_b divided by energy dissipated by F_i, all within a single wave period
L	Lift force due to water action
ℓ	Nominal track-ground contact length (i.e., contact length on a flat, unyielding surface)
ℓ_1, ℓ_2	For ℓ divided into two parts by the intersection of the vertical projection of the vehicle's CG, ℓ_1 and ℓ_2 are the shorter and longer parts of ℓ, respectively
M_o	Moment acting on tracked vehicle about point O, which promotes overturn of the vehicle about its lateral axis (with the vehicle viewed from its end)
M_p	Moment acting on tracked vehicle about point P, which promotes overturn of the vehicle about its longitudinal axis (with the vehicle viewed from its side)

MB	Maximum buoyancy
MBF, MFF	Maximum broadside force and maximum frontal force, respectively, acting on a vehicle due to water action
MI, MI_h, MI_ℓ	Mobility index; MI_h for the vehicle at its heaviest (fully loaded, in air); and MI_ℓ for the vehicle at its lightest (empty, fully submerged)
MLF	Maximum lift force acting on a vehicle due to water action
n	Exponent in the term $\left(\frac{d}{TL/2}\right)^n$, which is a part of N_s
N_s	Sand-track mobility number
OA	Obstacle angle
OH	Obstacle height
PH_{max}, PL_{max}, PW_{max}	Maximum payload height, length, and width, respectively
RCI	Rating cone index
RCI_x	Excess rating cone index
REC	Height of vehicle's trailing edge
RCGH	Running gear connection height (i.e., height required to attach running gear to chassis)
RI	Remolding index
RISR	Distance from center of rear idler or sprocket to outermost edge of track
RWR	Road wheel radius (plus track thickness)
RWW	Drive sprocket pitch radius
S_u	Shear strength obtained by a vane shear apparatus
SMR	Soil motion resistance
STAM	Surfzone Transition Analytical Methodology
SUBWT	Submerged weight of vehicle
t	Tread, distance between center lines of vehicle's tracks
T*	Time
TF, TF_{max}	Tractive force and maximum tractive force, respectively
TF_o	Tractive force required for obstacle override
TF_1	Tractive force required to overcome soil motion resistance and slope resistance (due to vehicle weight)

* T has a different meaning in the ratio G/T defined in paragraph 153.

TF_2	Sum of TF_o and TF_1
TH	Track height
TL	Track length between centroids of outermost road bogies (TL = ℓ)
TLC	Track length in contact with ground
TN	Number of tracks
TT	Track type
TVAR	Transmission type (0 = automatic, 1 = manual)
TW	Track width
U	Denominator in the ratio I/U, which is used by STAM to evaluate vehicle ability to resist side sliding on the nearshore ocean bottom
V	Speed of vehicle
V_{max}	Maximum vehicle speed
VA	Maximum angle vehicle can climb
VAA	Vehicle approach angle
VCI_1,VCI_{50}	One-pass and fifty-pass vehicle cone index, respectively
VDA	Vehicle departure angle
VEW	Vehicle effective weight
VEW_t	Theoretical vehicle effective weight, the value of VEW that would cause the road bogies of the vehicle to bottom out
VH	Vehicle height (overall)
VH_s	Vehicle submerged height
VHF	Vehicle height in feet
VL	Vehicle length (overall)
VLWOB	Vehicle length without blade and without mount between blade and chassis (for a bulldozer)
VT	Vehicle type
VW	Vehicle width (overall)
VWF	Vehicle width in feet
W_t	Weight of both vehicle tracks and connections thereto
WP	Wave period
W_{LC}	Weight of loaded vehicle chassis
Wet W_{LC}	Submerged weight of loaded vehicle chassis

XBC	Vehicle braking coefficient
α	Angle between the bottom of a tracked vehicle and the horizontal when the vehicle is viewed from the end
$\ddot{\alpha}$	Acceleration of angle α
β	Angle between the bottom of a tracked vehicle and the horizontal when the vehicle is viewed from the side
$\ddot{\beta}$	Acceleration of angle β
δ	Angle between the bottom of a tracked vehicle and the seafloor and local seafloor slope when the vehicle is atop an obstacle of height OH (with the vehicle viewed either from the end or the side)
λ	Ratio of IT to WP
μ	Coefficient of traction between the vehicle tracks and the seafloor soil
ϕ	Vehicle heading angle
θ	Seafloor slope

In accordance with letter from DAEN-RDC, DAEN-ASI dated 22 July 1977, Subject: Facsimile Catalog Cards for Laboratory Technical Publications, a facsimile catalog card in Library of Congress MARC format is reproduced below.

Turnage, Gerald W
Study and parametric analysis of trafficability, running gear, and stability considerations for nearshore, bottom-crawling vehicles / by Gerald W. Turnage, William C. Seabergh. Vicksburg, Miss. : U. S. Waterways Experiment Station ; Springfield, Va. : available from National Technical Information Service, 1978.
121, [59] p. : ill. ; 27 cm. (Technical report - U. S. Army Engineer Waterways Experiment Station ; M-78-3)
Prepared for Civil Engineering Laboratory, Naval Construction Battalion Center, Port Hueneme, California.
References: p. 116-121.

1. Coastal zone. 2. Mathematical models. 3. Mobility. 4. Ocean bottom vehicles. 5. Surfzone Transition Analytical Methodology (STAM). 6. Trafficability. 7. Vehicle performance. I. Seabergh, William C., joint author. II. United States. Naval Construction Battalion Center, Port Hueneme, Calif. Civil Engineering Laboratory. III. Series: United States. Waterways Experiment Station, Vicksburg, Miss. Technical report ; M-78-3.
TA7.W34 no.M-78-3